

ELECTROMAGNETIC PLANE WAVE SCATTERING BY
UNIFORMLY LOSSY DIELECTRIC PROLATE SPHEROIDS

CENTRE FOR NEWFOUNDLAND STUDIES

**TOTAL OF 10 PAGES ONLY
MAY BE XEROXED**

(Without Author's Permission)

SOUMYA NAG



Electromagnetic Plane Wave Scattering by Uniformly Lossy Dielectric Prolate Spheroids

By

© Soumya Nag, B. Eng.

A thesis submitted to the School of Graduate Studies in
partial fulfillment of the requirements for the degree of
Master of Engineering

Faculty of Engineering and Applied Science
Memorial University of Newfoundland

August 1994

St. John's

Newfoundland

Canada



National Library
of Canada

Acquisitions and
Bibliographic Services Branch

395 Wellington Street
Ottawa, Ontario
K1A 0N4

Bibliothèque nationale
du Canada

Direction des acquisitions et
des services bibliographiques

395, rue Wellington
Ottawa (Ontario)
K1A 0N4

Your file / Votre référence

Our file / Notre référence

The author has granted an irrevocable non-exclusive licence allowing the National Library of Canada to reproduce, loan, distribute or sell copies of his/her thesis by any means and in any form or format, making this thesis available to interested persons.

The author retains ownership of the copyright in his/her thesis. Neither the thesis nor substantial extracts from it may be printed or otherwise reproduced without his/her permission.

L'auteur a accordé une licence irrévocable et non exclusive permettant à la Bibliothèque nationale du Canada de reproduire, prêter, distribuer ou vendre des copies de sa thèse de quelque manière et sous quelque forme que ce soit pour mettre des exemplaires de cette thèse à la disposition des personnes intéressées.

L'auteur conserve la propriété du droit d'auteur qui protège sa thèse. Ni la thèse ni des extraits substantiels de celle-ci ne doivent être imprimés ou autrement reproduits sans son autorisation.

ISBN 0-612-01894-6

Canada

Abstract

Using modal series expansions of electromagnetic fields in terms of prolate spheroidal vector wave functions, an exact solution is obtained for the scattering by: (a) a single uniformly lossy dielectric prolate spheroid, (b) a system of two uniformly lossy dielectric prolate spheroids in arbitrary orientation, and (c) as an important special case a system of two uniformly lossy dielectric prolate spheroids in parallel configuration embedded in free space. In all the above cases, the excitation being a monochromatic plane electromagnetic wave of arbitrary polarization and angle of incidence. Since the dielectric materials of the scatterers are of complex relative permittivities, complex eigenvalues are evaluated for the spheroidal scalar wave functions of transmitted components of E -field and H -field expansions. Rotational-Translational Addition Theorems and Translational Addition Theorems for spheroidal vector wave functions are used to study the scattering by a system of two spheroids in arbitrary configuration and as a special case by a system of two spheroids in parallel configuration respectively. These theorems are used to transform the outgoing wave from one spheroid into the incoming wave at the other spheroid. The field solution determines the column vector of the unknown coefficients of the series expansions of the scattered and transmitted fields expressed in terms of the column vector of the known coefficients of the series expansions of the incident field and the system matrix which is independent of the direction and polarization of the incident wave. Numerical results in the form of plots for normalized bistatic and monostatic radar cross

sections are given for a variety of uniformly lossy dielectric prolate spheroids with resonant or near resonant lengths. Also for two-body scattering, different arbitrary configurations including parallel configurations of the spheroids at different distances of separation have been considered.

Acknowledgment

I would like to thank and express my gratitude to my supervisor Dr. B. P. Sinha for giving me an excellent opportunity to work under his supervision. His constant technical feedback and useful suggestions helped me immensely in my thesis work and have made my research really enjoyable.

I would also like to express my thanks to School of Graduate Studies and Dr. J. J. Sharp, Faculty of Engineering and Applied Science, Memorial University of Newfoundland for giving me financial support through out the period of my graduate studies.

Last but not the least, I am thankful to my friends Mr. Bibhas Bhattacharya and Mr. Tapas Banerjee for giving me valuable suggestions in the development of software pertaining to my thesis work.

Contents

Abstract	i
Acknowledgement	iii
1 Introduction	1
1.1 Literature Review	1
1.2 Organization of the Thesis	6
2 Prolate Spheroidal Coordinates and Prolate Spheroidal Wave Functions	9
2.1 Introduction	9
2.2 Prolate Spheroidal Coordinates	9
2.3 Vector Helmholtz Equations	13
2.4 Prolate Spheroidal Differential Equations	15
2.4.1 Prolate Angle Functions	17
2.4.2 Prolate Radial Functions	18
2.5 Prolate Spheroidal Vector Wave Functions	20
3 Electromagnetic Plane Wave Scattering by Single Uniformly Lossy Dielectric Prolate Spheroid	25
3.1 Introduction	25

3.2	Expansion of the Incident Electric Field in terms of Normalized Prolate Spheroidal Vector Wave Functions	27
3.3	Expansion of the Scattered Electric Field in terms of Normalized Prolate Spheroidal Vector Wave Functions	29
3.4	Expansion of the Transmitted Electric Field in terms of Normalized Prolate Spheroidal Vector Wave Functions	30
3.5	Expansion of H -field in terms of E -field	32
3.6	Expansion of the Incident Magnetic Field in terms of Normalized Prolate Spheroidal Vector Wave Functions	33
3.6.1	Limiting Case: $\gamma_p = 0$ and $\theta_i \rightarrow \pi/2$	34
3.7	Expansion of the Scattered Magnetic Field in terms of Normalized Prolate Spheroidal Vector Wave Functions	34
3.8	Expansion of the Transmitted Magnetic Field in terms of Normalized Prolate Spheroidal Vector Wave Functions	35
3.9	Applications of Boundary Conditions	35
3.9.1	ϕ -matching and η -matching	36
3.10	System Matrix $[G]$	37
3.11	Far-Field Expansions and Scattering Cross sections	38
3.12	Results of Numerical Computation	40
4	Electromagnetic Plane Wave Scattering by a System of Two Uniformly Lossy Dielectric Prolate Spheroids in Arbitrary Configuration	49
4.1	Introduction	49
4.2	Expansion of the Incident Electric Field in terms of Normalized Prolate Spheroidal Vector Wave Functions	50

4.3	Expansion of the Scattered Electric Field in terms of Normalized Prolate Spheroidal Vector Wave Functions	56
4.4	Expansion of the Transmitted Electric Field in terms of Normalized Prolate Spheroidal Vector Wave Functions	60
4.5	Expansion of Incident, Scattered and Transmitted Magnetic Fields in terms of Normalized Prolate Spheroidal Vector Wave Functions	62
4.6	Application of Boundary Conditions	63
4.7	System Matrix $[G]$	66
4.8	Far-Field Expansions and Scattering Cross sections	67
4.9	Results of Numerical Computation	71
5	Electromagnetic Plane Wave Scattering by a System of Two Parallel Uniformly Lossy Dielectric Prolate Spheroids	82
5.1	Introduction	82
5.2	Formulation of the Problem	84
5.3	Application of Boundary Conditions	87
5.4	Far-Field Expansions and Scattering Cross sections	89
5.5	Results of Numerical Computation	90
6	Conclusion	99
	Bibliography	101
A	Computation of Complex Eigen Values	107
B	Definition of Elements of $[G]$	120
C	Definition of $[\eta Q_m^{\pm(i)}], [\eta Q_{m+2}^{\pm(i)}], [\eta Q_{m+1}^{\pm(i)}], [\phi Q_m^{\pm(i)}], [\phi Q_{m+2}^{\pm(i)}], [\phi Q_{m+1}^{\pm(i)}]$	125

D	Definition of Integrals	130
E	Rotational-Translational Coefficients	138
E.1	The Euler Angles	138
E.2	Rotational-Translational Coefficients	139
E.3	Special Case: Translational Coefficients	143

List of Figures

2.1	Prolate Spheroidal Coordinate System.	11
2.2	Prolate spheroidal geometry and cartesian coordinates.	12
3.1	Scattering geometry for a single uniformly lossy dielectric prolate spheroid with arbitrary incidence and polarization of a plane electromagnetic wave.	26
3.2	Normalized bistatic cross section for TE polarization of incident wave, as a function of scattering angle for single uniformly lossy dielectric prolate spheroid with axial ratio 2 and 10, and of relative sizes $k_1 a = 1, 2, 3$ and 4 for complex relative permittivity $\epsilon_r = 2 - j0.5$	43
3.3	Normalized bistatic cross section for TE polarization of incident wave, as a function of scattering angle for single uniformly lossy dielectric prolate spheroid with axial ratio 2 and 10, and of relative sizes $k_1 a = 1, 2, 3$ and 4 for complex relative permittivity $\epsilon_r = 4 - j0.5$	44

3.4	Normalized bistatic cross section for <i>TE</i> polarization of incident wave, as a function of scattering angle for single uniformly lossy dielectric prolate spheroid with axial ratio 10, relative size $k_1 a = 2$ and with different values of complex relative permittivity: $\epsilon_r = 4 - j0$; $\epsilon_r = 4 - j0.2$; $\epsilon_r = 4 - j0.4$; $\epsilon_r = 4 - j0.6$; $\epsilon_r = 4 - j0.8$; $\epsilon_r = 4 - j1$; $\epsilon_r = 4 - j1.2$	45
3.5	Normalized monostatic cross section, as a function of aspect angle for single uniformly lossy dielectric prolate spheroid with axial ratio 2 and 10, and of relative sizes $k_1 a = 1, 2, 3$ and 4 for complex relative permittivity $\epsilon_r = 2 - j0.5$	46
3.6	Normalized monostatic cross section, as a function of aspect angle for single uniformly lossy dielectric prolate spheroid with axial ratio 2 and 10, and of relative sizes $k_1 a = 1, 2, 3$ and 4 for complex relative permittivity $\epsilon_r = 4 - j0.5$	47
3.7	Normalized monostatic cross section, as a function of aspect angle for single uniformly lossy dielectric prolate spheroid with axial ratio 10, relative size $k_1 a = 3$, and for different values of complex relative permittivity $\epsilon_r = 4 - j0$; $\epsilon_r = 4 - j0.4$; $\epsilon_r = 4 - j0.8$; $\epsilon_r = 4 - j1.2$	48
4.1	Scattering geometry for a system of two uniformly lossy dielectric prolate spheroids in general configuration with arbitrary incidence and polarization of a plane electromagnetic wave.	51

- 4.2 Normalized bistatic cross section for TE polarization of incident wave, as a function of scattering angle for two identical lossy dielectric prolate spheroids with axial ratios 2 and 10, each with semi-major axis length $a_A = a_B = \lambda/4$, complex relative permittivity $\epsilon_{rA} = \epsilon_{rB} = 2 - j0.5$, Euler angles $\alpha = 30^\circ, \beta = 45^\circ, \gamma = 60^\circ$, and displaced along z -axis ($\theta_0 = 0^\circ, \phi_0 = 0^\circ$) by: (a) $d = \lambda/2$, (b) $d = \lambda$ 75
- 4.3 Normalized bistatic cross section for TE polarization of incident wave, as a function of scattering angle for two identical lossy dielectric prolate spheroids with axial ratios 2 and 10, each with semi-major axis length $a_A = a_B = \lambda/4$, complex relative permittivity $\epsilon_{rA} = \epsilon_{rB} = 4 - j0.5$, Euler angles $\alpha = 30^\circ, \beta = 45^\circ, \gamma = 60^\circ$, and displaced along z -axis ($\theta_0 = 0^\circ, \phi_0 = 0^\circ$) by: (a) $d = \lambda/2$, (b) $d = \lambda$ 76
- 4.4 Normalized monostatic cross section as a function of aspect angle (θ_i) for two identical lossy dielectric prolate spheroids with axial ratios 2 and 10, each with semi-major axis length $a_A = a_B = \lambda/4$, complex relative permittivity $\epsilon_{rA} = \epsilon_{rB} = 2 - j0.5$, Euler angles $\alpha = 30^\circ, \beta = 45^\circ, \gamma = 60^\circ$, and displaced along z -axis ($\theta_0 = 0^\circ, \phi_0 = 0^\circ$) by: (a) $d = \lambda/2$, (b) $d = \lambda$ 77

- 4.5 Normalized monostatic cross section as a function of aspect angle (θ_i) for two identical lossy dielectric prolate spheroids with axial ratios 2 and 10, each with semi-major axis length $a_A = a_B = \lambda/4$, complex relative permittivity $\epsilon_{rA} = \epsilon_{rB} = 4 - j0.5$, Euler angles $\alpha = 30^\circ, \beta = 45^\circ, \gamma = 60^\circ$, and displaced along z -axis ($\theta_0 = 0^\circ, \phi_0 = 0^\circ$) by: (a) $d = \lambda/2$, (b) $d = \lambda$ 78
- 4.6 Normalized monostatic cross section as a function of aspect angle (θ_i) for two identical lossy dielectric prolate spheroids with axial ratios 2 and 10, each with semi-major axis length $a_A = a_B = \lambda/4$, Euler angles $\alpha = 30^\circ, \beta = 45^\circ, \gamma = 60^\circ$, and displaced along x -axis ($\theta_0 = 90^\circ, \phi_0 = 0^\circ$) by $d = \lambda/2$: (a) $\epsilon_{rA} = \epsilon_{rB} = 2 - j0.5$, (b) $\epsilon_{rA} = \epsilon_{rB} = 4 - j0.5$ 79
- 4.7 Normalized monostatic cross section as a function of aspect angle (θ_i) for two lossy dielectric prolate spheroids with axial ratios 2 and 10 respectively, each with semi-major axis length $a_A = a_B = \lambda/4$, Euler angles $\alpha = 30^\circ, \beta = 45^\circ, \gamma = 60^\circ$, and displaced along the direction $d = \lambda/2$, $\theta_0 = 60^\circ, \phi_0 = 20^\circ$: (a) $\epsilon_{rA} = 2 - j0.5, \epsilon_{rB} = 3 - j0.5$, (b) $\epsilon_{rA} = 3 - j0.5, \epsilon_{rB} = 4 - j0.5$, (c) $\epsilon_{rA} = 2 - j0.1, \epsilon_{rB} = 3 - j0.1$, (d) $\epsilon_{rA} = 3 - j0.1, \epsilon_{rB} = 4 - j0.1$ 80

- 4.8 Normalized monostatic cross section as a function of aspect angle (θ_s) for two lossy dielectric prolate spheroids with axial ratios 2 and 10 respectively, each with semi-major axis length $a_A = a_B = \lambda/4$ and complex relative permittivity $\epsilon_{rA} = 3 - j0.5$, $\epsilon_{rB} = 4 - j0.5$, and displaced along the direction $d = \lambda/2$, $\theta_0 = 60^\circ$, $\phi_0 = 20^\circ$; Euler angles are given by: (a) $\alpha = 0^\circ$, $\beta = 45^\circ$, $\gamma = 0^\circ$; (b) $\alpha = 30^\circ$, $\beta = 60^\circ$, $\gamma = 90^\circ$ 81
- 5.1 Scattering geometry for a system of two parallel uniformly lossy dielectric prolate spheroids with arbitrary incidence and polarization of a plane electromagnetic wave. 83
- 5.2 Normalized bistatic cross section $\pi\sigma(\theta)/\lambda^2$ for TE polarization of incident wave, as a function of scattering angle (θ) for two identical lossy dielectric prolate spheroids with axial ratios 2 and 10, each with semi-major axis length $a_A = a_B = \lambda/4$, complex relative permittivity $\epsilon_{rA} = \epsilon_{rB} = 2 - j0.5$, and displaced along z -axis $(\theta_0 = 0^\circ, \phi_0 = 0^\circ)$ by: (a) $d = \lambda/2$, (b) $d = \lambda$ 93
- 5.3 Normalized bistatic cross section $\pi\sigma(\theta)/\lambda^2$ for TE polarization of incident wave, as a function of scattering angle (θ) for two identical lossy dielectric prolate spheroids with axial ratios 2 and 10, each with semi-major axis length $a_A = a_B = \lambda/4$, complex relative permittivity $\epsilon_{rA} = \epsilon_{rB} = 4 - j0.5$, and displaced along z -axis $(\theta_0 = 0^\circ, \phi_0 = 0^\circ)$ by: (a) $d = \lambda/2$, (b) $d = \lambda$ 94

- 5.4 Normalized monostatic cross section $\pi\sigma(\theta_i, 0)/\lambda^2$ as a function of aspect angle (θ_i) for two identical lossy dielectric prolate spheroids with axial ratios 2 and 10, each with semi-major axis length $a_A = a_B = \lambda/4$, complex relative permittivity $\epsilon_{rA} = \epsilon_{rB} = 2 - j0.5$, and displaced along x -axis ($\theta_0 = 0^\circ, \phi_0 = 0^\circ$) by: (a) $d = \lambda/2$, (b) $d = \lambda$. 95
- 5.5 Normalized monostatic cross section $\pi\sigma(\theta_i, 0)/\lambda^2$ as a function of aspect angle (θ_i) for two identical lossy dielectric prolate spheroids with axial ratios 2 and 10, each with semi-major axis length $a_A = a_B = \lambda/4$, complex relative permittivity $\epsilon_{rA} = \epsilon_{rB} = 4 - j0.5$, and displaced along x -axis ($\theta_0 = 0^\circ, \phi_0 = 0^\circ$) by: (a) $d = \lambda/2$, (b) $d = \lambda$. 96
- 5.6 Normalized monostatic cross section as a function of aspect angle (θ_i) for two identical lossy dielectric prolate spheroids with axial ratios 2 and 10, each with semi-major axis length $a_A = a_B = \lambda/4$, and displaced along x -axis ($\theta_0 = 90^\circ, \phi_0 = 0^\circ$) by $d = \lambda/2$: (a) $\epsilon_{rA} = \epsilon_{rB} = 2 - j0.5$; (b) $\epsilon_{rA} = \epsilon_{rB} = 4 - j0.5$ 97
- 5.7 Normalized monostatic cross section as a function of aspect angle (θ_i) for two lossy dielectric prolate spheroids with axial ratios 2 and 10 respectively, each with semi-major axis length $a_A = a_B = \lambda/4$, and displaced along the direction $d = \lambda/2$, $\theta_0 = 60^\circ, \phi_0 = 20^\circ$: (a) $\epsilon_{rA} = 2 - j0.5, \epsilon_{rB} = 3 - j0.5$ (b) $\epsilon_{rA} = 2 - j0.1, \epsilon_{rB} = 3 - j0.1$ (c) $\epsilon_{rA} = 3 - j0.5, \epsilon_{rB} = 4 - j0.5$ (d) $\epsilon_{rA} = 3 - j0.1, \epsilon_{rB} = 4 - j0.1$. 98
- E.1 The Euler Angles. 139

Chapter 1

Introduction

1.1 Literature Review

The study of electromagnetic scattering by a system of two (or more) spheroidal objects has gained considerable interest in the last few decades. This is because the geometries of many objects of practical interest can be approximated by spheroids.

Solving scalar Helmholtz equation in spheroidal coordinates is the starting point in solving problems of electromagnetic scattering by spheroids. Flammer [1] and Stratton et al. [2] have studied extensively the spheroidal wave functions. Solution of scalar Helmholtz equation in terms of spheroidal coordinate system and expressions of spheroidal vector wave functions are available in details in [1] and [2].

The exact analytical solution to the electromagnetic scattering by conducting prolate spheroids for axial incidence has been given by Schultz [3]. Later Siegel et al. [4] obtained some numerical results for scattering by a thin prolate spheroid (axial ratio 10 : 1) by varying the relative size of the spheroid from 0.1 to 6.

The exact solution to the problem of electromagnetic scattering by a conducting prolate spheroid for arbitrary angle of incidence and polarization was given

by Reitlinger [5]. But his work involved complexity in numerical computation. Nevertheless, his work provided a foundation in finding analytical solutions to more complex problems involving scattering by spheroidal objects.

Because of the complexity of the spheroidal geometry, non-orthogonality of spheroidal wave functions and increasing difficulties in numerical computations beyond the Rayleigh region [6], no progress was made in the resonance region after the work of Siegel et al. [4], although extensive works have been carried out at both low frequencies and high frequencies. It was not until 1974 that Sinha obtained for the first time an exact analytical solution to the electromagnetic scattering by a conducting prolate spheroid in resonance region [6]. He also developed fast, accurate and simplified algorithms for computing spheroidal eigen values and spheroidal wave functions thereby overcoming the shortcomings in Reitlinger's work. Furthermore, he proved that results obtained by Siegel were accurate for values of axial ratio upto 2.5. Later Sinha and MacPhie presented numerical results of backscattering radar cross section at different values of axial ratio for a single conducting spheroid [7].

Dalmas and Deleuil also studied the electromagnetic scattering by a perfectly conducting spheroid by using \vec{M}^r and \vec{N}^r spheroidal vector wave functions [8]-[10]. Using these vector wave functions, Asano and Yamamoto presented the analytical solution of light scattering by a spheroidal particle at arbitrary incidence and polarization of incident wave [11].

Scattering of electromagnetic waves by arbitrarily shaped dielectric bodies lying in the resonance region has been studied by Barber and Yeh [12]. In [12] plots of differential scattering cross section vs. scattering angle are presented in azimuthal plane and equatorial plane for bodies like spheres, prolate spheroids,

oblate spheroids and cylinders having different geometries and dielectric constants. Asano and Sato [13] analyzed the problem of light scattering by randomly oriented identical dielectric spheroidal particles and computed extinction, scattering and absorption cross sections and asymmetry factor of prolate and oblate spheroids. Asano also investigated the light scattering properties of spheroidal particles oriented randomly with their long axes horizontal [14]. Later Cooray [15] worked on the scattering problem by a perfect dielectric prolate spheroid by employing modal series expansion of electromagnetic waves.

Extensive research is available in literature regarding scattering of electromagnetic wave by a system of two (or more) spherical and spheroidal objects. Bruning and Lo [16] studied extensively the scattering of electromagnetic wave by a system of two spheres by applying the translational addition theorem for spherical vector wave functions [17], which is an extension of the theorem for scalar wave functions developed by Stein [18].

It was not until the mid 1980s that Sinha and MacPhie [19] developed the translational addition theorems for scalar and vector spheroidal wave functions in which the outgoing wave from one spheroid is transformed into the incoming wave to the other spheroid assuming the simplest form for the vector wave functions, as they translate like a scalar wave function. Utilizing these theorems, Sinha and MacPhie obtained the exact solution for the scattering behavior of plane electromagnetic wave by two parallel conducting prolate spheroids [20]. In Appendix II of [20] the computation was simplified by obtaining the spheroidal translational addition coefficients in terms of the spherical translational addition coefficients. Dalmas and Deleuil also studied the multiple scattering of electromagnetic waves by two infinitely conducting prolate spheroids in [21] using Translational Addition

Theorems for prolate spheroidal vector wave functions \vec{M}^r and \vec{N}^r [22]. Lately, Cooray et al. [23] worked on the scattering problem by two perfect dielectric prolate spheroids in parallel orientation.

Further generalization of the two-spheroid scattering problem has been possible due to formulation of Rotational-Translational Addition Theorems for vector spheroidal wave functions in [24]-[26]. Utilizing these theorems, electromagnetic scattering by a system of two perfectly conducting and two lossless dielectric spheroids in arbitrary orientation were analytically studied by Cooray and Ciric in [27], [28] and [29].

By means of modal series expansions of electromagnetic fields in terms of prolate spheroidal vector wave functions, an exact analytical solution for more realistic situation of electromagnetic plane wave scattering by uniformly lossy dielectric prolate spheroids has been given in the present thesis. Scattering of plane electromagnetic wave by (i) a single uniformly lossy dielectric prolate spheroid, (ii) by a system of two uniformly lossy dielectric prolate spheroids in arbitrary configuration, and (iii) as a special case scattering by a system of two uniformly lossy dielectric prolate spheroids in parallel orientation, have been separately studied in resonance region. The parallel configuration of two or more prolate spheroids has practical importance. Hence it is felt that analytical study of this special case of the more general case of arbitrary orientation of the spheroids be developed separately by using translational addition theorems, so that those interested in this special case may not necessarily be involved in the complexity of the general formulation.

In this thesis, the analysis for single body is carried out by using $\vec{M}^{\alpha, \nu, \lambda}$ and $\vec{N}^{\alpha, \nu, \lambda}$ vector wave functions following the procedure employed by Sinha and

MacPhie [7] for conducting prolate spheroid. The scattering by a single lossy dielectric prolate spheroid has also been analyzed by Zimmer [30] who employed \vec{M}^r and \vec{N}^r vector wave functions.

In the present work the dielectric media of the scatterers are assumed to be uniformly (or homogeneous) lossy and non-ferromagnetic. Since the propagation constant of the media inside the scatterers is complex in nature, complex eigenvalues are evaluated for the spheroidal scalar wave functions of transmitted components of E -field and H -field expansions. Oguchi has calculated the eigen values of spheroidal wave functions for complex values of propagation constants in [31]. Zimmer also has computed complex eigen values for spheroidal wave functions assuming $e^{-j\omega t}$ time variation of time-harmonic electromagnetic field [30]. Subsequently Sebak and Sinha have calculated complex eigen values corresponding to prolate spheroidal functions in order to study the scattering by a conducting spheroidal object with lossy dielectric coating at axial incidence [32]. In the present work, the algorithm developed in [33] for real eigen value computation has been used to compute complex eigen values.

By applying appropriate boundary conditions, the field solution is obtained in the form $S = [G]I$, where S and I are respectively the column vector of the unknown coefficients of the series expansions of the scattered and transmitted fields taken together and the column vector of the known coefficients of the series expansions of the incident field. $[G]$ is the system matrix that depends only on the scattering system and the frequency of the incident radiation, and is independent of the direction and polarization of the incident wave. The solution in the above form eliminates the need for repeatedly solving a new set of simultaneous equations in order to obtain the expansion coefficients of scattered and

transmitted fields for a new angle of incidence.

It is worthwhile to note that the oblate spheroidal vector wave functions can be obtained from the prolate ones by the transformations $\xi \rightarrow j\xi$ and $h \rightarrow -jh$, where ξ is the spheroidal radial coordinate; $h = kF$, F being semi-interfocal distance of the spheroid and k being the propagation constant of the medium [1].

1.2 Organization of the Thesis

This thesis deals with the exact analytical solution of scattering by uniformly lossy dielectric prolate spheroids — the incident excitation being unit amplitude monochromatic plane electromagnetic wave of arbitrary incidence and polarization and having wavelength λ . Electromagnetic scattering by a single uniformly lossy dielectric prolate spheroid, by a system of two uniformly lossy dielectric prolate spheroids in arbitrary configuration, and by a system of two uniformly lossy dielectric prolate spheroids in parallel orientation have been considered separately. In Section 1.1 we have discussed the available research in literature pertaining to electromagnetic scattering by spheroidal objects and have given the general outline of the problem presented in this thesis. The organization of other chapters is as follows:

- In Chapter 2, a brief idea of spheroidal coordinate system is presented first. Then solution of scalar wave equation in spheroidal coordinates and expressions of various spheroidal wave functions are considered. Finally, prolate spheroidal vector wave functions are discussed.
- Chapter 3 deals with the analytical solution of scattering of plane electromagnetic wave by single uniformly lossy dielectric prolate spheroid. Inci-

dent, scattered and transmitted components of electric and magnetic fields are expressed in terms of normalized prolate spheroidal vector wave functions. Appropriate boundary conditions are then applied on the surface of the spheroid to solve a set of simultaneous linear algebraic equations relating the unknown expansion coefficients corresponding to scattered and transmitted fields expressed in terms of known expansion coefficients of the incident field. Finally the scattered field is calculated in the far zone and numerical results are presented in the form of curves of normalized bistatic and monostatic radar cross sections for a variety of uniformly lossy dielectric prolate spheroids.

- In Chapter 4, the exact solution for the problem of electromagnetic scattering by two uniformly lossy dielectric prolate spheroids in arbitrary orientation has been discussed. Rotational-Translational Addition Theorems for spheroidal vector wave functions have been used here — a vector spheroidal wave function defined in one spheroidal coordinate system (ξ, η, ϕ) has been expressed in terms of a series expansion of vector spheroidal wave functions defined in another spheroidal coordinate system (ξ', η', ϕ') , which is rotated and translated with respect to the first one. Applications of appropriate boundary conditions and derivation of the system equation have been discussed then. Finally numerical results in the form of curves for normalized bistatic and monostatic radar cross sections are given for a variety of two-body system of uniformly lossy dielectric prolate spheroids in arbitrary orientation having resonant or near resonant lengths and different distances of separation.

- In Chapter 5 we present an exact solution for electromagnetic scattering by two uniformly lossy dielectric prolate spheroids in parallel orientation. The Translational Addition Theorems, which transform the outgoing wave from one spheroid into the incoming wave at the other spheroid, have been used here. Incidentally translational addition theorems [19] can be considered as a special case of rotational-translational addition theorems when Euler angles $\alpha \rightarrow 0^\circ$, $\beta \rightarrow 0^\circ$ and $\gamma \rightarrow 0^\circ$. Applications of appropriate boundary conditions and derivation of the system equation have been discussed. Numerical results in the form of curves for normalized bistatic and monostatic radar cross sections have been obtained in the resonance region for a variety of two-body system of uniformly lossy dielectric prolate spheroids in parallel orientation having different distances of separation.
- Finally in Chapter 6 concluding remarks are presented.

Chapter 2

Prolate Spheroidal Coordinates and Prolate Spheroidal Wave Functions

2.1 Introduction

In this chapter we give a brief overview of prolate spheroidal coordinate system followed by derivation of vector Helmholtz equations for \vec{E} -field and \vec{H} -field of an electromagnetic wave. We then discuss the solution of scalar wave equations in spheroidal coordinates. Finally we obtain solutions of vector wave equation by applying certain vector differential operators to the scalar wave functions. The resulting solutions are called vector wave functions.

2.2 Prolate Spheroidal Coordinates

There are two types of spheroidal coordinate system: *prolate* and *oblate*. The prolate and oblate spheroidal coordinate system are formed by rotating the two-dimensional elliptic coordinate system, consisting of confocal ellipses and hyperbolas, about the major and minor axes of the ellipses, respectively. It is customary to make the z -axis the axis of revolution in each case [1].

Since in this thesis we are considering the scattering problem from prolate spheroids, we concentrate on the description of prolate spheroidal coordinate system; however description of oblate spheroidal coordinate system can be found in pp. 6 - 7, [1]. Fig. 2.1 shows the prolate spheroidal coordinate system.

Let the semi-interfocal distances of the confocal ellipses be denoted by F , as shown in Fig. 2.2. Then for a single ellipse the spheroidal coordinates, denoted by (ξ, η, ϕ) of a point P in space distant r_1 and r_2 respectively from the foci F_1 and F_2 , are given by :

$$\left. \begin{aligned} \xi &= (r_1 + r_2)/(2F) \\ \eta &= (r_1 - r_2)/(2F) \\ \phi &= \phi \end{aligned} \right\} \quad (2.1)$$

where ξ is radial coordinate, η is angular coordinate and ϕ is azimuthal coordinate. It can be shown that prolate spheroidal coordinates (ξ, η, ϕ) are given in terms of rectangular coordinates by the following relations pp. 17-18, [6]:

$$\xi = \frac{1}{2F} \left[(x^2 + y^2 + (z + F)^2)^{1/2} + (x^2 + y^2 + (z - F)^2)^{1/2} \right] \quad (2.2)$$

$$\eta = \frac{1}{2F} \left[(x^2 + y^2 + (z + F)^2)^{1/2} - (x^2 + y^2 + (z - F)^2)^{1/2} \right] \quad (2.3)$$

$$\phi = \tan^{-1}(y/x) \quad (2.4)$$

By inverse transformation we can also obtain:

$$x = F(1 - \eta^2)^{1/2}(\xi^2 - 1)^{1/2} \cos \phi \quad (2.5)$$

$$y = F(1 - \eta^2)^{1/2}(\xi^2 - 1)^{1/2} \sin \phi \quad (2.6)$$

$$z = F\xi\eta \quad (2.7)$$

with $-1 \leq \eta \leq 1$, $1 \leq \xi \leq \infty$, $0 \leq \phi \leq 2\pi$.

In prolate spheroidal system the surface $\xi = \text{constant} > 1$ is an elongated ellipsoid of revolution with major axis of length $2F\xi$ and minor axis of length

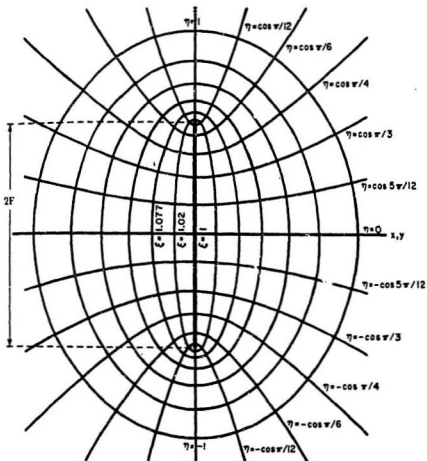


Figure 2.1: Prolate Spheroidal Coordinate System.

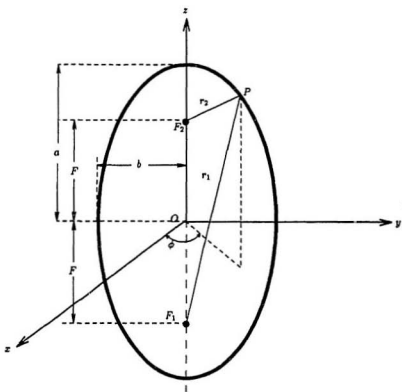


Figure 2.2: Prolate spheroidal geometry and cartesian coordinates.

$2F(\xi - 1)^{1/2}$. The degenerate surface $\xi = 1$ is a straight line along the z -axis from $z = -F$ to $z = +F$. The surface $|\eta| = \text{constant} < 1$ is a hyperboloid of revolution of two sheets with an asymptotic cone whose generating line passes through the origin and is inclined at an angle $\theta = \cos^{-1} \eta$ to the z -axis. The degenerate surface $|\eta| = 1$ is that part of the z -axis for which $|z| > F$. The surface $\phi = \text{constant}$ is a plane through the z -axis forming the angle ϕ with the $x - z$ plane [1].

It is to be noted that the confocal quadric surfaces in space intersect each other at right angles, i.e. the tangent planes of the three surfaces passing through any given point in space are mutually perpendicular. Thus prolate spheroidal coordinate system is a system of orthogonal curvilinear coordinates. In each case the coordinates (ξ, η, ϕ) form a left-handed system, since $\hat{\xi} \times \hat{\eta} = -\hat{\phi}$; $\hat{\eta} \times \hat{\phi} = -\hat{\xi}$; $\hat{\phi} \times \hat{\xi} = -\hat{\eta}$.

In the limit when the interfocal distance $2F$ becomes zero, both the prolate and oblate spheroidal systems reduce to the spherical coordinate system. For finite $2F$, the surface $\xi = \text{constant}$ in each case becomes spherical as ξ approaches to infinity; thus

$$F\xi \rightarrow r, \quad \eta \rightarrow \cos \theta, \quad \text{as } \xi \rightarrow \infty \quad (2.8)$$

where r and θ are spherical radial and angular coordinates respectively.

2.3 Vector Helmholtz Equations

We know that a time-harmonic electromagnetic field ($e^{j\omega t}$ time variation, ω being angular frequency) satisfies Maxwell's equations:

$$\nabla \times \vec{E} = -j\omega\mu\vec{H} \quad (2.9)$$

$$\nabla \times \vec{H} = j\omega\epsilon\vec{E} + \vec{J} = j\omega\epsilon'\vec{E} \quad (2.10)$$

where

$$\epsilon' = \epsilon - j\sigma/\omega \quad (2.11)$$

is called *complex permittivity* of the medium; ϵ , μ and σ are the permittivity, permeability and conductivity of the medium respectively. \vec{J} is volume distribution of electric current per unit area.

Let λ_0 be wavelength of the electromagnetic wave in free space; ϵ_0 and μ_0 be the permittivity and permeability of free space respectively, and c be velocity of propagation of wave in free space. Then propagation constant of free space is given by

$$k_0 = 2\pi/\lambda_0 = \omega/c = \omega(\mu_0\epsilon_0)^{1/2} \quad (2.12)$$

Substituting ω from (2.12) in (2.9) and (2.10) we get

$$\nabla \times \vec{E} = -j \frac{\mu}{(\mu_0\epsilon_0)^{1/2}} k_0 \vec{H} \quad (2.13)$$

$$\nabla \times \vec{H} = j \frac{\epsilon'}{(\mu_0\epsilon_0)^{1/2}} k_0 \vec{E} \quad (2.14)$$

Taking curl on both sides of (2.13) we get

$$\nabla \nabla \cdot \vec{E} - \nabla^2 \vec{E} = \left(\frac{\mu\epsilon'}{\mu_0\epsilon_0} \right) k_0^2 \vec{E} \quad (2.15)$$

For charge free space

$$\nabla \cdot \vec{E} = 0 \quad (2.16)$$

From (2.15) and (2.16) we have

$$\nabla^2 \vec{E} + \left(\frac{\mu\epsilon'}{\mu_0\epsilon_0} \right) k_0^2 \vec{E} = 0 \quad (2.17)$$

Taking curl on both sides of (2.14) we get

$$\nabla \nabla \cdot \vec{H} - \nabla^2 \vec{H} = \left(\frac{\mu \epsilon'}{\mu_0 \epsilon_0} \right) k_0^2 \vec{H} \quad (2.18)$$

From Maxwell's equation

$$\nabla \cdot \vec{H} = 0 \quad (2.19)$$

From (2.18) and (2.19) we have

$$\nabla^2 \vec{H} + \left(\frac{\mu \epsilon'}{\mu_0 \epsilon_0} \right) k_0^2 \vec{H} = 0 \quad (2.20)$$

Setting

$$k = \left(\frac{\mu \epsilon'}{\mu_0 \epsilon_0} \right)^{1/2} k_0 = n_r k_0 \quad (2.21)$$

where $n_r = \sqrt{\mu \epsilon' / \mu_0 \epsilon_0}$ is the complex refractive index of the medium, vector Helmholtz equations for \vec{E} and \vec{H} fields of electromagnetic wave can be given as

$$\nabla^2 \vec{E} + k^2 \vec{E} = 0 \quad (2.22)$$

$$\nabla^2 \vec{H} + k^2 \vec{H} = 0 \quad (2.23)$$

2.4 Prolate Spheroidal Differential Equations

Prolate spheroidal coordinate system is one of the eleven coordinate systems¹ in which the scalar wave equation

$$(\nabla^2 + k^2) \psi = 0 \quad (2.24)$$

is separable, where k is the medium wave number. This equation, in prolate spheroidal coordinate system, can be written as

$$\left[\frac{\partial}{\partial \eta} (1 - \eta^2) \frac{\partial}{\partial \eta} + \frac{\partial}{\partial \xi} (1 - \xi^2) \frac{\partial}{\partial \xi} + \frac{\xi^2 - \eta^2}{(\xi^2 - 1)(1 - \eta^2)} \frac{\partial^2}{\partial \phi^2} + k^2 (\xi^2 - \eta^2) \right] \psi = 0 \quad (2.25)$$

¹cartesian, circular cylinder, elliptic cylinder, parabolic cylinder, spherical, conical, parabolic, prolate spheroidal, oblate spheroidal, ellipsoidal and paraboloidal.

where we set $h = kF$.

Using the separation of variables principle, the solution of (2.25) can be obtained in the form [1]

$$\psi_{mn}^{(i)} = S_{mn}(h, \eta) R_{mn}^{(i)}(h, \xi) \frac{\cos m\phi}{\sin m\phi}, \quad i = 1, 2, 3, 4 \quad (2.26)$$

where $R_{mn}^{(i)}(h, \xi)$ and $S_{mn}(h, \eta)$ are called *prolate radial function* and *prolate angle function* respectively. $R_{mn}^{(i)}(h, \xi)$ and $S_{mn}(h, \eta)$ satisfy the ordinary differential equations

$$\frac{d}{d\eta} \left[(1 - \eta^2) \frac{d}{d\eta} S_{mn}(h, \eta) \right] + \left[\lambda_{mn} - h^2 \eta^2 - \frac{m^2}{1 - \eta^2} \right] S_{mn}(h, \eta) = 0 \quad (2.27)$$

$$\frac{d}{d\xi} \left[(\xi^2 - 1) \frac{d}{d\xi} R_{mn}^{(i)}(h, \xi) \right] - \left[\lambda_{mn} - h^2 \xi^2 + \frac{m^2}{\xi^2 - 1} \right] R_{mn}^{(i)}(h, \xi) = 0 \quad (2.28)$$

where $\lambda_{mn}(h)$ and m are separation constants. Those values of $\lambda_{mn}(h)$ for which (2.27) admits solutions that are finite at $\eta = \pm 1$ are the eigenvalues of the differential equation (2.27). Here $n = |m|, |m| + 1, |m| + 2, \dots$, and m is any integer including zero.

h is real or complex accordingly the propagation constant of the medium under consideration is real or complex. Computations of eigenvalues of spheroidal wave functions for *real* values of propagation constants and for *complex* values of propagation constants are respectively shown in [33] and Appendix A of the present thesis.

It is worthwhile to note that the oblate spheroidal scalar wave function can be obtained from the prolate one by utilizing the transformations $\xi \rightarrow j\xi$ and $h \rightarrow -jh$ in (2.26).

2.4.1 Prolate Angle Functions

The associated eigenfunctions $S_{mn}(h, \eta)$ are the prolate spheroidal angle functions of first kind, of order m and degree n , corresponding to eigenvalues $\lambda_{mn}(h)$ in (2.27). There are two types of angle functions: $S_{mn}^{(1)}(h, \eta)$ — angle function of first kind, and $S_{mn}^{(2)}(h, \eta)$ — angle function of second kind. In most boundary-value problems, the physical quantities are defined over the entire domain $-1 \leq \eta \leq 1$, $0 \leq \phi \leq 2\pi$. The usual requirement that the wave function be finite at $\eta = \pm 1$ confines the η -dependence of the wave function to that of the angle function of first kind, because the angle function of second kind, $S_{mn}^{(2)}(h, \eta)$ are singular at these points. Henceforth we will use the notation $S_{mn}(h, \eta)$ to refer to angle function of first kind.

When h goes to zero, angle function of first kind reduces to associated Legendre functions of the first kind of integral order and degree. So we have

$$\lambda_{mn}(0) = n(n+1), \quad n \geq m \quad (2.29)$$

When h is not equal to zero, angle function of first kind is of the form

$$S_{mn}(h, \eta) = \sum_{r=0,1}^{\infty} ' d_r^{mn}(h) P_{m+r}^{m+r}(\eta) \quad (2.30)$$

where $d_r^{mn}(h)$ are prolate spheroidal expansion coefficients. The prime on the summation symbol indicates that the summation is over only even values of r when $(n-m)$ is even and over only odd values of r when $(n-m)$ is odd. $P_{m+r}^{m+r}(\eta)$ is associated Legendre function of first kind. The expansion coefficients $d_r^{mn}(h)$ are given by the recurrence formula in equation (3.1.4) of [1]. Examination of equation (3.1.4) in [1] reveals that as $r \rightarrow \infty$, either $d_r^{mn}(h)/d_{r-2}^{mn}(h)$ increases as $-4r^2/h^2$, or goes to zero as $-h^2/(4r^2)$. We choose the latter as it leads to a convergent series. Numerical computation of angle function is given in [6].

From general theory of Sturm-Liouville differential equations, it follows $S_{mn}(h, \eta)$ form an orthogonal set in the interval $(-1, 1)$ [1]:

$$\int_{-1}^1 S_{mn}(h, \eta) S_{m'n'}(h, \eta) d\eta = \delta_{nn'} N_{mn}(h) \quad (2.31)$$

where $\delta_{nn'}$ is Kronecker delta function and

$$N_{mn}(h) = 2 \sum_{r=0,1}^{\infty} \frac{(r+2m)!(a_r^{mn}(h))^2}{(2r+2m+1)r!} \quad (2.32)$$

is the normalization factor.

2.4.2 Prolate Radial Functions

Prolate spheroidal radial functions $R_{mn}^{(i)}(h, \xi)$ ($i = 1, 2, 3, 4$) satisfy the differential equation (2.28), where $1 \leq \xi \leq \infty$. The eigenvalues $\lambda_{mn}(h)$ which occur in (2.28) are those to which angle functions $S_{mn}(h, \eta)$ belong.

In physical problems one usually requires both the radial functions of the first kind, $R_{mn}^{(1)}(h, \xi)$, and those of the second kind, $R_{mn}^{(2)}(h, \xi)$. Two useful combinations of these functions are known as radial functions of the third kind and radial functions fourth kinds, given by $R_{mn}^{(3)}(h, \xi)$ and $R_{mn}^{(4)}(h, \xi)$ respectively.

The radial functions of the first kind $R_{mn}^{(1)}(h, \xi)$ and radial functions of second kind $R_{mn}^{(2)}(h, \xi)$ are respectively given by the series [2]:

$$R_{mn}^{(1)}(h, \xi) = \left(\frac{\xi^2 - 1}{\xi^2} \right)^{m/2} \sum_{r=0,1}^{\infty} a_r^{mn}(h) j_{m+r}(h\xi) \quad (2.33)$$

$$R_{mn}^{(2)}(h, \xi) = \left(\frac{\xi^2 - 1}{\xi^2} \right)^{m/2} \sum_{r=0,1}^{\infty} a_r^{mn}(h) n_{m+r}(h\xi) \quad (2.34)$$

where $j_{m+r}(h\xi)$ and $n_{m+r}(h\xi)$ are spherical Bessel function and Neumann function respectively, and $a_r^{mn}(h)$ are convergent expansion coefficients such that as $r \rightarrow \infty$ $a_r^{mn}(h)/a_{r-2}^{mn}(h) \rightarrow h^2/(4r^2) \rightarrow 0$. The expansion coefficients $a_r^{mn}(h)$ are given by the recurrence relation in equation (3.24) of [6].

The radial function of third kind and radial function of fourth kind are respectively given as:

$$R_{mn}^{(3)}(h, \xi) = R_{mn}^{(1)}(h, \xi) + jR_{mn}^{(2)}(h, \xi) \quad (2.35)$$

$$R_{mn}^{(4)}(h, \xi) = R_{mn}^{(1)}(h, \xi) - jR_{mn}^{(2)}(h, \xi) \quad (2.36)$$

The following asymptotic properties of the spherical Bessel, Neumann, and Hankel functions are worth noting, p. 31, [1]:

$$\left. \begin{aligned} j_n(h\xi) &= \sqrt{\frac{\pi}{2h\xi}} J_{n+\frac{1}{2}}(h\xi) \xrightarrow{h\xi \rightarrow \infty} \frac{1}{h\xi} \cos\left(h\xi - \frac{1}{2}(n+1)\pi\right) \\ n_n(h\xi) &= \left(-1\right)^{n+1} j_{-(n+1)}(h\xi) \\ &= \sqrt{\frac{\pi}{2h\xi}} N_{n+\frac{1}{2}}(h\xi) \xrightarrow{h\xi \rightarrow \infty} \frac{1}{h\xi} \sin\left(h\xi - \frac{1}{2}(n+1)\pi\right) \\ h_n^{(1)}(h\xi) &= j_n(h\xi) + jn_n(h\xi) \xrightarrow{h\xi \rightarrow \infty} \frac{1}{h\xi} e^{[h\xi - \frac{1}{2}(n+1)\pi]} \\ h_n^{(2)}(h\xi) &= j_n(h\xi) - jn_n(h\xi) \xrightarrow{h\xi \rightarrow \infty} \frac{1}{h\xi} e^{-[h\xi - \frac{1}{2}(n+1)\pi]} \end{aligned} \right\} \quad (2.37)$$

Thus the asymptotic behavior of $R_{mn}^{(1)}(h, \xi)$, $R_{mn}^{(2)}(h, \xi)$, $R_{mn}^{(3)}(h, \xi)$ and $R_{mn}^{(4)}(h, \xi)$ is readily obtained as

$$R_{mn}^{(1)}(h, \xi) \xrightarrow{h\xi \rightarrow \infty} \frac{1}{h\xi} \cos\left(h\xi - \frac{1}{2}(n+1)\pi\right) \quad (2.38)$$

$$R_{mn}^{(2)}(h, \xi) \xrightarrow{h\xi \rightarrow \infty} \frac{1}{h\xi} \sin\left(h\xi - \frac{1}{2}(n+1)\pi\right) \quad (2.39)$$

$$R_{mn}^{(3)}(h, \xi) \xrightarrow{h\xi \rightarrow \infty} \frac{1}{h\xi} e^{[h\xi - \frac{1}{2}(n+1)\pi]} \quad (2.40)$$

$$R_{mn}^{(4)}(h, \xi) \xrightarrow{h\xi \rightarrow \infty} \frac{1}{h\xi} e^{-[h\xi - \frac{1}{2}(n+1)\pi]} \quad (2.41)$$

At very large distance from the spheroid $R_{mn}^{(3)}(h, \xi)$ and $R_{mn}^{(4)}(h, \xi)$ have the properties of diverging spherical waves. As $R_{mn}^{(4)}(h, \xi)$ has the property of outgoing spherical wave for $h\xi \rightarrow \infty$, it will be used to describe the scattered fields of electromagnetic wave. Series representation of $R_{mn}^{(1)}(h, \xi)$ shows fast convergence, whereas series for $R_{mn}^{(2)}(h, \xi)$ does not converge rapidly for small value of $h\xi$ or

$h\xi \approx 1$. An integral method introduced by Sinha and MacPhie in [34] improves the convergence of $R_{mn}^{(2)}(h, \xi)$.

2.5 Prolate Spheroidal Vector Wave Functions

Before defining prolate spheroidal vector wave functions let us discuss in brief the fundamental set of solutions of any vector wave equation, pp. 392 – 393, [37].

Within any closed domain of a homogeneous, isotropic medium from which sources have been excluded, all vectors characterizing the electromagnetic field — the field vectors \vec{E} , \vec{B} , \vec{D} and \vec{H} , the vector potential and the Hertzian vectors — satisfy one and the same differential equation. If \vec{C} denotes any such vector, then

$$\nabla^2 \vec{C} + k^2 \vec{C} = 0 \quad (2.42)$$

where $k^2 = \epsilon\mu\omega^2 - j\sigma\mu\omega$ ($e^{j\omega t}$ time variation of \vec{C} is assumed).

By the operator ∇^2 acting on a vector we mean $\nabla^2 = \nabla \nabla \cdot - \nabla \times \nabla \times$; therefore in place of (2.42) we can write

$$\nabla \nabla \cdot \vec{C} - \nabla \times \nabla \times \vec{C} + k^2 \vec{C} = 0 \quad (2.43)$$

Now the vector equation in (2.43) can always be replaced by a simultaneous system of three scalar equations, but the solution of this system for any component of \vec{C} is impractical in most cases. It is only when \vec{C} is resolved into its rectangular components that three independent equations are obtained. Thus, in this case

$$\nabla^2 C_j + k^2 C_j = 0, \quad j = x, y, z \quad (2.44)$$

Let the scalar function ψ be a solution of the equation

$$\nabla^2 \psi + k^2 \psi = 0 \quad (2.45)$$

and let \hat{a} be any constant vector of unit length. We now can construct three independent vector solutions of (2.43) as follows:

$$\left. \begin{aligned} \vec{L} &= \nabla\psi \\ \vec{M} &= \nabla \times \hat{a}\psi \\ \vec{N} &= (1/k)\nabla \times \vec{M} \end{aligned} \right\} \quad (2.46)$$

If \vec{C} is placed equal to \vec{L} , \vec{M} or \vec{N} we can verify that (2.43) is satisfied identically by (2.46) subject to (2.45). Since \hat{a} is a constant vector \vec{M} can also be written as

$$\vec{M} = \vec{L} \times \hat{a} = (1/k)\nabla \times \vec{N} \quad (2.47)$$

For one and the same generating function ψ the vector \vec{M} is perpendicular to the vector \vec{L} , or

$$\vec{L} \cdot \vec{M} = 0 \quad (2.48)$$

The vector functions \vec{L} , \vec{M} and \vec{N} have the following properties:

$$\nabla \times \vec{L} = 0, \quad \nabla \cdot \vec{L} = \nabla^2\psi = -k^2\psi \quad (2.49)$$

Also \vec{M} and \vec{N} are solenoidal, i.e.

$$\nabla \cdot \vec{M} = 0, \quad \nabla \cdot \vec{N} = 0 \quad (2.50)$$

Let us now define the spheroidal vector wave functions. The scalar function satisfying the scalar Helmholtz equation expressed in terms of spheroidal coordinates has the form given in (2.26):

$$\psi_{mn}^{(i)}(\xi, \eta, \phi) = S_{mn}(h, \eta) R_{mn}^{(i)}(h, \xi) \begin{matrix} \cos \\ \sin \end{matrix} m\phi \quad (2.51)$$

where the superscripts ϵ and o refer to even ϕ -dependency and odd ϕ -dependency respectively and $i = 1, 2, 3, 4$.

The spheroidal vector wave functions can be defined as [1]:

$$\vec{M}_{mn}^{za(i)}(h; \xi, \eta, \phi) = \nabla \psi_{mn}^{za(i)}(h; \xi, \eta, \phi) \times \hat{a} \quad (2.52)$$

$$\vec{N}_{mn}^{za(i)}(h; \xi, \eta, \phi) = k^{-1} \nabla \times \vec{M}_{mn}^{za(i)}(h; \xi, \eta, \phi) \quad (2.53)$$

where \hat{a} is arbitrary unit constant vector or radius (position) vector. In spheroidal coordinate system, none of the unit vectors $\hat{\xi}$, $\hat{\eta}$, $\hat{\phi}$ has the properties required for \hat{a} . Hence we choose cartesian coordinate system in which each of the unit vectors \hat{x} , \hat{y} , \hat{z} is a constant unit vector, The unit vectors in cartesian coordinates are related to the spheroidal coordinate unit vectors by the relations [1]:

$$\left. \begin{aligned} \hat{x} &= -\eta \left(\frac{\xi^2 - 1}{\xi^2 - \eta^2} \right)^{1/2} \cos \phi \hat{\eta} + \xi \left(\frac{1 - \eta^2}{\xi^2 - \eta^2} \right)^{1/2} \cos \phi \hat{\xi} - \sin \phi \hat{\phi} \\ \hat{y} &= -\eta \left(\frac{\xi^2 - 1}{\xi^2 - \eta^2} \right)^{1/2} \sin \phi \hat{\eta} + \xi \left(\frac{1 - \eta^2}{\xi^2 - \eta^2} \right)^{1/2} \sin \phi \hat{\xi} + \cos \phi \hat{\phi} \\ \hat{z} &= \xi \left(\frac{1 - \eta^2}{\xi^2 - \eta^2} \right)^{1/2} \hat{\eta} + \eta \left(\frac{\xi^2 - 1}{\xi^2 - \eta^2} \right)^{1/2} \hat{\xi} \end{aligned} \right\} \quad (2.54)$$

Thus the cartesian unit vectors in (2.54) generate three distinct classes of prolate spheroidal vector wave functions \vec{M} and \vec{N} , given by:

$$\vec{M}_{mn}^{za(i)}(h; \xi, \eta, \phi) = \nabla \psi_{mn}^{za(i)}(h; \xi, \eta, \phi) \times \hat{a}, \quad a = x, y, z \quad (2.55)$$

$$\vec{N}_{mn}^{za(i)}(h; \xi, \eta, \phi) = k^{-1} \nabla \times \vec{M}_{mn}^{za(i)}(h; \xi, \eta, \phi), \quad a = x, y, z \quad (2.56)$$

Also with regard to the position vector \vec{r} , the \vec{M} and \vec{N} vectors are expressed as

$$\vec{M}_{mn}^{za(i)}(h; \xi, \eta, \phi) = \nabla \psi_{mn}^{za(i)}(h; \xi, \eta, \phi) \times \vec{r} \quad (2.57)$$

$$\vec{N}_{mn}^{za(i)}(h; \xi, \eta, \phi) = k^{-1} \nabla \times \vec{M}_{mn}^{za(i)}(h; \xi, \eta, \phi) \quad (2.58)$$

In this thesis the analysis for single body is carried out by using $\vec{M}^{x,y,z}$ and $\vec{N}^{x,y,z}$ vectors following the procedure employed by Sinha and MacPhie for conducting prolate spheroid [7]. ²

²Zimmer employed \vec{M}^* and \vec{N}^* vectors to analyze the scattering problem by a single lossy dielectric prolate spheroid [30].

In the functions $\vec{M}_{mn}^{z\pm(i)}$, $\vec{M}_{mn}^{z\pm(i)}$, $\vec{N}_{mn}^{z\pm(i)}$ and $\vec{N}_{mn}^{z\pm(i)}$ the ϕ -dependence of the various components is equal to the product of either $\cos \phi$ or $\sin \phi$ with $\cos m\phi$ or $\sin m\phi$. Therefore it is convenient to define the following additional spheroidal vector wave functions, (where the components of those labeled with the index $m+1$ have either a $\cos(m+1)\phi$ or $\sin(m+1)\phi$ ϕ -dependence, while the components of those labeled with $m-1$ have either a $\cos(m-1)\phi$ or $\sin(m-1)\phi$ one) p. 70 [1]:

$$\vec{M}_{m+1,n}^{z+(i)}(h; \xi, \eta, \phi) = \frac{1}{2} \left[\vec{M}_{mn}^{z\pm(i)}(h; \xi, \eta, \phi) \mp \frac{1}{2} \vec{M}_{mn}^{z\pm(i)}(h; \xi, \eta, \phi) \right] \quad (2.59)$$

$$\vec{M}_{m-1,n}^{z-(i)}(h; \xi, \eta, \phi) = \frac{1}{2} \left[\vec{M}_{mn}^{z\pm(i)}(h; \xi, \eta, \phi) \pm \frac{1}{2} \vec{M}_{mn}^{z\pm(i)}(h; \xi, \eta, \phi) \right] \quad (2.60)$$

$$\vec{N}_{m+1,n}^{z+(i)}(h; \xi, \eta, \phi) = k^{-1} \nabla \times \vec{M}_{m+1,n}^{z+(i)}(h; \xi, \eta, \phi) \quad (2.61)$$

$$\vec{N}_{m-1,n}^{z-(i)}(h; \xi, \eta, \phi) = k^{-1} \nabla \times \vec{M}_{m-1,n}^{z-(i)}(h; \xi, \eta, \phi) \quad (2.62)$$

Explicit expressions of the vector wave functions defined above are given in Table V, pp. 74 - 78, [1].

According to Sinha and MacPhie [20], it is possible to express the sinusoidal variation of ϕ in equation (2.51) as complex exponential variation. Also for any integer $n > 0$ since $-n \leq m \leq n$, it is possible to normalize spheroidal vector wave functions \vec{M} and \vec{N} in terms of $|m|$. Normalization of spheroidal vector wave functions and their representations in exponential form are explicitly given in [20] and Appendix A of [15]. Orthogonality property of complex exponential, given below, will be used later:

$$\int_0^{2\pi} e^{jm\phi} e^{-jm'\phi} d\phi = 2\pi \delta_{mm'} \quad (2.63)$$

where $\delta_{mm'}$ is Kronecker delta function.

It is worthwhile to note here that notations for \vec{M} and \vec{N} followed through this thesis are the ones used by Sinha and MacPhie [20]. Flammer's $\vec{M}_{m+1,n}^{z+(i)}$ and

$\vec{N}_{m+1,n}^{+(i)}$ become $\vec{M}_{mn}^{+(i)}$ and $\vec{N}_{mn}^{+(i)}$ in [20] respectively, and Flammer's $\vec{M}_{m-1,n}^{-(i)}$ and $\vec{N}_{m-1,n}^{-(i)}$ become $\vec{M}_{mn}^{-(i)}$ and $\vec{N}_{mn}^{-(i)}$ in [20] respectively so that $\vec{M}_{mn}^{\pm(i)}$ and $\vec{N}_{mn}^{\pm(i)}$ have $(m \pm 1)\phi$ ϕ -dependence. However Flammer's $\vec{M}_{mn}^{+(i)}$ and $\vec{N}_{mn}^{+(i)}$ remain same as that in [20] having $m\phi$ ϕ -dependence.

Chapter 3

Electromagnetic Plane Wave Scattering by Single Uniformly Lossy Dielectric Prolate Spheroid

3.1 Introduction

In this chapter we study scattering of plane electromagnetic wave by single uniformly lossy dielectric prolate spheroid. Incident, scattered and transmitted components of electric and magnetic fields are expressed in terms of normalized prolate spheroidal vector wave functions (defined in Appendix A of [15]). Since the dielectric medium of the scatterer is of complex relative permittivity, complex eigenvalues are evaluated for the spheroidal scalar wave functions of transmitted components of E -field and H -field expansions. Appropriate boundary conditions are then applied on the surface of the spheroid to solve a set of simultaneous linear algebraic equations relating the unknown expansion coefficients corresponding to scattered and transmitted fields expressed in terms of known expansion coefficients of the incident field. Finally we elaborate on the computation of radar cross sections in far field for single uniformly lossy dielectric prolate spheroid.

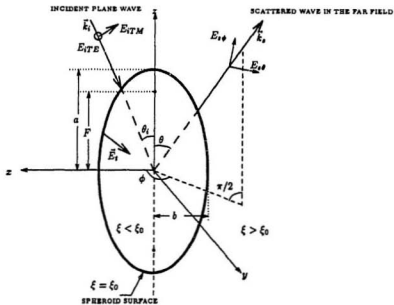


Figure 3.1: Scattering geometry for a single uniformly lossy dielectric prolate spheroid with arbitrary incidence and polarization of a plane electromagnetic wave.

3.2 Expansion of the Incident Electric Field in terms of Normalized Prolate Spheroidal Vector Wave Functions

Let us consider a monochromatic plane electromagnetic wave of wavelength λ and of unit amplitude propagating in free space. This wave is propagating in the $x - z$ plane ($\phi_i = 0$) at an angle $\theta_i (\leq \pi/2)$ made with the z -axis, and is incident on single uniformly lossy dielectric prolate spheroid as shown in Fig. 3.1. Let $\xi = \xi_0$ be the value of ξ on the surface of the spheroid, and a be the length of semimajor axis of the spheroid. The media outside and inside the scatterer are assumed to be non-ferromagnetic (i.e. their permeabilities are equal to the permeability of free space μ_0).

Let the electric field \vec{E}_i of the incident plane wave be linearly polarized in an arbitrary direction. This can be decomposed into two orthogonally polarized \vec{E} vectors \vec{E}_{iTE} and \vec{E}_{iTM} . \vec{H}_i vector is decomposed into orthogonally polarized \vec{H} vectors \vec{H}_{iTE} and \vec{H}_{iTM} . \vec{E}_{iTE} and \vec{H}_{iTM} lie perpendicular to the plane of incidence whereas \vec{E}_{iTM} and \vec{H}_{iTE} lie in the plane of incidence. Thus the polarization angle γ_p (the angle which the incident electric field makes with the normal to the plane of incidence ($x - z$ plane)) is such that for TE polarization $\gamma_p = 0$ and for TM polarization $\gamma_p = \pi/2$.

According to Flammer: an incident plane wave can be expanded in terms of $\vec{M}_{mn}^{+(1)}$ and $\vec{M}_{mn}^{- (1)}$. The electric field of unit amplitude incident on a spheroid is given as [20] and [15]

$$\vec{E}_i = \sum_{m=-\infty}^{\infty} \sum_{n=|m|}^{\infty} \left[p_{mn}^+ \vec{M}_{mn}^{+(1)} + p_{mn}^- \vec{M}_{mn}^{- (1)} \right] \quad (3.1)$$

where

$$P_{mn}^{\pm} = \frac{2j^{n-1}}{N_{|m|n}(h_1)} S_{|m|n}(h_1, \cos \theta_i) \left(\frac{\cos \gamma_p}{\cos \theta_i} \mp j \sin \gamma_p \right) \quad (3.2)$$

where $h_1 = (2\pi/\lambda)F$, $N_{|m|n}(h_1)$ is the normalization factor given by equation (2.32); $S_{|m|n}(h_1, \cos \theta_i)$ is the prolate spheroidal angle function (defined in Chapter 2).

If the expansion of \vec{E}_i given in (3.1) is arranged in the ϕ -sequence $(0)\phi, (\pm 1)\phi, (\pm 2)\phi, \dots$, then the series expansion in (3.1) can be written in the form of associated matrix field expansions given in [20] and [15]:

$$\vec{E}_i = \vec{M}_i^{(1)T} \mathbf{I} \quad (3.3)$$

where T indicate transpose of a matrix, and

$$\vec{M}_i = \begin{bmatrix} \vec{M}_{i0} \\ \vec{M}_{i1} \\ \vec{M}_{i2} \\ \vdots \end{bmatrix}; \quad \mathbf{I} = \begin{bmatrix} p_0 \\ p_1 \\ p_2 \\ \vdots \end{bmatrix} \quad (3.4)$$

with

$$\vec{M}_{i0}^T = [\vec{M}_{-1}^{+(1)T} \vec{M}_{1}^{-(1)T}] \quad (3.5)$$

$$\vec{M}_{i\sigma}^T = [\vec{M}_{\sigma-1}^{+(1)T} \vec{M}_{\sigma+1}^{-(1)T}; \vec{M}_{-(\sigma+1)}^{+(1)T} \vec{M}_{-(\sigma-1)}^{-(1)T}], \quad \sigma \geq 1 \quad (3.6)$$

where

$$\vec{M}_i^{\pm(i)T} = [\vec{M}_{r_i|r_i}^{\pm(i)T} \vec{M}_{r_i|r_i+1}^{\pm(i)T} \vec{M}_{r_i|r_i+2}^{\pm(i)T} \dots], \quad i = 1, \dots, 4. \quad (3.7)$$

Also

$$P_0^T = [p_{-1}^{+T} p_1^{-T}] \quad (3.8)$$

$$P_{\sigma}^T = [p_{\sigma-1}^{+T} p_{\sigma+1}^{-T}; p_{-(\sigma+1)}^{-T} p_{-(\sigma-1)}^{-T}], \quad \sigma \geq 1 \quad (3.9)$$

with

$$P_r^{\pm T} = [P_{r,|r|}^{\pm} P_{r,|r|+1}^{\pm} P_{r,|r|+2}^{\pm} \dots] \quad (3.10)$$

where P_{mn}^{\pm} ($n = |m|, |m| + 1, |m| + 2, \dots$) is given by equation (3.2).

3.3 Expansion of the Scattered Electric Field in terms of Normalized Prolate Spheroidal Vector Wave Functions

In response to the electromagnetic field incident on spheroid, there will be scattered component of electric field outside the spheroid ($\xi > \xi_0$) which must satisfy the radiation condition. Knowing

$$R_{mn}^{(4)}(h, \xi) \xrightarrow{h\xi \rightarrow \infty} \frac{1}{h\xi} e^{-[h\xi - \frac{1}{2}(n+1)\pi]} \quad (3.11)$$

we can expand the scattered E -field in terms of normalized prolate vector wave functions. Also the components of the scattered field must have the same ϕ -dependence as the corresponding elements of the incident field. Thus according to [20] we can write

$$\begin{aligned} \vec{E}_s = & \sum_{m=0}^{\infty} \sum_{n=m}^{\infty} \alpha_{mn}^+ \vec{M}_{mn}^{+(4)} + \alpha_{m+1,n}^s \vec{M}_{m+1,n}^{s(4)} + \sum_{n=0}^{\infty} \alpha_{-1n}^+ \vec{M}_{-1n}^{+(4)} + \alpha_{0n}^s \vec{M}_{0n}^{s(4)} \\ & + \sum_{m=0}^{\infty} \sum_{n=m}^{\infty} \alpha_{-mn}^- \vec{M}_{-mn}^{-(4)} + \alpha_{-(m+1),n}^s \vec{M}_{-(m+1),n}^{s(4)} \end{aligned} \quad (3.12)$$

where all \vec{M} -vectors in the above equation are evaluated with respect to h_1 ($= 2\pi F/\lambda$) which is real. α^+ -s, α^- -s and α^s -s are the unknown expansion coefficients corresponding to the series expansion of scattered E -field that have to be evaluated.

If same ϕ -sequence of azimuthal harmonics used for the incident field is used in this case, then the scattered field from the spheroid can be written in the

generalized column vector product similar to that for \vec{E}_i , [20]

$$\vec{E}_s = \vec{M}_s^{(4)T} \alpha \quad (3.13)$$

where

$$\vec{M}_s = \begin{bmatrix} \vec{M}_{s0} \\ \vec{M}_{s1} \\ \vec{M}_{s2} \\ \vdots \end{bmatrix}; \quad \alpha = \begin{bmatrix} \alpha_0 \\ \alpha_1 \\ \alpha_2 \\ \vdots \end{bmatrix} \quad (3.14)$$

with

$$\vec{M}_{s0}^T = [\vec{M}_{-1}^{+(4)T} \vec{M}_0^{+(4)T}] \quad (3.15)$$

$$\vec{M}_{s\sigma}^T = [\vec{M}_{\sigma-1}^{+(4)T} \vec{M}_\sigma^{+(4)T} \vec{M}_{-(\sigma-1)}^{-(4)T} \vec{M}_{-\sigma}^{-(4)T}], \quad \sigma \geq 1 \quad (3.16)$$

with $\vec{M}_r^{\pm(4)}$ defined in (3.7) for $i = 4$, and

$$\vec{M}_r^{+(4)T} = [\vec{M}_{r,|r|}^{+(4)} \vec{M}_{r,|r|+1}^{+(4)} \vec{M}_{r,|r|+2}^{+(4)} \cdots] \quad (3.17)$$

Also

$$\alpha_0^T = [\alpha_{-1}^{+T} \alpha_0^{+T}] \quad (3.18)$$

$$\alpha_\sigma^T = [\alpha_{\sigma-1}^{+T} \alpha_\sigma^{+T} \alpha_{-(\sigma-1)}^{-T} \alpha_{-\sigma}^{-T}], \quad \sigma \geq 1 \quad (3.19)$$

with

$$\alpha_r^{\pm T} = [\alpha_{r,|r|}^{\pm} \alpha_{r,|r|+1}^{\pm} \alpha_{r,|r|+2}^{\pm} \cdots] \quad (3.20)$$

$$\alpha_r^{\pm T} = [\alpha_{r,|r|}^{\pm} \alpha_{r,|r|+1}^{\pm} \alpha_{r,|r|+2}^{\pm} \cdots] \quad (3.21)$$

3.4 Expansion of the Transmitted Electric Field in terms of Normalized Prolate Spheroidal Vector Wave Functions

Since the medium inside the scatterer (spheroid) is composed of dielectric material, there will also be a transmitted component of E -field inside the spheroid

which is non-plane wave type.

Now inside a lossy dielectric medium, propagation constant or wave number k is given by

$$k = (2\pi/\lambda) \cdot \sqrt{\epsilon'/\epsilon_0} \quad (3.22)$$

where $\epsilon' = \epsilon - j\sigma/\omega$, ϵ_0 is permittivity of free space, and conductivity (σ) of the medium inside the spheroid is not equal to zero. $\epsilon_r = \epsilon'/\epsilon_0$ is called complex relative permittivity of the medium. Thus inside the lossy dielectric spheroid k is complex, and is of the form $k = k' - jk''$, where k' and k'' are real quantities.

For the expansion of the transmitted E -field, the vector wave functions of first kind are to be considered and also they have to be evaluated with respect to $h_2 (= (2\pi F/\lambda)\sqrt{\epsilon_r})$, which is complex. Thus the transmitted E -field inside the spheroid expressed in terms of normalized prolate spheroidal vector wave functions is given as [23]

$$\begin{aligned} \vec{E}_t = & \sum_{m=0}^{\infty} \sum_{n=m}^{\infty} \beta_{mn}^+ \vec{M}_{mn}^{+(1)} + \beta_{m+1,n}^s \vec{M}_{m+1,n}^{s(1)} + \sum_{n=0}^{\infty} \beta_{-1n}^+ \vec{M}_{-1n}^{+(1)} + \beta_{0n}^s \vec{M}_{0n}^{s(1)} \\ & + \sum_{m=0}^{\infty} \sum_{n=m}^{\infty} \beta_{-mn}^- \vec{M}_{-mn}^{-(1)} + \beta_{-(m+1),n}^s \vec{M}_{-(m+1),n}^{s(1)} \end{aligned} \quad (3.23)$$

β^{+} -s, β^{-} -s and β^s -s are the unknown expansion coefficients corresponding to the series expansion of transmitted E -field that have to be evaluated. All the \vec{M} -vectors in the equation (3.23) are evaluated with respect to h_2 .

If the terms in the expansion of E_t are arranged in the ϕ -sequence of $(0)\phi$, $(\pm 1)\phi$, $(\pm 2)\phi$, ... then we can have

$$\vec{E}_t = \vec{M}_t^{(1)T} \beta \quad (3.24)$$

where

$$\vec{M}_t = \begin{bmatrix} \vec{M}_{t0} \\ \vec{M}_{t1} \\ \vec{M}_{t2} \\ \vdots \end{bmatrix}; \quad \beta = \begin{bmatrix} \beta_0 \\ \beta_1 \\ \beta_2 \\ \vdots \end{bmatrix} \quad (3.25)$$

with

$$\vec{M}_{t0}^T = [\vec{M}_{-1}^{+(1)T} \vec{M}_0^{+(1)T}] \quad (3.26)$$

$$\vec{M}_{t\sigma}^T = [\vec{M}_{\sigma-1}^{+(1)T} \vec{M}_\sigma^{+(1)T} \vec{M}_{-(\sigma-1)}^{-(1)T} \vec{M}_{-\sigma}^{-(1)T}], \quad \sigma \geq 1 \quad (3.27)$$

with $\vec{M}_r^{\pm(1)}$ defined in (3.7) for $i = 1$, and

$$\vec{M}_r^{+(1)T} = [\vec{M}_{r,|r|}^{+(1)} \vec{M}_{r,|r|+1}^{+(1)} \vec{M}_{r,|r|+2}^{+(1)} \cdots] \quad (3.28)$$

Also

$$\beta_0^T = [\beta_{-1}^{+T} \beta_0^{+T}] \quad (3.29)$$

$$\beta_\sigma^T = [\beta_{\sigma-1}^{+T} \beta_\sigma^{+T} \beta_{-(\sigma-1)}^{-T} \beta_{-\sigma}^{-T}], \quad \sigma \geq 1 \quad (3.30)$$

with

$$\beta_r^{\pm T} = [\beta_{r,|r|}^{\pm} \beta_{r,|r|+1}^{\pm} \beta_{r,|r|+2}^{\pm} \cdots] \quad (3.31)$$

$$\beta_r^{\pm T} = [\beta_{r,|r|}^{\pm} \beta_{r,|r|+1}^{\pm} \beta_{r,|r|+2}^{\pm} \cdots] \quad (3.32)$$

3.5 Expansion of H -field in terms of E -field

We know from Maxwell's equations for a time harmonic electromagnetic field

$$\vec{H} = \left(\frac{j}{\omega\mu} \right) \nabla \times \vec{E} \quad (3.33)$$

Again we know that $\omega = (2\pi/\lambda)/(\mu_0\epsilon_0)^{1/2}$ and $k = (\epsilon/\epsilon_0)^{1/2}(2\pi/\lambda)$, Assuming that the media outside and inside the spheroid are non-ferromagnetic, we can

write

$$\vec{H} = j k^{-1} (\epsilon/\mu_0)^{1/2} \nabla \times \vec{E} \quad (3.34)$$

where k is the wavenumber (or propagation constant) and ϵ is the permittivity of the medium (real or complex). We can obtain expansions of the different H -fields inside and outside the scatterer in terms of appropriate normalized spheroidal vector wave functions from those of the corresponding E -fields. We do this by replacing \vec{M} by \vec{N} and multiplying each expansion by the appropriate value of $j(\epsilon/\mu_0)^{1/2}$.

3.6 Expansion of the Incident Magnetic Field in terms of Normalized Prolate Spheroidal Vector Wave Functions

Utilizing equation (3.34), the incident H -field can be expressed as

$$\vec{H}_i = j(\epsilon_1/\mu_0)^{1/2} \left(\frac{1}{k_1}\right) (\nabla \times \vec{E}_i) \quad (3.35)$$

where k_1 and ϵ_1 are the propagation constant and permittivity of the medium outside the spheroid respectively. Using (3.1) and the relation

$$\vec{N}_{mn}^{(i)} = \frac{1}{k} (\nabla \times \vec{M}_{mn}^{(i)}) \quad (3.36)$$

we get

$$\vec{H}_i = \sum_{m=-\infty}^{\infty} \sum_{n=|m|}^{\infty} [p_{mn}^+ \vec{N}_{mn}^{+(1)} + p_{mn}^- \vec{N}_{mn}^{-(1)}] \quad (3.37)$$

where p_{mn}^{\pm} are defined in (3.2). Equation (3.37) can be written in the matrix form similar to that of \vec{E}_i as

$$\vec{H}_i = j(\epsilon_1/\mu_0)^{1/2} \vec{N}_i^{(1)T} \mathbf{I} \quad (3.38)$$

$\vec{N}_i^{(1)T}$ has the same form as that of $\vec{M}_i^{(1)T}$ defined in (3.4) - (3.7) but with \vec{M} replaced by \vec{N} . It has also been defined in (3.4) and (3.9) - (3.10).

3.6.1 Limiting Case: $\gamma_p = 0$ and $\theta_i \rightarrow \pi/2$

The series expansion of incident E -field and H -field becomes indeterminate when angle of incidence $\theta_i \rightarrow 90^\circ$ for TE polarization (i.e. $\gamma_p = 0$) of incident excitation. The limiting expressions for p_{mn}^\pm for $\theta_i \rightarrow 90^\circ$ corresponding to TE polarization of incident fields are given by Sinha and MacPhie in [7]:

$$p_{mn}^\pm = \begin{cases} 0, & (n - |m|) \text{ even} \\ \frac{2j^{n-1}}{N_{|m|n}} \cdot \frac{(-1)^{(n-|m|-1)/2} (n + |m| + 1)!}{2^n \left(\frac{n-|m|-1}{2}\right)! \left(\frac{n+|m|+1}{2}\right)!}, & (n - |m|) \text{ odd} \end{cases} \quad (3.39)$$

$N_{|m|n}$ is the normalization factor given by equation (2.32).

3.7 Expansion of the Scattered Magnetic Field in terms of Normalized Prolate Spheroidal Vector Wave Functions

Using (3.34) we can write for \vec{H}_s

$$\vec{H}_s = j(\epsilon_1/\mu_0)^{1/2} \left(\frac{1}{k_1}\right) (\nabla \times \vec{E}_s) \quad (3.40)$$

Using (3.12) and the relation given in (3.36)

$$\begin{aligned} \vec{H}_s = & j(\epsilon_1/\mu_0)^{1/2} \left[\sum_{m=0}^{\infty} \sum_{n=m}^{\infty} \alpha_{mn}^+ \vec{N}_{mn}^{+(4)} + \alpha_{m+1,n}^+ \vec{N}_{m+1,n}^{+(4)} + \sum_{n=0}^{\infty} \alpha_{-1n}^+ \vec{N}_{-1n}^{+(4)} + \alpha_{0n}^+ \vec{N}_{0n}^{+(4)} \right. \\ & \left. + \sum_{m=0}^{\infty} \sum_{n=m}^{\infty} \alpha_{-mn}^- \vec{N}_{-mn}^{-(4)} + \alpha_{-(m+1),n}^- \vec{N}_{-(m+1),n}^{-(4)} \right] \end{aligned} \quad (3.41)$$

Equation (3.41) can be written in the matrix form similar to that of \vec{E}_s as

$$\vec{H}_s = j(\epsilon_1/\mu_0)^{1/2} \vec{N}_s^{(4)T} \alpha \quad (3.42)$$

$\vec{N}_i^{(4)T}$ has the same form as that of $\vec{M}_i^{(4)T}$ defined in (3.14) – (3.17) but with \vec{M} replaced by \vec{N} . α has also been defined in (3.14) and (3.18) – (3.21).

3.8 Expansion of the Transmitted Magnetic Field in terms of Normalized Prolate Spheroidal Vector Wave Functions

Using (3.34) we can write for \vec{H}_t

$$\vec{H}_t = j(\epsilon_2/\mu_0)^{1/2} \left(\frac{1}{k_2} \right) (\nabla \times \vec{E}_t) \quad (3.43)$$

where k_2 and ϵ_2 are the propagation constant and complex permittivity of the medium inside the spheroid respectively.

Using (3.23) and the relation given in (3.36)

$$\begin{aligned} \vec{H}_t = & j(\epsilon_2/\mu_0)^{1/2} \sum_{m=0}^{\infty} \sum_{n=m}^{\infty} \beta_{mn}^+ \vec{N}_{mn}^{+(1)} + \beta_{m+1,n}^z \vec{N}_{m+1,n}^{z(1)} + \sum_{n=0}^{\infty} \beta_{-1n}^+ \vec{N}_{-1n}^{+(1)} + \beta_{0n}^z \vec{N}_{0n}^{z(1)} \\ & + \sum_{m=0}^{\infty} \sum_{n=m}^{\infty} \beta_{-mn}^- \vec{N}_{-mn}^{-(1)} + \beta_{-(m+1),n}^z \vec{N}_{-(m+1),n}^{z(1)} \end{aligned} \quad (3.44)$$

Equation (3.44) can be written in the matrix form similar to that of \vec{E}_t as

$$\vec{H}_t = j(\epsilon_2/\mu_0)^{1/2} \vec{N}_i^{(1)T} \beta \quad (3.45)$$

$\vec{N}_i^{(1)T}$ has the same form as that of $\vec{M}_i^{(1)T}$ defined in (3.25) – (3.28) but with \vec{M} replaced by \vec{N} . β has also been defined in (3.25) and (3.30) – (3.32).

3.9 Applications of Boundary Conditions

Boundary conditions require that across the surface of spheroid ($\xi = \xi_0$) the tangential components (η and ϕ) of the E -field and as well as those of H -field

(assuming no surface current) must be continuous. These conditions can be expressed equivalently:

$$\left. \begin{aligned} \vec{E}_{i\eta} + \vec{E}_{e\eta} &= \vec{E}_{i\eta} \\ \vec{E}_{i\phi} + \vec{E}_{e\phi} &= \vec{E}_{i\phi} \\ \vec{H}_{i\eta} + \vec{H}_{e\eta} &= \vec{H}_{i\eta} \\ \vec{H}_{i\phi} + \vec{H}_{e\phi} &= \vec{H}_{i\phi} \end{aligned} \right\} \quad (3.46)$$

at $\xi = \xi_0$ and for all values of η and ϕ in the ranges $-1 \leq \eta \leq 1$ and $0 \leq \phi \leq 2\pi$ respectively.

By expanding each E -field and H -field in terms of normalized prolate spheroidal vector wave functions, we can rewrite (3.46) as

$$(\vec{M}_i^{(1)T} \mathbf{I} + \vec{M}_i^{(4)T} \boldsymbol{\alpha}) \times \hat{\xi}|_{\xi=\xi_0} = \vec{M}_i^{(1)T} \beta \times \hat{\xi}|_{\xi=\xi_0} \quad (3.47)$$

$$(\vec{N}_i^{(1)T} \mathbf{I} + \vec{N}_i^{(4)T} \boldsymbol{\alpha}) \times \hat{\xi}|_{\xi=\xi_0} = (\epsilon_2/\epsilon_1)^{1/2} \vec{N}_i^{(1)T} \beta \times \hat{\xi}|_{\xi=\xi_0} \quad (3.48)$$

3.9.1 ϕ -matching and η -matching

In (3.47) and (3.48) the coefficients of the same ϕ -dependent exponential terms on both sides of each equation should be equal and the equality should hold good for each corresponding term under the summation of m . Also those terms on both sides of (3.47) and (3.48) that are under summation of n cannot be matched term by term.

Thus according to [15] and [23] for ϕ -matching and η -matching both sides of (3.47) and (3.48) are scalar multiplied by the vector functions

$$\left\{ \begin{array}{l} l_\eta \hat{\eta} \\ l_\phi \hat{\phi} \end{array} \right\} S_{|m|, |m|+N} e^{\pm j(m \pm 1)\phi}, \quad N = 0, 1, 2, \dots$$

and the products are integrated over the surface of the spheroid with respect to both η ($-1 \leq \eta \leq 1$) and ϕ ($0 \leq \phi \leq 2\pi$), where l_η and l_ϕ are given by

$$\left. \begin{aligned} l_\eta &= j2F(\xi_0^2 - \eta^2)^{1/2} \\ l_\phi &= 2F(\xi_0^2 - \eta^2) \end{aligned} \right\} \quad (3.49)$$

for equation (3.47) and by

$$\left. \begin{aligned} l_\eta &= 2F^2(\xi_0^2 - \eta^2)^{5/2}/(\xi_0^2 - 1)^{1/2} \\ l_\phi &= j2F^2(\xi_0^2 - \eta^2)/(\xi_0^2 - 1) \end{aligned} \right\} \quad (3.50)$$

for equation (3.48). Using the orthogonality properties of complex exponentials, given in (2.63), and angle functions, given in (2.31), we obtain a set of coupled algebraic equations of the form:

$$[P_M] \beta + [Q_M] \alpha = [R_M] \mathbf{I} \quad (3.51)$$

$$[P_N] \beta + [Q_N] \alpha = [R_N] \mathbf{I} \quad (3.52)$$

where the elements of $[P_M]$, $[Q_M]$, $[R_M]$, $[P_N]$, $[Q_N]$ and $[R_N]$ are defined in Appendix B.

3.10 System Matrix $[G]$

Combining (3.51) and (3.52) we can write

$$\begin{bmatrix} [Q_M] & [P_M] \\ [Q_N] & [P_N] \end{bmatrix} \cdot \begin{bmatrix} \alpha \\ \beta \end{bmatrix} = \begin{bmatrix} [R_M] \mathbf{I} \\ [R_N] \mathbf{I} \end{bmatrix} \quad (3.53)$$

Equation (3.53) can be written in the form

$$S = [G] \mathbf{I} \quad (3.54)$$

where

$$S = \begin{bmatrix} \alpha \\ \beta \end{bmatrix} \quad (3.55)$$

$$[G] = \begin{bmatrix} [Q_M] & [P_M] \\ [Q_N] & [P_N] \end{bmatrix}^{-1} \cdot \begin{bmatrix} [R_M] \\ [R_N] \end{bmatrix} \quad (3.56)$$

$[G]$ is the generalized system matrix which is independent of the direction and polarization of the incident wave. Thus the solution in the above form eliminates

the need for repeatedly solving a new set of simultaneous equations in order to obtain the expansion coefficients of scattered and transmitted fields for a new angle of incidence.

3.11 Far-Field Expansions and Scattering Cross sections

Once the unknown expansion coefficients corresponding to series expansion of scattered and transmitted fields are determined by solving the system equation (3.54), we can find the magnitude of the scattered field at a particular distance from the spheroid by substituting the values of coefficients corresponding to series expansion of scattered field in equation (3.12). However, of practical interest is the scattered field in the far zone for $|r| \rightarrow \infty$, r being the distance from the spheroid to the point of observation.

At very large distance from the spheroid $h_1 \xi \rightarrow \infty$. So as $h_1 \xi \rightarrow \infty$,

$$\left. \begin{aligned} h_1 \xi &\rightarrow kr \\ \eta &\rightarrow \cos \theta \\ \hat{\eta} &\rightarrow -\hat{\theta} \end{aligned} \right\} \quad (3.57)$$

Also as $h_1 \xi \rightarrow \infty$, it can be shown that [20] and [15]:

$$R_{mn}^{(s)}(h_1, \xi) \rightarrow j^{n+1} \frac{e^{-jk_1 r}}{k_1 r} \quad (3.58)$$

$$\frac{d}{d\xi} R_{mn}^{(s)}(h_1, \xi) \rightarrow j^n k_1 r \frac{e^{-jk_1 r}}{k_1 r} \quad (3.59)$$

The asymptotic forms of spheroidal vector functions are obtained by neglecting ξ^{-2} and its higher inverse power terms. Thus in the far zone the scattered E -field with respect to the origin O of spheroid A , is given by [20]

$$\vec{E}_s = \frac{e^{-jk_1 r}}{kr} \left[F_\theta(\theta, \phi) \hat{\theta} + F_\phi(\theta, \phi) \hat{\phi} \right] \quad (3.60)$$

where

$$F_{\theta}(\theta, \phi) = - \sum_{m=0}^{\infty} \sum_{n=m}^{\infty} j^{n+1} \left[\frac{S_{mn}}{2} \{(\alpha_{mn}^{+} - \alpha_{mn}^{-}) \cos(m+1)\phi\} + \frac{S_{1n}}{2} \alpha_{-1n}^{+} \right] \quad (3.61)$$

$$F_{\phi}(\theta, \phi) = \sum_{m=0}^{\infty} \sum_{n=m}^{\infty} j^n \left[\frac{1}{2} \eta S_{mn} \{(\alpha_{mn}^{+} + \alpha_{mn}^{-}) \cos(m+1)\phi\} + j(\alpha_{mn}^{+} - \alpha_{mn}^{-}) \sin(m+1)\phi - \sqrt{1-\eta^2} S_{m+1,n} \cdot \{(\alpha_{m+1,n}^{+} + \alpha_{-(m+1),n}^{+}) \cos(m+1)\phi\} + j(\alpha_{m+1,n}^{+} - \alpha_{-(m+1),n}^{+}) \sin(m+1)\phi \right] + \frac{1}{2} \eta S_{1n} \alpha_{-1n}^{+} - \sqrt{1-\eta^2} S_{0n} \alpha_{0n}^{+} \quad (3.62)$$

$\hat{\theta}$ and $\hat{\phi}$ are the unit vectors in the direction of increasing θ and ϕ respectively.

The scattering cross section is defined as 4π times the ratio of the scattered power delivered per unit solid angle in the direction of the receiver to the power per unit area incident at the scatterer. This can be shown to be independent of r .

The bistatic radar cross section $\sigma(\theta, \phi)$ is defined as

$$\sigma(\theta, \phi) = \lim_{r \rightarrow \infty} 4\pi r^2 \frac{|\vec{E}_s \cdot \hat{\tau}|^2}{|\vec{E}_i|^2} \quad (3.63)$$

where $\hat{\tau}$ represents the polarization of the receiver at the observation point (r, θ, ϕ) . With $\hat{\tau}$ in the same direction as \vec{E}_s , the normalized bistatic radar cross section is given by

$$\frac{\pi \sigma(\theta, \phi)}{\lambda^2} = |F_{\theta}(\theta, \phi)|^2 + |F_{\phi}(\theta, \phi)|^2 \quad (3.64)$$

The normalized bistatic radar cross section in E -Plane and H -Plane are obtained by substituting $\phi = \pi/2$ and $\phi = 0$ in (3.64). For normalized backscattering

(monostatic) radar cross section $\theta = \theta_i$ and $\phi = 0$ in (3.64), so that the corresponding backscattering cross section becomes

$$\frac{\pi\sigma(\theta_i, 0)}{\lambda^2} = |F_\theta(\theta_i, 0)|^2 + |F_\phi(\theta_i, 0)|^2 \quad (3.65)$$

For evaluation of monostatic radar cross section we substitute $\phi = 0$ in (3.64) because we have assumed that the incident wave is propagating in the $x-z$ plane ($\phi_i = 0$).

3.12 Results of Numerical Computation

For *TE* or *TM* polarization of incident field, the unknown expansion coefficients corresponding to series expansion of scattered and transmitted fields have been determined by solving the system equation (3.54) by using Gauss elimination technique [36]. Since the series expansions of the *E* and *H*-fields in terms of the spheroidal vector wave functions are infinite in extent, all the matrices of (3.54) have infinite size. Thus to obtain numerical results of desired accuracy one has to truncate the series and matrices accordingly.

The truncation scheme used here, is the one that was developed by Sinha and MacPhie for conducting prolate spheroid [7] and [20]. According to their scheme for each value of m , $n = |m|, |m| + 1, |m| + 2, \dots, |m| + n_t - 1$ with $n_t = \text{Int}(k_1 a + 4)$. $k_1 = 2\pi/\lambda$, $k_1 a$ is the relative size of the spheroid, and $\text{Int}(\Delta)$ is the smallest integer which is not less than (Δ) . For each m , N in $S_{|m|, |m|+N}$ can be given as $N = 0, 1, 2, \dots, n_t - 1$. It is found that ϕ -harmonics $(0)\phi, (\pm 1)\phi, (\pm 2)\phi$ give at least two significant digit accuracy in the computed results of the radar cross sections. This limits the values of m to $-1, 0, 1$. However since we are using spheroidal vector wave functions normalized with respect to $|m|$, we evaluate the

radar cross sections for $m = 0, 1$. Another truncation scheme is given in [11] which uses \vec{M}^r and \vec{N}^r vectors in scattering formulation.

Also in order to study the scattering characteristics in the resonance region, where the wavelength of the incident radiation is comparable to the length of semi-major axis of the spheroid, we choose spheroids with different values of $k_1 a$ varying from 1 to 4.

Numerical results are presented in the form of normalized bistatic and monostatic (backscattering) radar cross sections in the far field for single uniformly lossy dielectric prolate spheroid, with axial ratio $a/b = 2$ and 10, and with different values of complex relative permittivity (ϵ_r).

In this thesis we determine bistatic radar cross section for TE polarization of nose-on incident wave ($\theta_i = 0$), since for axial incidence the known expansion coefficients p_{mn}^\pm have same magnitude for TE and TM polarizations of incident plane wave. Thus when $\theta_i = 0$, evaluation of bistatic radar cross section in E -Plane and H -Plane is independent of the polarization (TE or TM) of the incident excitation.

Fig. 3.2-3.4 give plots of normalized bistatic cross section for TE polarization of incident wave in both E -plane ($\phi = 90^\circ$) and H -plane ($\phi = 0^\circ$) for a single uniformly lossy dielectric prolate spheroid having axial ratio $a/b = 2$ and $a/b = 10$, and with different values of relative size ($k_1 a$) and complex relative permittivity ϵ_r . In Fig. 3.2 we consider $\epsilon_r = 2 - j0.5$ and in Fig. 3.3 we consider $\epsilon_r = 4 - j0.5$. From Fig. 3.2 and Fig. 3.3 we observe that as the axial ratio changes from 2 to 10 there is a decrement in magnitude of bistatic cross section in both E -plane and H -plane. This is due to the reduction in the available scattering area for the thin spheroid with axial ratio 10. Also for a given value of

axial ratio and complex relative permittivity, bistatic cross sections tend to show more fluctuations as the value of relative size ($k_1 a$) increases. For given values of $k_1 a$ and a/b , Fig. 3.4 presents the plots of bistatic cross section for various values of frequency dependent part of ϵ_r . We choose seven different values of ϵ_r : $\epsilon_r = 4 - j0$; $\epsilon_r = 4 - j0.2$; $\epsilon_r = 4 - j0.4$; $\epsilon_r = 4 - j0.6$; $\epsilon_r = 4 - j0.8$; $\epsilon_r = 4 - j1$; $\epsilon_r = 4 - j1.2$.

In Fig. 3.5 and Fig. 3.6 we present the plots of normalized monostatic (backscattering) cross section $\pi\sigma(\theta_i, 0)/\lambda^2$ as function of aspect angle θ_i in terms of TE and TM polarizations of incident field for a single uniformly lossy dielectric prolate spheroid having axial ratio $a/b = 2$ and $a/b = 10$, and with different values of relative size ($k_1 a$) and complex relative permittivity ϵ_r . In Fig. 3.5 and Fig. 3.6 we consider $\epsilon_r = 2 - j0.5$ and $\epsilon_r = 4 - j0.5$ respectively. It is observed that that magnitudes of monostatic cross section corresponding to TE and TM polarization of incident wave are the same at axial incidence ($\theta_i = 0^\circ$). This is because for axial incidence the known expansion coefficients p_{mn}^\pm corresponding to the incident fields have same magnitude for TE and TM polarization of incident excitation.

Fig. 3.7 shows normalized monostatic cross section, as a function of aspect angle for single uniformly lossy dielectric prolate spheroid with axial ratio 10, relative size $k_1 a = 3$, and for different values of complex relative permittivity $\epsilon_r = 4 - j0$; $\epsilon_r = 4 - j0.4$; $\epsilon_r = 4 - j0.8$; $\epsilon_r = 4 - j1.2$.

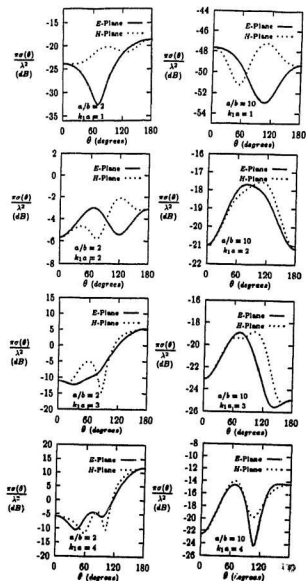


Figure 3.2: Normalized bistatic cross section for TE polarization of incident wave, as a function of scattering angle for single uniformly lossy dielectric prolate spheroid with axial ratio 2 and 10, and of relative sizes $k_1 a = 1, 2, 3$ and 4 for complex relative permittivity $\epsilon_r = 2 - j0.5$.

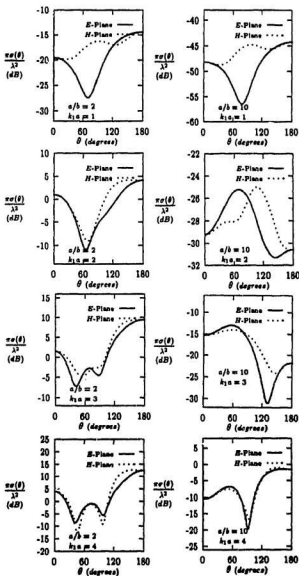


Figure 3.3: Normalized bistatic cross section for TE polarization of incident wave, as a function of scattering angle for single uniformly lossy dielectric prolate spheroid with axial ratio 2 and 10, and of relative sizes $k_1 a = 1, 2, 3$ and 4 for complex relative permittivity $\epsilon_r = 4 - j0.5$.

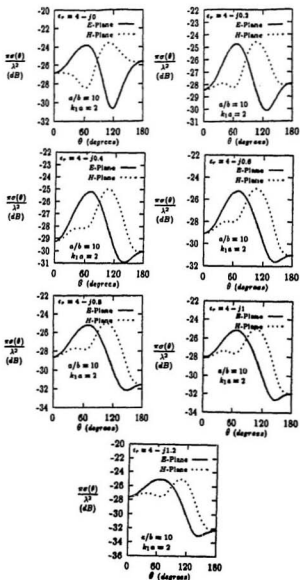


Figure 3.4: Normalized bistatic cross section for TE polarization of incident wave, as a function of scattering angle for single uniformly lossy dielectric prolate spheroid with axial ratio 10, relative size $k_1 a = 2$ and with different values of complex relative permittivity: $\epsilon_r = 4 - j0$; $\epsilon_r = 4 - j0.2$; $\epsilon_r = 4 - j0.4$; $\epsilon_r = 4 - j0.6$; $\epsilon_r = 4 - j0.8$; $\epsilon_r = 4 - j1$; $\epsilon_r = 4 - j1.2$.

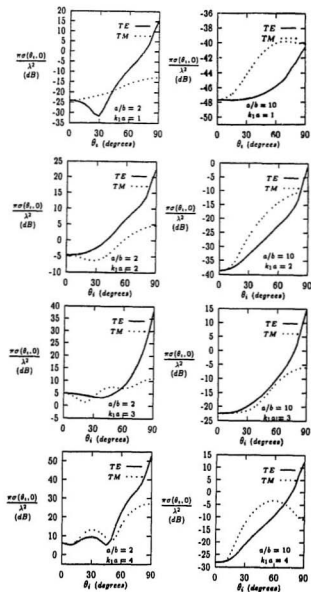


Figure 3.5: Normalized monostatic cross section, as a function of aspect angle for single uniformly lossy dielectric prolate spheroid with axial ratio 2 and 10, and of relative sizes $k_1 a = 1, 2, 3$ and 4 for complex relative permittivity $\epsilon_r = 2 - j0.5$.

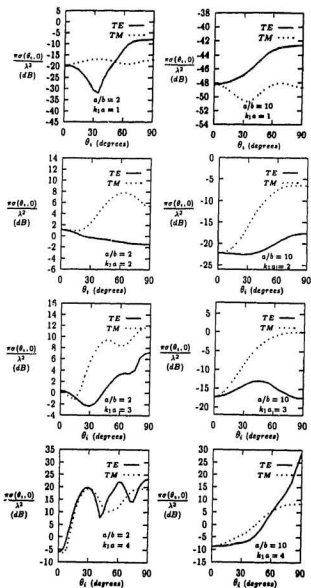


Figure 3.6: Normalized monostatic cross section, as a function of aspect angle for single uniformly lossy dielectric spheroid with axial ratio 2 and 10, and of relative sizes $k_1 a = 1, 2, 3$ and 4 for complex relative permittivity $\epsilon_r = 4 - j0.5$.

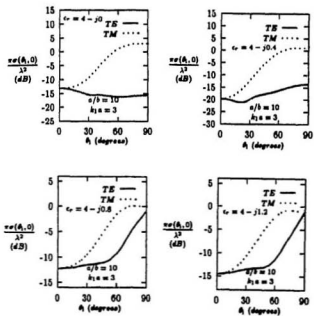


Figure 3.7: Normalized monostatic cross section, as a function of aspect angle for single uniformly lossy dielectric prolate spheroid with axial ratio 10, relative size $k_1 a = 3$, and for different values of complex relative permittivity $\epsilon_r = 4 - j0$; $\epsilon_r = 4 - j0.4$; $\epsilon_r = 4 - j0.8$; $\epsilon_r = 4 - j1.2$.

Chapter 4

Electromagnetic Plane Wave Scattering by a System of Two Uniformly Lossy Dielectric Prolate Spheroids in Arbitrary Configuration

4.1 Introduction

By means of modal series expansions of electromagnetic fields in terms of prolate spheroidal vector wave functions (following the procedures shown in chapter 3), an exact solution is obtained for the electromagnetic plane wave scattering by two uniformly lossy dielectric prolate spheroids in arbitrary orientation. Since the spheroids are arbitrarily oriented, rotational-translational addition theorems for spheroidal vector wave functions are employed in order to transform the outgoing wave from one spheroid into the incoming wave at the other spheroid. By applying appropriate boundary conditions on surfaces of the spheroids we solve unknown expansion coefficients corresponding to scattered and transmitted fields. Finally numerical results in the form of curves for normalized bistatic and monostatic radar cross sections are given for a variety of two-body system of uniformly

lossy dielectric prolate spheroids in arbitrary orientation having resonant or near resonant lengths and different distances of separation.

4.2 Expansion of the Incident Electric Field in terms of Normalized Prolate Spheroidal Vector Wave Functions

Consider a system of two arbitrarily oriented uniformly lossy dielectric prolate spheroids as shown in Fig. 4.1. Unprimed coordinates refer to spheroid A and primed coordinates refer to spheroid B . The system (x', y', z') is obtained from (x, y, z) by rotating the latter through Euler angles (α, β, γ) (defined in [38], also refer Appendix E) to $(x_{||}, y_{||}, z_{||})$ which is parallel to (x', y', z') , and then followed by a translation of distance d . The center O' of spheroid B has spherical coordinates (d, θ_d, ϕ_d) with respect to $Ox_{||}y_{||}z_{||}$ and (d, θ_0, ϕ_0) with respect to $Oxyz$. A point P has spheroidal coordinates (ξ, η, ϕ) and (ξ', η', ϕ') with respect to (x, y, z) -system and (x', y', z') -system respectively.

Let us consider a monochromatic plane electromagnetic wave of wavelength λ and of unit amplitude propagating in free space. This wave is propagating in the x - z plane ($\phi_i = 0$) at an angle $\theta_i (\leq \pi/2)$ made with the z -axis, and is incident on A - B system. The media outside and inside the scatterers are assumed to be non-ferromagnetic (i.e. their permeabilities are equal to the permeability of free space μ_0).

Let the electric field \vec{E}_i of the incident plane wave be linearly polarized in an arbitrary direction. This can be decomposed into two orthogonally polarized \vec{E} vectors $\vec{E}_{i,TE}$ and $\vec{E}_{i,TM}$. \vec{H}_i vector is decomposed into orthogonally polarized \vec{H} vectors $\vec{H}_{i,TE}$ and $\vec{H}_{i,TM}$. $\vec{E}_{i,TE}$ and $\vec{H}_{i,TM}$ lie perpendicular to the plane of

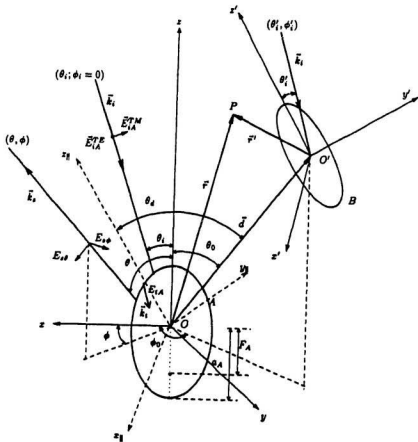


Figure 4.1: Scattering geometry for a system of two uniformly lossy dielectric prolate spheroids in general configuration with arbitrary incidence and polarization of a plane electromagnetic wave.

incidence whereas \vec{E}_{iTM} and \vec{H}_{iTE} lie in the plane of incidence. Thus the polarization angle γ_p (the angle which the incident electric field makes with the normal to the plane of incidence (x - z plane)) is such that for TE polarization $\gamma_p = 0$ and for TM polarization $\gamma_p = \pi/2$. The electric field of unit amplitude incident on spheroid A is given as [20] and [15]

$$\vec{E}_{iA} = \sum_{m=-\infty}^{\infty} \sum_{n=|m|}^{\infty} [p_{mn}^+ \vec{M}_{mn}^{+(1)} + p_{mn}^- \vec{M}_{mn}^{-(1)}] \quad (4.1)$$

where

$$p_{mn}^{\pm} = \frac{2^{j^{n-1}}}{N_{|m|n}(h_1)} S_{|m|n}(h_1, \cos \theta_i) \left(\frac{\cos \gamma_p}{\cos \theta_i} \mp j \sin \gamma_p \right) \quad (4.2)$$

$N_{|m|n}(h_1)$ is the normalization factor given by (2.32); $S_{|m|n}(h_1, \cos \theta_i)$ is the prolate angle function (defined in Chapter 2). $h_1 = (2\pi/\lambda)F_A$, which is real. All the \vec{M} -vectors in the above equation are evaluated with respect to h_1 .

If the expansion of \vec{E}_{iA} is arranged in ϕ -sequence $(0)\phi, (\pm 1)\phi, (\pm 2)\phi, \dots$, then the series expansion in equation (4.1) can be given as:

$$\vec{E}_{iA} = \vec{M}_{iA}^{(1)T} \mathbf{I}_A \quad (4.3)$$

where

$$\vec{M}_{iA} = \begin{bmatrix} \vec{M}_{i0} \\ \vec{M}_{i1} \\ \vec{M}_{i2} \\ \vdots \end{bmatrix}; \quad \mathbf{I}_A = \begin{bmatrix} p_0 \\ p_1 \\ p_2 \\ \vdots \end{bmatrix} \quad (4.4)$$

where

$$\vec{M}_{i0}^T = [\vec{M}_{-1}^{+(1)T} \vec{M}_{1}^{-(1)T}] \quad (4.5)$$

$$\vec{M}_{i\sigma}^T = [\vec{M}_{\sigma-1}^{+(1)T} \vec{M}_{\sigma+1}^{-(1)T}; \vec{M}_{-(\sigma+1)}^{+(1)T} \vec{M}_{-(\sigma-1)}^{-(1)T}], \quad \sigma \geq 1 \quad (4.6)$$

with

$$\vec{M}_r^{\pm(i)T} = \left[\vec{M}_{r,|r|}^{\pm(i)T} \vec{M}_{r,|r|+1}^{\pm(i)T} \vec{M}_{r,|r|+2}^{\pm(i)T} \cdots \right], i = 1, 2, 3, 4. \quad (4.7)$$

Also

$$P_0^T = \left[P_{-1}^T P_1^{-T} \right] \quad (4.8)$$

$$P_\sigma^T = \left[P_{\sigma-1}^T P_{\sigma+1}^{-T} P_{-(\sigma+1)}^T P_{-(\sigma-1)}^{-T} \right], \sigma \geq 1 \quad (4.9)$$

with

$$P_r^{\pm T} = \left[P_{r,|r|}^{\pm} P_{r,|r|+1}^{\pm} P_{r,|r|+2}^{\pm} \cdots \right] \quad (4.10)$$

The limiting expressions for p_{mn}^{\pm} when $\gamma_p = 0$ and $\theta \rightarrow \pi/2$ are given in [7] (also refer section 3.6.1).

E-field incident on spheroid *B* is given in terms of primed coordinate system as [27]:

$$\vec{E}_{iB} = e^{-j\vec{k}_i \cdot \vec{r}} \sum_{m=-\infty}^{+\infty} \sum_{n=|m|}^{\infty} \left[P_{mn}^{+'} \vec{M}_{mn}^{+(1)'} + P_{mn}^{-'} \vec{M}_{mn}^{-(1)'} + P_{mn}^{*' } \vec{M}_{mn}^{*(1)'} \right] \quad (4.11)$$

where,

$$P_{mn}^{\pm'} = \frac{2^{j^{n-1}}}{N_{mn}(h_1')} S_{mn}(h_1', \cos \theta_i') e^{-jm\phi_i'} \left[(c_{xz'} \mp j c_{xy'}) \sin \gamma_p \right. \\ \left. + \begin{cases} \left(c_{xz'} \mp j c_{xy'} \frac{\cos \gamma_p}{\cos \theta_i} \right), \forall \theta_i \text{ except when } \gamma_p = 0, \theta_i \rightarrow \frac{\pi}{2} \\ - (c_{xz'} \mp j c_{xy'}) \frac{\cos \gamma_p}{\sin \theta_i} \right] \text{ for } \gamma_p = 0, \theta_i \rightarrow \frac{\pi}{2} \end{cases} \quad (4.12)$$

$$P_{mn}^{*' } = \frac{2^{j^{n-1}}}{N_{mn}(h_1')} S_{mn}(h_1', \cos \theta_i') e^{-jm\phi_i'} [c_{yz'} \sin \gamma_p \\ + \begin{cases} c_{xz'} \frac{\cos \gamma_p}{\cos \theta_i}, \forall \theta_i \text{ except when } \gamma_p = 0, \theta_i \rightarrow \frac{\pi}{2} \\ -c_{xz'} \frac{\cos \gamma_p}{\sin \theta_i} \end{cases} \text{ for } \gamma_p = 0, \theta_i \rightarrow \frac{\pi}{2} \quad (4.13)$$

where $\vec{k}_i = -k_0(\hat{x} \sin \theta_i + \hat{z} \cos \theta_i)$. All the \vec{M}' -vectors are evaluated with respect to $h'_i (= 2\pi F_B/\lambda)$, which is real. In (4.12) and (4.13) θ'_i, ϕ'_i respectively are the spherical angular and azimuthal coordinates of the direction of incident monochromatic plane wave with respect to the primed coordinate system. $c_{ax'}, c_{ay'}, c_{az'}$, ($a = x, y, z$) are the direction cosines that relate the unit vectors $\hat{x}, \hat{y}, \hat{z}$ and $\hat{x}', \hat{y}', \hat{z}'$ by

$$\hat{a} = c_{ax'}\hat{x}' + c_{ay'}\hat{y}' + c_{az'}\hat{z}', \quad \hat{a} = \hat{x}, \hat{y}, \hat{z} \quad (4.14)$$

where

$$\begin{aligned} c_{xx'} &= \cos \alpha \cos \beta \cos \gamma - \sin \alpha \sin \gamma \\ c_{xy'} &= -(\cos \alpha \cos \beta \sin \gamma + \sin \alpha \cos \gamma) \\ c_{xz'} &= \cos \alpha \sin \beta \\ c_{yx'} &= \sin \alpha \cos \beta \cos \gamma + \cos \alpha \sin \gamma \\ c_{yy'} &= \cos \alpha \cos \gamma - \sin \alpha \cos \beta \sin \gamma \\ c_{yz'} &= \sin \alpha \sin \beta \\ c_{zx'} &= -\sin \beta \cos \gamma \\ c_{zy'} &= \sin \beta \sin \gamma \\ c_{zz'} &= \cos \beta \end{aligned} \quad (4.15)$$

α, β, γ are the three Euler angles. If the expansion of \vec{E}_{iB} is arranged in the ϕ' -sequence, $(0)\phi', (\pm 1)\phi', (\pm 2)\phi', \dots$ then we get in the matrix form

$$\vec{E}_{iB} = \vec{M}_{iB}^{(1)T} \mathbf{I}_B \quad (4.16)$$

where

$$\vec{M}_{iB} = \begin{bmatrix} \vec{M}'_{i0} \\ \vec{M}'_{i1} \\ \vec{M}'_{i2} \\ \vdots \end{bmatrix}; \quad \mathbf{I}_B = \begin{bmatrix} p'_0 \\ p'_1 \\ p'_2 \\ \vdots \end{bmatrix} e^{-jk_i \cdot \vec{d}} \quad (4.17)$$

$$\vec{M}'_{i0}{}^T = \left[\vec{M}_1^{+(1)T} \vec{M}_1^{-(1)T} \vec{M}_0^{s(1)T} \right] \quad (4.18)$$

$$\vec{M}'_{i\sigma}{}^T = \left[\vec{M}_{\sigma-1}^{+(1)T} \vec{M}_{\sigma+1}^{-(1)T} \vec{M}_\sigma^{s(1)T} \vec{M}_{-(\sigma+1)}^{+(1)T} \vec{M}_{-(\sigma-1)}^{-(1)T} \vec{M}_\sigma^{s(1)T} \right], \quad \sigma \geq 1 \quad (4.19)$$

with

$$\vec{M}_r^{\pm(1)T} = \left[\vec{M}_{r,|r|}^{\pm(1)'} \vec{M}_{r,|r|+1}^{\pm(1)'} \vec{M}_{r,|r|+2}^{\pm(1)'} \dots \right] \quad (4.20)$$

$$\vec{M}_r^{s(1)T} = \left[\vec{M}_{r,|r|}^{s(1)'} \vec{M}_{r,|r|+1}^{s(1)'} \vec{M}_{r,|r|+2}^{s(1)'} \dots \right] \quad (4.21)$$

Also

$$\mathbf{p}_0^T = \left[p_1^{-T} p_1^{-T} p_0^{sT} \right] \quad (4.22)$$

$$\mathbf{p}_\sigma^T = \left[p_{\sigma-1}^{+T} p_{\sigma+1}^{-T} p_\sigma^{sT} p_{-(\sigma+1)}^{+T} p_{-(\sigma-1)}^{-T} p_\sigma^{sT} \right], \quad \sigma \geq 1 \quad (4.23)$$

with

$$\mathbf{p}_r^{\pm T} = \left[p_{r,|r|}^{\pm} p_{r,|r|+1}^{\pm} p_{r,|r|+2}^{\pm} \dots \right] \quad (4.24)$$

$$\mathbf{p}_r^{sT} = \left[p_{r,|r|}^{s'} p_{r,|r|+1}^{s'} p_{r,|r|+2}^{s'} \dots \right] \quad (4.25)$$

The exponential factor in the expression for \mathbf{I}_B is necessary since $\vec{r}' = \vec{r} - \vec{d}$, and the global reference point for the incident wave is the center O of spheroid A . If the spheroids are identical and Euler angles $\alpha \rightarrow 0^\circ, \beta \rightarrow 0^\circ, \gamma \rightarrow 0^\circ$ (i.e. the spheroids are parallel to each other), it is obvious $\mathbf{I}_B = \mathbf{I}_A e^{-jk_i \cdot \vec{d}}$.

4.3 Expansion of the Scattered Electric Field in terms of Normalized Prolate Spheroidal Vector Wave Functions

According to [20] the scattered E -field from spheroid A can be expanded in the form:

$$\begin{aligned} \vec{E}_{sA} = & \sum_{m=0}^{\infty} \sum_{n=m}^{\infty} \alpha_{mn}^+ \vec{M}_{mn}^{+(4)} + \alpha_{m+1,n}^+ \vec{M}_{m+1,n}^{+(4)} + \sum_{n=0}^{\infty} \alpha_{-1n}^+ \vec{M}_{-1n}^{+(4)} + \alpha_{0n}^+ \vec{M}_{0n}^{+(4)} \\ & + \sum_{m=0}^{\infty} \sum_{n=m}^{\infty} \alpha_{-mn}^- \vec{M}_{-mn}^{-(4)} + \alpha_{-(m+1),n}^- \vec{M}_{-(m+1),n}^{-(4)} \end{aligned} \quad (4.26)$$

where all \vec{M} -vectors in the above equation are evaluated with respect to h_1 which is real. α^+ -s, α^- -s and α^+ -s are the unknown expansion coefficients corresponding to the series expansion of scattered E -field from spheroid A that have to be evaluated.

If same ϕ -sequence of azimuthal harmonics used for the incident field is used in this case, then the scattered field from the spheroid can be written in the generalized column vector product similar to that for \vec{E}_i , [20]:

$$\vec{E}_{sA} = \vec{M}_s^{(4)T} \alpha \quad (4.27)$$

where

$$\vec{M}_s = \begin{bmatrix} \vec{M}_{s0} \\ \vec{M}_{s1} \\ \vec{M}_{s2} \\ \vdots \end{bmatrix}; \quad \alpha = \begin{bmatrix} \alpha_0 \\ \alpha_1 \\ \alpha_2 \\ \vdots \end{bmatrix} \quad (4.28)$$

with

$$\vec{M}_{s0}^T = [\vec{M}_{-1}^{+(4)T} \vec{M}_0^{+(4)T}] \quad (4.29)$$

$$\vec{M}_{s\sigma}^T = [\vec{M}_{\sigma-1}^{+(4)T} \vec{M}_\sigma^{+(4)T} \vec{M}_{-(\sigma-1)}^{-(4)T} \vec{M}_{-\sigma}^{-(4)T}], \quad \sigma \geq 1 \quad (4.30)$$

with $\vec{M}_r^{\pm(4)}$ defined in (4.7) for $i = 4$, and

$$\vec{M}_r^{(4)T} = [\vec{M}_{r,|r|}^{(4)} \vec{M}_{r,|r|+1}^{(4)} \vec{M}_{r,|r|+2}^{(4)} \cdots] \quad (4.31)$$

Also

$$\alpha_0^T = [\alpha_0^{+T} \alpha_0^{-T}] \quad (4.32)$$

$$\alpha_\sigma^T = [\alpha_{\sigma-1}^{+T} \alpha_\sigma^{+T} \alpha_{-(\sigma-1)}^{-T} \alpha_\sigma^{-T}], \quad \sigma \geq 1 \quad (4.33)$$

with

$$\alpha_r^{\pm T} = [\alpha_{r,|r|}^{\pm} \alpha_{r,|r|+1}^{\pm} \alpha_{r,|r|+2}^{\pm} \cdots] \quad (4.34)$$

$$\alpha_r^{*T} = [\alpha_{r,|r|}^* \alpha_{r,|r|+1}^* \alpha_{r,|r|+2}^* \cdots] \quad (4.35)$$

In presence of spheroid B there will be a non-plane wave type of field that will be incident on spheroid A , which is the E -field scattered from spheroid B . The scattered E -field from spheroid B can be expanded in terms of primed coordinates in a manner similar to that for scattered E -field from spheroid A . The scattered field \vec{E}_{sB} acts as a secondary incident field for the spheroid A . Thus we have

$$\begin{aligned} \vec{E}_{sB} = & \sum_{m=0}^{\infty} \sum_{n=m}^{\infty} \beta_{mn}^+ \vec{M}_{mn}^{+(4)'} + \beta_{m+1,n}^+ \vec{M}_{m+1,n}^{+(4)'} + \sum_{n=0}^{\infty} \beta_{-1n}^+ \vec{M}_{-1n}^{+(4)'} + \beta_{0n}^+ \vec{M}_{0n}^{+(4)'} \\ & + \sum_{m=0}^{\infty} \sum_{n=m}^{\infty} \beta_{-mn}^- \vec{M}_{-mn}^{-(4)'} + \beta_{-(m+1),n}^- \vec{M}_{-(m+1),n}^{-(4)'} \end{aligned} \quad (4.36)$$

where all \vec{M}' -vectors in the above equation are evaluated with respect to h_1' which is real. β^+ -s, β^- -s and β^* -s are the unknown expansion coefficients corresponding to the series expansion of scattered E -field from spheroid B that have to be evaluated.

This scattered field from spheroid B can be written in the generalized column vector product similar to that for spheroid A as

$$\vec{E}_{sB} = \vec{M}_{sB}^{(4)T} \beta \quad (4.37)$$

We can use a sequence of ϕ' -harmonics for spheroid B similar to that used in case of spheroid A , and form the following column matrices for the scattered E -field from spheroid B :

$$\vec{M}_{sB} = \begin{bmatrix} \vec{M}'_{s0} \\ \vec{M}'_{s1} \\ \vec{M}'_{s2} \\ \vdots \end{bmatrix}; \quad \beta = \begin{bmatrix} \beta_0 \\ \beta_1 \\ \beta_2 \\ \vdots \end{bmatrix} \quad (4.38)$$

in which the various sub-vectors \vec{M}'_{sr} and β_r are analogous to those for spheroid A , but with the vector wave functions evaluated with respect to primed coordinates.

To impose the boundary conditions on the surface of spheroid A , the field in primed coordinates has to be expressed in terms of vector wave functions of first kind in unprimed coordinates. Since the spheroids are arbitrarily oriented, it is necessary to invoke the rotational-translational addition theorems [24]–[26], which transform each outgoing normalized spheroidal vector wave functions in primed coordinates into a series of incoming normalized spheroidal vector wave functions in unprimed coordinates for $r \leq d$ [27]:

$$\vec{M}_{sB}^{(4)} = [\Gamma] \vec{M}_{sA}^{(1)} \quad (4.39)$$

Utilizing (4.37) and (4.39) we can have:

$$\vec{E}_{sBA} = \vec{M}_{sA}^{(1)T} [\Gamma]^T \beta \quad (4.40)$$

The elements of matrix $[\Gamma]$ are the rotational-translational addition field expansion coefficients given in [24] – [26] (also refer Appendix E). The column vector \vec{M}_{sA} is such that

$$\vec{M}_{sA}^T = [\vec{M}_{sA,0}^T \vec{M}_{sA,1}^T \vec{M}_{sA,2}^T \cdots] \quad (4.41)$$

$$(4.42)$$

where

$$\vec{M}_{BA,0}^T = [\vec{M}_{-1}^{+(1)T} \vec{M}_1^{-(1)T} \vec{M}_0^{s(1)T}] \quad (4.43)$$

$$\vec{M}_{BA,\sigma}^T = [\vec{M}_{\sigma-1}^{+(1)T} \vec{M}_{\sigma+1}^{-(1)T} \vec{M}_\sigma^{s(1)T} \vec{M}_{-(\sigma+1)}^{+(1)T} \vec{M}_{-(\sigma-1)}^{-(1)T} \vec{M}_{-\sigma}^{s(1)T}], \quad \sigma \geq 1 \quad (4.44)$$

with

$$\vec{M}_r^{\pm(1)T} = [\vec{M}_{r,|r|}^{\pm(1)T} \vec{M}_{r,|r|+1}^{\pm(1)T} \vec{M}_{r,|r|+2}^{\pm(1)T} \dots] \quad (4.45)$$

$$\vec{M}_r^{s(1)T} = [\vec{M}_{r,|r|}^{s(1)T} \vec{M}_{r,|r|+1}^{s(1)T} \vec{M}_{r,|r|+2}^{s(1)T} \dots] \quad (4.46)$$

where all \vec{M} -vectors in the above equation are evaluated with respect to h_1 which is real. Also in the presence of spheroid A there will be a non-plane wave type of field incident on spheroid B , which is the E -field scattered from spheroid A . This scattered field from spheroid A has been shown to be of the form:

$$\vec{E}_{sA} = \vec{M}_{sA}^{(4)T} \alpha \quad (4.47)$$

To impose the boundary conditions on the surface of spheroid B , this field in unprimed coordinates has to be expressed in terms of vector wave functions of first kind in primed coordinates. By utilizing the rotational-translational Addition Theorems each outgoing normalized spheroidal vector wave functions in unprimed coordinates is transformed into a series of incoming normalized spheroidal vector wave functions in primed coordinates for $r' \leq d$ [27]:

$$\vec{M}_{sA}^{(4)} = [\Gamma^r] \vec{M}_{AB}^{(1)} \quad (4.48)$$

Utilizing (4.47), (4.48) we can have:

$$\vec{E}_{sAB} = \vec{M}_{AB}^{(1)T} [\Gamma^r]^T \alpha \quad (4.49)$$

The elements of matrix $[\Gamma^r]$ are the rotational-translational addition field expansion coefficients given in [24] - [26] (also refer Appendix E). $\vec{M}_{AB}^{(1)}$ has the same

form as that of $\vec{M}_{BA}^{(1)}$ but with vector wave functions evaluated with respect to primed coordinates.

4.4 Expansion of the Transmitted Electric Field in terms of Normalized Prolate Spheroidal Vector Wave Functions

Since the spheroids are composed of dielectric material, there will be transmitted component of E -field inside the spheroids which is non-plane wave type. Thus the transmitted E -field inside spheroid A can be expanded in terms of normalized prolate spheroidal vector wave functions, given by [23]:

$$\begin{aligned} \vec{E}_{tA} = & \sum_{m=0}^{\infty} \sum_{n=m}^{\infty} \gamma_{mn}^+ \vec{M}_{mn}^{+(1)} + \gamma_{m+1,n}^s \vec{M}_{m+1,n}^{s(1)} + \sum_{n=0}^{\infty} \gamma_{-1n}^+ \vec{M}_{-1n}^{+(1)} + \gamma_{0n}^s \vec{M}_{0n}^{s(1)} \\ & + \sum_{m=0}^{\infty} \sum_{n=m}^{\infty} \gamma_{-mn}^- \vec{M}_{-mn}^{-(1)} + \gamma_{-(m+1),n}^s \vec{M}_{-(m+1),n}^{s(1)} \end{aligned} \quad (4.50)$$

γ^{+} -s, γ^{-} -s and γ^s -s are the unknown expansion coefficients corresponding to the series expansion of transmitted E -field that have to be evaluated. All the \vec{M} -vectors in the equation (4.50) are evaluated with respect to $h_2 = (2\pi F_A/\lambda)\sqrt{\epsilon_{rA}}$.

If the above expansion for \vec{E}_{tA} is also arranged in ϕ -sequence $(0)\phi, (\pm 1)\phi, (\pm 2)\phi, \dots$ then \vec{E}_{tA} can be written in the matrix form

$$\vec{E}_{tA} = \vec{M}_{tA}^{(1)T} \gamma \quad (4.51)$$

where, in terms of unprimed coordinate system of spheroid A , $\vec{M}_{tA}^{(1)}$ is a column vector whose elements are the normalized spheroidal vector wave functions of first kind evaluated with respect to h_2 which is complex, and γ represents a column

vector whose elements are the corresponding unknown expansion coefficients.

$$\vec{M}_{tA} = \begin{bmatrix} \vec{M}_{t0} \\ \vec{M}_{t1} \\ \vec{M}_{t2} \\ \vdots \end{bmatrix}; \quad \gamma = \begin{bmatrix} \gamma_0 \\ \gamma_1 \\ \gamma_2 \\ \vdots \end{bmatrix} \quad (4.52)$$

where

$$\vec{M}_{t0}^T = [\vec{M}_{-1}^{+(1)T} \vec{M}_0^{+(1)T}] \quad (4.53)$$

$$\vec{M}_{t\sigma}^T = [\vec{M}_{\sigma-1}^{+(1)T} \vec{M}_{\sigma}^{+(1)T} \vec{M}_{-(\sigma-1)}^{- (1)T} \vec{M}_{-\sigma}^{- (1)T}], \quad \sigma \geq 1 \quad (4.54)$$

with $\vec{M}_r^{\pm(1)}$ defined in (4.7) for $i = 1$, and

$$\vec{M}_r^{s(1)T} = [\vec{M}_{r,|r|}^{s(1)} \vec{M}_{r,|r|+1}^{s(1)} \vec{M}_{r,|r|+2}^{s(1)} \cdots] \quad (4.55)$$

Also

$$\gamma_0^T = [\gamma_{-1}^{+T} \gamma_0^{+T}] \quad (4.56)$$

$$\gamma_{\sigma}^T = [\gamma_{\sigma-1}^{+T} \gamma_{\sigma}^{+T} \gamma_{-(\sigma-1)}^{-T} \gamma_{-\sigma}^{-T}], \quad \sigma \geq 1 \quad (4.57)$$

with

$$\gamma_r^{\pm T} = [\gamma_{r,|r|}^{\pm} \gamma_{r,|r|+1}^{\pm} \gamma_{r,|r|+2}^{\pm} \cdots] \quad (4.58)$$

$$\gamma_r^{sT} = [\gamma_{r,|r|}^s \gamma_{r,|r|+1}^s \gamma_{r,|r|+2}^s \cdots] \quad (4.59)$$

The transmitted E -field inside spheroid B can be expressed in terms of normalized prolate spheroidal vector wave functions similar to that for spheroid A .

$$\begin{aligned} \vec{E}_{tB} = & \sum_{m=0}^{\infty} \sum_{n=m}^{\infty} \delta_{mn}^+ \vec{M}_{mn}^{+(1)} + \delta_{m+1,n}^s \vec{M}_{m+1,n}^{s(1)} + \sum_{n=0}^{\infty} \delta_{-1n}^+ \vec{M}_{-1n}^{+(1)} + \delta_{0n}^s \vec{M}_{0n}^{s(1)} \\ & + \sum_{m=0}^{\infty} \sum_{n=m}^{\infty} \delta_{-mn}^- \vec{M}_{-mn}^{-(1)} + \delta_{-(m+1),n}^s \vec{M}_{-(m+1),n}^{s(1)} \end{aligned} \quad (4.60)$$

Thus in matrix form we can write

$$\vec{E}_{tB} = \vec{M}'_{tB(1)T} \delta \quad (4.61)$$

where, in terms of primed coordinate system of spheroid B , $\vec{M}'_{tB(1)}$ is a column vector whose elements are the normalized spheroidal vector wave functions of first kind evaluated with respect to $h'_2 (= (2\pi F_B/\lambda) \cdot \sqrt{\epsilon_r B})$ which is complex, and δ represents a column vector whose elements are the corresponding unknown expansion coefficients.

$$\vec{M}'_{tB} = \begin{bmatrix} \vec{M}'_{tB10} \\ \vec{M}'_{tB11} \\ \vec{M}'_{tB12} \\ \vdots \end{bmatrix}; \quad \delta = \begin{bmatrix} \delta_0 \\ \delta_1 \\ \delta_2 \\ \vdots \end{bmatrix} \quad (4.62)$$

in which the various sub-vectors \vec{M}'_{tr} and δ_r are analogous to those for spheroid A , but with vector wave functions evaluated in primed coordinates.

4.5 Expansion of Incident, Scattered and Transmitted Magnetic Fields in terms of Normalized Prolate Spheroidal Vector Wave Functions

Using the Maxwell's equation

$$\vec{H} = j k^{-1} (\epsilon/\mu)^{1/2} \nabla \times \vec{E} \quad (4.63)$$

where k is the wavenumber (or propagation constant), ϵ and μ are the permittivity and permeability of the medium respectively, we can obtain expansions of the different H -fields inside and outside the scatterers in terms of appropriate normalized spheroidal vector wave functions from those of the corresponding E -fields. We do this by replacing \vec{M} by \vec{N} and multiplying each expansion by the

appropriate value of $j(\epsilon/\mu)^{1/2}$. Assuming media outside and inside the scatterers are non-ferromagnetic, we can write for spheroid A :

$$\vec{H}_{iA} = j(\epsilon_1/\mu_0)^{1/2} \vec{N}_{iA}^{(1)T} \mathbf{I}_A \quad (4.64)$$

$$\vec{H}_{eBA} = j(\epsilon_1/\mu_0)^{1/2} \vec{N}_{BA}^{(1)T} [\Gamma]^T \beta \quad (4.65)$$

$$\vec{H}_{iA} = j(\epsilon_1/\mu_0)^{1/2} \vec{N}_{iA}^{(4)T} \alpha \quad (4.66)$$

$$\vec{H}_{iA} = j(\epsilon_A/\mu_0)^{1/2} \vec{N}_{iA}^{(1)T} \gamma \quad (4.67)$$

where ϵ_1 and ϵ_A are the permittivities of the media outside and inside the scatterer A respectively, μ_0 is permeability of free space.

Similarly for spheroid B we have

$$\vec{H}_{iB} = j(\epsilon_1/\mu_0)^{1/2} \vec{N}_{iB}^{(1)T} \mathbf{I}_B \quad (4.68)$$

$$\vec{H}_{eAB} = j(\epsilon_1/\mu_0)^{1/2} \vec{N}_{AB}^{(1)T} [\Gamma]^T \beta \quad (4.69)$$

$$\vec{H}_{iB} = j(\epsilon_1/\mu_0)^{1/2} \vec{N}_{iB}^{(4)T} \alpha \quad (4.70)$$

$$\vec{H}_{iB} = j(\epsilon_B/\mu_0)^{1/2} \vec{N}_{iB}^{(1)T} \gamma \quad (4.71)$$

in which ϵ_1 and ϵ_B are the permittivities of the media outside and inside the scatterer B respectively.

4.6 Application of Boundary Conditions

From the analysis shown in the previous sections we find that the total E -field outside the spheroid A in the system of unprimed spheroidal coordinates can be given as

$$\vec{E}_A = \vec{E}_{iA} + \vec{E}_{eBA} + \vec{E}_{eA} = \vec{M}_{iA}^{(1)T} \mathbf{I}_A + \vec{M}_{BA}^{(1)T} [\Gamma]^T \beta + \vec{M}_{iA}^{(4)T} \alpha \quad (4.72)$$

and the total E -field inside the spheroid A is given as

$$\vec{E}_{iA} = \vec{M}_{iA}^{(1)T} \gamma \quad (4.73)$$

The total H -field outside and inside the spheroid A in the system of unprimed spheroidal coordinates can be respectively given as

$$\vec{H}_A = \vec{H}_{iA} + \vec{H}_{eBA} + \vec{H}_{eA} = j(\epsilon_1/\mu_0)^{1/2} \left(\vec{N}_{iA}^{(1)T} \mathbf{I}_A + \vec{N}_{BA}^{(1)T} [\Gamma]^T \beta + \vec{N}_{eA}^{(4)T} \alpha \right) \quad (4.74)$$

and

$$\vec{H}_{iA} = j(\epsilon_A/\mu_0)^{1/2} \vec{N}_{iA}^{(1)T} \gamma \quad (4.75)$$

Similarly total E -field outside and inside the spheroid B in the system of primed spheroidal coordinates can be respectively given as

$$\vec{E}_B = \vec{E}_{iB} + \vec{E}_{eAB} + \vec{E}_{eB} = \vec{M}_{iB}^{(1)T} \mathbf{I}_B + \vec{M}_{AB}^{(1)T} [\Gamma']^T \alpha + \vec{M}_{eB}^{(4)T} \beta \quad (4.76)$$

and

$$\vec{E}_{iB} = \vec{M}_{iB}^{(1)T} \delta \quad (4.77)$$

The total H -field outside and inside the spheroid B in the system of primed spheroidal coordinates can be respectively given as

$$\vec{H}_B = \vec{H}_{iB} + \vec{H}_{eAB} + \vec{H}_{eB} = j(\epsilon_1/\mu_0)^{1/2} \left(\vec{N}_{iB}^{(1)T} \mathbf{I}_B + \vec{N}_{AB}^{(1)T} [\Gamma']^T \alpha + \vec{N}_{eB}^{(4)T} \beta \right) \quad (4.78)$$

and

$$\vec{H}_{iB} = j(\epsilon_B/\mu_0)^{1/2} \vec{N}_{iB}^{(1)T} \delta \quad (4.79)$$

Boundary conditions require that across the surface of each spheroid the tangential components (η and ϕ) of the E -field and as well as those of H -field (assuming no surface current) must be continuous.

Spheroid A:

Let us first consider spheroid A . Application of the boundary conditions on equations (4.72)-(4.75) yields:

$$(\vec{M}_{iA}^{(1)T} I_A + \vec{M}_{\beta A}^{(1)T} [\Gamma]^T \beta + \vec{M}_{\alpha A}^{(4)T} \alpha \times \hat{\xi}|_{\xi=\xi_A} = \vec{M}_{iA}^{(1)T} \gamma \times \hat{\xi}|_{\xi=\xi_A} \quad (4.80)$$

$$(\vec{N}_{iA}^{(1)T} I_A + \vec{N}_{\beta A}^{(1)T} [\Gamma]^T \beta + \vec{N}_{\alpha A}^{(4)T} \alpha) \times \hat{\xi}|_{\xi=\xi_A} = \left(\frac{\epsilon_A}{\epsilon_1}\right)^{1/2} \vec{N}_{iA}^{(1)T} \gamma \times \hat{\xi}|_{\xi=\xi_A} \quad (4.81)$$

Following the procedures developed in [15], both sides of (4.80), (4.81) are scalar multiplied by the vector functions

$$\left\{ \begin{array}{l} l_\eta \hat{\eta} \\ l_\phi \hat{\phi} \end{array} \right\} S_{|m|, |m|+N} e^{\pm j(m \pm 1)\phi}, \quad N = 0, 1, 2, \dots$$

and the products are integrated over the surface of the spheroid A with respect to both η ($-1 \leq \eta \leq 1$) and ϕ ($0 \leq \phi \leq 2\pi$), where

$$l_\eta = j2F_A(\xi_A^2 - \eta^2)^{1/2}$$

$$l_\phi = 2F_A(\xi_A^2 - \eta^2)$$

for equation (4.80) and

$$l_\eta = 2F_A^2(\xi_A^2 - \eta^2)^{3/2}/(\xi_A^2 - 1)^{1/2}$$

$$l_\phi = j2F_A^2(\xi_A^2 - \eta^2)/(\xi_A^2 - 1)$$

for equation (4.81). Using the orthogonality properties of angle functions and complex exponentials, we obtain the following set of coupled algebraic equations of the form:

$$[P_{MA}] \gamma + [0] \delta + [Q_{MA}] \alpha + [R_{MBA}] [\Gamma]^T \beta = [R_{MA}] [I_A] \quad (4.82)$$

$$[P_{NA}] \gamma + [0] \delta + [Q_{NA}] \alpha + [R_{NBA}] [\Gamma]^T \beta = [R_{NA}] [I_A] \quad (4.83)$$

where the elements of $[P_{MA}]$, $[Q_{MA}]$, $[R_{MBA}]$, $[P_{NA}]$, $[Q_{NA}]$, $[R_{NBA}]$, $[R_{MA}]$ and $[R_{NA}]$ are defined in Appendix B.

Spheroid B:

For spheroid B by applying boundary conditions and performing subsequent η -integration and ϕ -integration in a manner similar to that of spheroid A , we obtain the following set of coupled algebraic equations:

$$[0] \gamma + [P_{MB}] \delta + [R_{MAB}][\Gamma]^T \alpha + [Q_{MB}] \beta = [R_{MB}] \mathbf{I}_B \quad (4.84)$$

$$[0] \gamma + [P_{NB}] \delta + [R_{NAB}][\Gamma]^T \alpha + [Q_{NB}] \beta = [R_{NB}] \mathbf{I}_B \quad (4.85)$$

where the elements of $[P_{MB}]$, $[Q_{MB}]$, $[R_{MAB}]$, $[P_{NB}]$, $[Q_{NB}]$, $[R_{NAB}]$, $[R_{MB}]$ and $[R_{NB}]$ are defined in Appendix B.

4.7 System Matrix $[G]$

Combining (4.82), (4.83), (4.84) and (4.85) we can write:

$$\begin{bmatrix} [P_{MA}] & [0] & [Q_{MA}] & [R_{MBA}][\Gamma]^T \\ [P_{NA}] & [0] & [Q_{NA}] & [R_{NBA}][\Gamma]^T \\ [0] & [P_{MB}] & [R_{MAB}][\Gamma]^T & [Q_{MB}] \\ [0] & [P_{NB}] & [R_{NAB}][\Gamma]^T & [Q_{NB}] \end{bmatrix} \cdot \begin{bmatrix} \gamma \\ \delta \\ \alpha \\ \beta \end{bmatrix} = \begin{bmatrix} [R_{MA}] \mathbf{I}_A \\ [R_{NA}] \mathbf{I}_A \\ [R_{MB}] \mathbf{I}_B \\ [R_{NB}] \mathbf{I}_B \end{bmatrix} \quad (4.86)$$

Equation (4.86) can be written in the form

$$S = [G] \mathbf{I} \quad (4.87)$$

where

$$S = \begin{bmatrix} \gamma \\ \delta \\ \alpha \\ \beta \end{bmatrix} \quad (4.88)$$

$$\mathbf{I} = \begin{bmatrix} \mathbf{I}_A \\ \mathbf{I}_B \end{bmatrix} \quad (4.89)$$

$$[G] = \begin{bmatrix} [P_{MA}] & [0] & [Q_{MA}] & [R_{MBA}][\Gamma]^T \\ [P_{NA}] & [0] & [Q_{NA}] & [R_{NBA}][\Gamma]^T \\ [0] & [P_{MB}] & [R_{MAB}][\Gamma']^T & [Q_{MB}] \\ [0] & [P_{NB}] & [R_{NAB}][\Gamma']^T & [Q_{NB}] \end{bmatrix}^{-1} \begin{bmatrix} [R_{MA}] & [0] \\ [R_{NA}] & [0] \\ [0] & [R_{MB}] \\ [0] & [R_{NB}] \end{bmatrix} \quad (4.90)$$

$[G]$ is the generalized system matrix which is independent of the direction and polarization of the incident wave. Solution in the form $S = [G]\mathbf{I}$ eliminates the process of repeatedly solving a new set of equations for new angle of incidence, which is a great advantage in numerical computation.

4.8 Far-Field Expansions and Scattering Cross sections

Let the distances from the centers of spheroids A and B to the point of observation P be denoted by \bar{r} and \bar{r}' respectively. Of practical interest is the scattered field in the far zone of the A - B system for $|\bar{r}| \rightarrow \infty$. To calculate the far-field scattering cross sections we have to evaluate the asymptotic values of $h_1\xi$, $h_1'\xi'$, η , $\dot{\eta}$, η' and $\dot{\eta}'$. The asymptotic forms of spheroidal vector functions are obtained by neglecting ξ^{-2} and its higher inverse power terms. According to [20]:

$$\left. \begin{array}{l} h_1\xi \rightarrow kr \\ \eta \rightarrow \cos\theta \\ \dot{\eta} \rightarrow -\dot{\theta} \\ h_1'\xi' \rightarrow kr' \\ \eta' \rightarrow \cos\theta' \\ \dot{\eta}' \rightarrow -\dot{\theta}' \end{array} \right\} \quad (4.91)$$

Also as $r \rightarrow \infty$ it can be shown that [20]:

$$\left. \begin{aligned} R_{mn}^{(4)}(h_1, \xi) &\rightarrow j^{n+1} \frac{e^{-jk_r r}}{kr} \\ \frac{d}{d\xi} R_{mn}^{(4)}(h_1, \xi) &\rightarrow j^n k F \frac{e^{-jk_r r}}{kr} \\ R_{mn}^{(4)}(h'_1, \xi') &\rightarrow j^{n+1} \frac{e^{-jk_r r}}{kr} e^{j\vec{k}_s \cdot \vec{d}} \\ \frac{d}{d\xi'} R_{mn}^{(4)}(h'_1, \xi') &\rightarrow j^n k F' \frac{e^{-jk_r r}}{kr} e^{j\vec{k}_s \cdot \vec{d}} \end{aligned} \right\} \quad (4.92)$$

where

$$\vec{k}_s = k_0 (\hat{x} \sin \theta \cos \phi + \hat{y} \sin \theta \sin \phi + \hat{z} \cos \theta) \quad (4.93)$$

$$\vec{d} = d (\hat{x} \sin \theta_0 \cos \phi_0 + \hat{y} \sin \theta_0 \sin \phi_0 + \hat{z} \cos \theta_0) \quad (4.94)$$

$h_1 = 2\pi F_A/\lambda$ and $h'_1 = 2\pi F_B/\lambda$. \vec{k}_s is the k -vector of the far-scattered field where spheroidal coordinates are asymptotic to spherical coordinates. Thus in the far zone the scattered E -field with respect to the origin O of spheroid A , which is chosen to be the global origin, is given by [20] and [27]:

$$\begin{aligned} \vec{E}_s &= \vec{E}_{sA} + \vec{E}_{sB} \\ &= \frac{e^{-jk_r r}}{kr} \left[F_{\theta A}(\theta, \phi) \hat{\theta} + F_{\phi A}(\theta, \phi) \hat{\phi} + F_{\theta' B}(\theta', \phi') \hat{\theta}' + F_{\phi' B}(\theta', \phi') \hat{\phi}' \right] \\ &= \frac{e^{-jk_r r}}{kr} \left[F_{\theta A}(\theta, \phi) \hat{\theta} + F_{\phi A}(\theta, \phi) \hat{\phi} + F_{\theta' B}(\theta', \phi') \{g_1 \hat{\theta} + g_2 \hat{\phi}\} \right. \\ &\quad \left. + F_{\phi' B}(\theta', \phi') \{g_3 \hat{\theta} + g_4 \hat{\phi}\} \right] \\ &= \frac{e^{-jk_r r}}{kr} \left[F_{\theta}(\theta, \phi) \hat{\theta} + F_{\phi}(\theta, \phi) \hat{\phi} \right] \end{aligned} \quad (4.95)$$

where

$$F_{\theta}(\theta, \phi) = F_{\theta A}(\theta, \phi) + g_1 F_{\theta' B}(\theta', \phi') + g_3 F_{\phi' B}(\theta', \phi') \quad (4.96)$$

$$F_{\phi}(\theta, \phi) = F_{\phi A}(\theta, \phi) + g_2 F_{\theta' B}(\theta', \phi') + g_4 F_{\phi' B}(\theta', \phi') \quad (4.97)$$

$$[g_1 \ g_2]^T = [\Omega][C][\cos \theta' \cos \phi' \ \cos \theta' \sin \phi' \ -\sin \theta']^T \quad (4.98)$$

$$[g_3 \ g_4]^T = [\Omega][C][-\sin \phi' \ \cos \phi' \ 0]^T \quad (4.99)$$

$$F_\theta(\theta, \phi) = -\sum_{m=0}^{\infty} \sum_{n=m}^{\infty} j^{n+1} \left[\frac{S_{mn}}{2} \{(\alpha_{mn}^+ - \alpha_{mn}^-) \cos(m+1)\phi\} \right. \\ \left. + j(\alpha_{mn}^+ + \alpha_{mn}^-) \sin(m+1)\phi \right] + \frac{S_{1n}}{2} \alpha_{-1n}^+ \quad (4.100)$$

$$F_\phi(\theta, \phi) = \sum_{m=0}^{\infty} \sum_{n=m}^{\infty} j^n \left[\frac{1}{2} \eta S_{mn} \{(\alpha_{mn}^+ + \alpha_{mn}^-) \cos(m+1)\phi\} \right. \\ \left. + j(\alpha_{mn}^+ - \alpha_{mn}^-) \sin(m+1)\phi \right] \\ - \sqrt{1 - \eta^2} S_{m+1,n} \{(\alpha_{m+1,n}^e + \alpha_{-(m+1),n}^e) \cos(m+1)\phi\} \\ + j(\alpha_{m+1,n}^e - \alpha_{-(m+1),n}^e) \sin(m+1)\phi \} \\ + \frac{1}{2} \eta S_{1n} \alpha_{-1n}^+ - \sqrt{1 - \eta^2} S_{0n} \alpha_{0n}^e \quad (4.101)$$

$$[\Omega] = \begin{bmatrix} \cos \theta \cos \phi & \cos \theta \sin \phi & -\sin \theta \\ -\sin \phi & \cos \phi & 0 \end{bmatrix} \quad (4.102)$$

$$[C] = \begin{bmatrix} c_{xx'} & c_{xy'} & c_{xz'} \\ c_{yx'} & c_{yy'} & c_{yz'} \\ c_{zx'} & c_{zy'} & c_{zz'} \end{bmatrix} \quad (4.103)$$

The expressions for $F_{\psi B}(\theta', \phi')$ and $F_{\psi A}(\theta', \phi')$ are obtained from those of $F_{\theta A}(\theta, \phi)$ and $F_{\phi A}(\theta, \phi)$ respectively by replacing α -s by β -s and multiplying each expression by an overall phase factor $\exp[j\vec{k}_s \cdot \vec{d}]$ to account for the vector displacement \vec{d} from the global origin O . Also the functions in primed variables θ', ϕ' are expressed in terms of unprimed variables θ, ϕ as follows. The direction of the scattered wave vector \vec{k}_s in the far-field with respect to primed coordinate system is given by

$$\vec{k}_s = k_0 (\hat{x}' \sin \theta' \cos \phi' + \hat{y}' \sin \theta' \sin \phi' + \hat{z}' \cos \theta') \quad (4.104)$$

Substituting $\hat{x}, \hat{y}, \hat{z}$ in (4.93) in terms of $\hat{x}', \hat{y}', \hat{z}'$ (refer to (4.14)) we get from (4.93) and (4.104) the following set of relations, from which knowing θ, ϕ and the direction cosines $c_{ax'}, c_{ay'}, c_{az'}$ ($a = x, y$ or z) (refer to (4.15)), we can determine θ' and ϕ' :

$$\left. \begin{aligned} \sin \theta' \cos \phi' &= c_{xx'} \sin \theta \cos \phi + c_{yx'} \sin \theta \sin \phi + c_{zx'} \cos \theta \\ \sin \theta' \sin \phi' &= c_{xy'} \sin \theta \cos \phi + c_{yy'} \sin \theta \sin \phi + c_{zy'} \cos \theta \\ \cos \theta' &= c_{xz'} \sin \theta \cos \phi + c_{yz'} \sin \theta \sin \phi + c_{zz'} \cos \theta \end{aligned} \right\}$$

The expressions needed for calculations of bistatic and monostatic radar cross sections in the far field are given by equations (3.63) - (3.65).

4.9 Results of Numerical Computation

Numerical results are presented in the form of normalized bistatic and monostatic (backscattering) radar cross sections in the far field for a system of two uniformly lossy dielectric prolate spheroids in arbitrary orientation, each with axial ratio $a/b = 2$ and 10, and with different values of complex relative permittivity (ϵ_r), Euler angles (α, β, γ) and displacement of their centers specified by (d, θ_0, ϕ_0).

Since the series expansions of the E and H -fields in terms of the spheroidal vector wave functions are infinite in extent, all the matrices of (4.86) have infinite size. Thus to obtain numerical results of desired accuracy one has to truncate the series and matrices accordingly. The truncation procedure discussed in Chapter 3 is followed here. Since F_p and F_q in equations (4.100) and (4.101) respectively are true for $m \geq 0$, we compute the radar cross sections for $m = 0, 1$.

At this point it is pertinent to mention about the limitation on the distance between the spheroids for some non-axially displaced cases while using rotational-translational addition theorems. For a distance d of separation between two spheroids (as shown in Fig. 4.1) the rotational-translational addition theorems for spheroidal vector wave functions, employed to transform the outgoing wave from spheroid B into the incoming wave at spheroid A , are valid strictly within the region enclosed by a sphere of radius d and having center at global origin O . Thus rotational-translational addition theorems can hold good for all points on spheroid A only when $a_A \leq d$, where a_A is the semi-major axis length of spheroid A and d is the radius of the sphere of convergence. Similar arguments are true for spheroid B .

In order to study the scattering characteristics in the resonance region, where

the wavelength of the incident radiation is comparable to the length of semi-major axis of each spheroid, we choose $a_A = a_B = a = \lambda/4$. This restricts the value of d to $d \geq \lambda/4$. So since $k_1 a = \pi/2$, in order to truncate the series and matrices all the results in this thesis have been obtained with $n = |m|, |m| + 1, |m| + 2, \dots, |m| + 5$ for each value of m corresponding to the above ϕ -harmonics, and $N = 0, 1, 2, \dots, 5$.

Fig. 4.2(a) shows the computed normalized bistatic cross section $\pi\sigma(\theta)/\lambda^2$ as a function of scattering angle θ corresponding to the axial excitation ($\theta_i = 0$) of incident wave for two identical uniformly lossy dielectric spheroids each of semimajor axis length of $\lambda/4$, complex relative permittivity being $\epsilon_{rA} = \epsilon_{rB} = 2 - j0.5$, and axially displaced (center of spheroid B lying on the axis of symmetry of spheroid A i.e. z -axis) by $d = \lambda/2$ Fig. 4.2(b) presents the normalized bistatic cross section for the same spheroids and excitation but with their centers separated by a distance $d = \lambda$ along z -axis. In Fig. 4.3 we present the normalized bistatic cross section by choosing complex relative permittivity $\epsilon_{rA} = \epsilon_{rB} = 4 - j0.5$. In both Fig. 4.2 and Fig. 4.3 we consider the Euler angles to be $\alpha = 30^\circ, \beta = 45^\circ, \gamma = 60^\circ$.

From Fig. 4.2 and Fig. 4.3 we observe that as the axial ratio changes from 2 to 10 there is a decrease in magnitude of bistatic cross section in both E -plane and H -plane. This is due to the reduction in the available scattering area for the thin spheroid with axial ratio 10. Also with the increase of $d = \lambda/2$ to $d = \lambda$ we observe that E -plane and H -plane bistatic cross sections show more oscillations, which is due to more pronounced effect of multiple scattering. Also the absence of perfect nulls may be attributed to multiple scattering.

Fig. 4.4(a) shows the computed normalized monostatic cross section $\pi\sigma(\theta_i, 0)/\lambda^2$ as a function of aspect angle θ_i in terms of TE and TM polarization of incident

wave for two identical uniformly lossy dielectric spheroids each of semimajor axis length of $\lambda/4$, complex relative permittivity being $\epsilon_{rA} = \epsilon_{rB} = 2 - j0.5$, and axially displaced (center of spheroid B lying on the axis of symmetry of spheroid A i.e. z -axis) by $\lambda/2$. Fig. 4.4(b) presents the normalized monostatic cross section for the same spheroids and excitation but with their centers separated by a distance λ along z -axis. In Fig. 4.5 we present the normalized monostatic cross section by choosing complex relative permittivity $\epsilon_{rA} = \epsilon_{rB} = 4 - j0.5$. In both Fig. 4.4 and Fig. 4.5 we consider the Euler angles to be $\alpha = 30^\circ, \beta = 45^\circ, \gamma = 60^\circ$.

From each of the four figures in Fig. 4.4 and Fig. 4.5 respectively, we find that the minima of monostatic cross section corresponding to TE polarization of incident field and that corresponding to TM polarization of incident field occur at almost same value of θ_i . However, since the spheroids are arbitrarily oriented, at $\theta_i = 0^\circ$ the value of backscattering cross section corresponding to TE polarization of incident excitation is different from that corresponding to TM polarization of incident wave, unlike what we have observed in [20], [23] and [43]. The same observation holds good for $\theta_i = 180^\circ$. We can also notice that minima occur at almost at the same positions as in Fig. 4.2 and Fig. 4.3, and also as d increases monostatic cross section, corresponding to both TE and TM polarization of incident wave, show more oscillations which is due to more pronounced effect of multiple scattering.

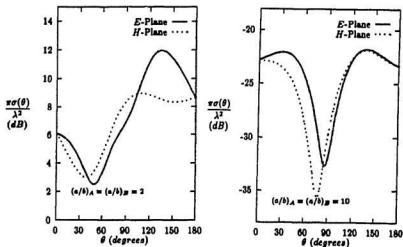
Fig. 4.6 gives the plots of normalized backscattering cross section for broadside displacement of two identical spheroids separated by $d = \lambda/2$ in the direction of x -axis ($\theta_0 = 90^\circ, \phi = 0^\circ$), with Euler angles $\alpha = 30^\circ, \beta = 45^\circ, \gamma = 60^\circ$ and complex relative permittivity: (a) $\epsilon_{rA} = \epsilon_{rB} = 2 - j0.5$; (b) $\epsilon_{rA} = \epsilon_{rB} = 4 - j0.5$. From this figure we find that that for axial ratio $a/b = 10$ of the spheroids, there

is a significant difference in the value of monostatic cross section at $\theta_i = 0^\circ$ for *TE* and *TM* polarization of incident wave unlike what has been explained in [20], [23] and [43].

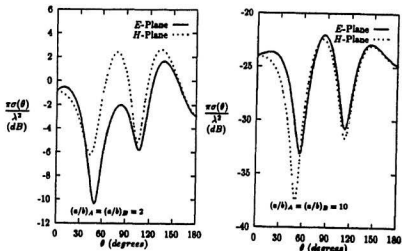
In Fig. 4.7 the variation of monostatic cross section as function of aspect angle is presented for two spheroids of different values of axial ratio and complex relative permittivity. The center O' of spheroid B has spherical coordinates: $d = \lambda/2, \theta_0 = 60^\circ, \phi_0 = 20^\circ$ with respect to $Oxyz$ -system; the Euler angles are chosen to be $\alpha = 30^\circ, \beta = 45^\circ, \gamma = 60^\circ$: (a) $\epsilon_{rA} = 2 - j0.5, \epsilon_{rB} = 3 - j0.5$, (b) $\epsilon_{rA} = 3 - j0.5, \epsilon_{rB} = 4 - j0.5$, (c) $\epsilon_{rA} = 2 - j0.1, \epsilon_{rB} = 3 - j0.1$, (d) $\epsilon_{rA} = 3 - j0.1, \epsilon_{rB} = 4 - j0.1$.

In Fig. 4.8 the variation of monostatic cross section as function of aspect angle is presented for two spheroids of different values of axial ratio and complex relative permittivity. Complex relative permittivity of the spheroids are chosen to be $\epsilon_{rA} = 3 - j0.5, \epsilon_{rB} = 4 - j0.5$. The center O' of spheroid B has spherical coordinates: $d = \lambda/2, \theta_0 = 60^\circ, \phi_0 = 20^\circ$ with respect to $Oxyz$ -system. In Fig. 4.8(a) Euler angles are chosen to be $\alpha = 0^\circ, \beta = 45^\circ, \gamma = 0^\circ$, whereas in Fig. 4.8(b) we take Euler angles to be $\alpha = 30^\circ, \beta = 60^\circ, \gamma = 90^\circ$.

It is to be noted, while obtaining results for monostatic cross section we have to consider the variation of aspect angle (θ_i) from 0° to 180° (unlike what have been shown in [20], [23] and [43]) because of the spatial asymmetry of the arbitrarily oriented spheroids.

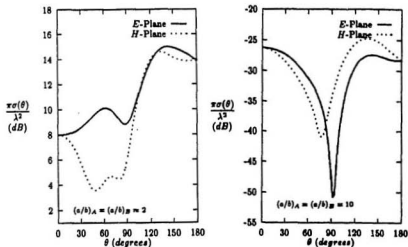


(a) $d = \lambda/2$.

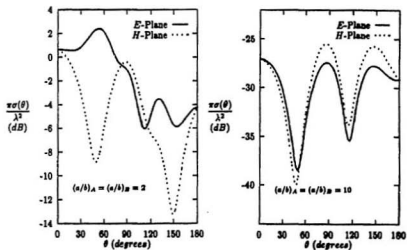


(b) $d = \lambda$.

Figure 4.2: Normalized bistatic cross section for TE polarization of incident wave, as a function of scattering angle for two identical lossy dielectric prolate spheroids with axial ratios 2 and 10, each with semi-major axis length $a_A = a_B = \lambda/4$, complex relative permittivity $\epsilon_{r,A} = \epsilon_{r,B} = 2 - j0.5$, Euler angles $\alpha = 30^\circ$, $\beta = 45^\circ$, $\gamma = 60^\circ$, and displaced along x -axis ($\theta_0 = 0^\circ$, $\phi_0 = 0^\circ$) by: (a) $d = \lambda/2$, (b) $d = \lambda$.



(a) $d = \lambda/2$.



(b) $d = \lambda$.

Figure 4.3: Normalized bistatic cross section for TE polarization of incident wave, as a function of scattering angle for two identical lossy dielectric prolate spheroids with axial ratios 2 and 10, each with semi-major axis length $a_A = a_B = \lambda/4$, complex relative permittivity $\epsilon_{rA} = \epsilon_{rB} = 4 - j0.5$, Euler angles $\alpha = 30^\circ, \beta = 45^\circ, \gamma = 60^\circ$, and displaced along x -axis ($\theta_0 = 0^\circ, \phi_0 = 0^\circ$) by: (a) $d = \lambda/2$, (b) $d = \lambda$.

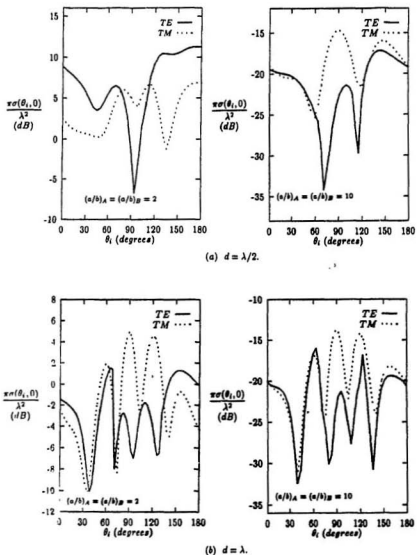


Figure 4.4: Normalized monostatic cross section as a function of aspect angle (θ_i) for two identical lossy dielectric prolate spheroids with axial ratios 2 and 10, each with semi-major axis length $a_A = a_B = \lambda/4$, complex relative permittivity $\epsilon_{rA} = \epsilon_{rB} = 2 - j0.5$, Euler angles $\alpha = 30^\circ, \beta = 45^\circ, \gamma = 60^\circ$, and displaced along z -axis ($\theta_0 = 0^\circ, \phi_0 = 0^\circ$) by: (a) $d = \lambda/2$, (b) $d = \lambda$.

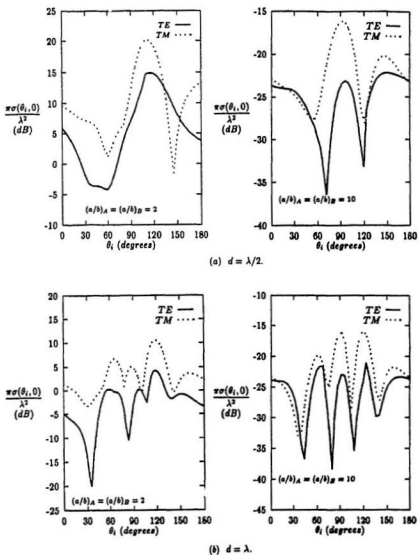


Figure 4.5: Normalized monostatic cross section as a function of aspect angle (θ_i) for two identical lossy dielectric prolate spheroids with axial ratios 2 and 10, each with semi-major axis length $a_A = a_B = \lambda/4$, complex relative permittivity $\epsilon_{r,A} = \epsilon_{r,B} = 4 - j0.5$, Euler angles $\alpha = 30^\circ, \beta = 45^\circ, \gamma = 60^\circ$, and displaced along z-axis ($\theta_0 = 0^\circ, \phi_0 = 0^\circ$) by: (a) $d = \lambda/2$, (b) $d = \lambda$.

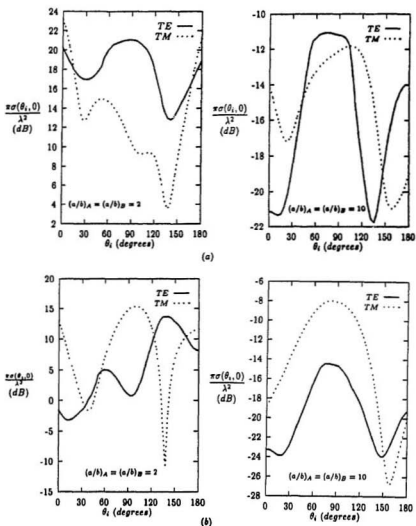


Figure 4.6: Normalized monostatic cross section as a function of aspect angle (θ_i) for two identical lossy dielectric prolate spheroids with axial ratios 2 and 10, each with semi-major axis length $a_A = a_B = \lambda/4$, Euler angles $\alpha = 30^\circ, \beta = 45^\circ, \gamma = 60^\circ$, and displaced along x -axis ($\theta_0 = 90^\circ, \phi_0 = 0^\circ$) by $d = \lambda/2$: (a) $\epsilon_{rA} = \epsilon_{rB} = 2 - j0.5$, (b) $\epsilon_{rA} = \epsilon_{rB} = 4 - j0.5$.

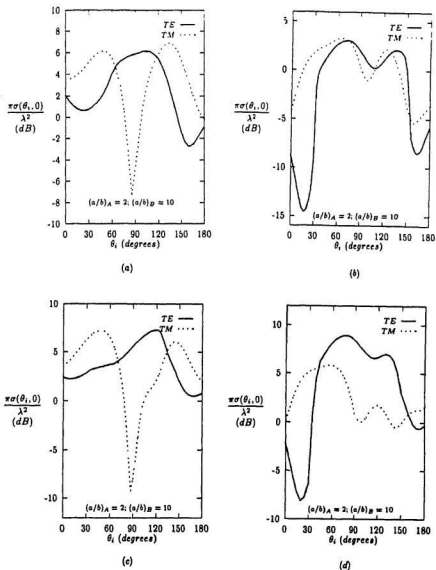


Figure 4.7: Normalized monostatic cross section as a function of aspect angle (θ_i) for two lossy dielectric prolate spheroids with axial ratios 2 and 10 respectively, each with semi-major axis length $a_A = a_B = \lambda/4$, Euler angles $\alpha = 30^\circ, \beta = 45^\circ, \gamma = 60^\circ$, and displaced along the direction $d = \lambda/2, \theta_0 = 60^\circ, \phi_0 = 20^\circ$: (a) $\epsilon_{rA} = 2 - j0.5, \epsilon_{rB} = 3 - j0.5$, (b) $\epsilon_{rA} = 3 - j0.5, \epsilon_{rB} = 4 - j0.5$, (c) $\epsilon_{rA} = 2 - j0.1, \epsilon_{rB} = 3 - j0.1$, (d) $\epsilon_{rA} = 3 - j0.1, \epsilon_{rB} = 4 - j0.1$.

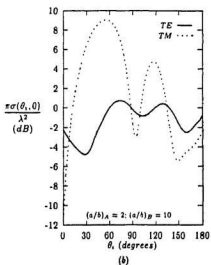
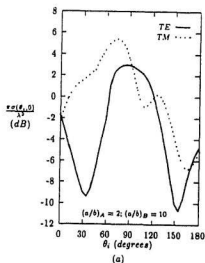


Figure 4.8: Normalized monostatic cross section as a function of aspect angle (θ_i) for two lossy dielectric prolate spheroids with axial ratios 2 and 10 respectively, each with semi-major axis length $a_A = a_B = \lambda/4$ and complex relative permittivity $\epsilon_{rA} = 3 - j0.5$, $\epsilon_{rB} = 4 - j0.5$, and displaced along the direction $d = \lambda/2$, $\theta_0 = 60^\circ$, $\phi_0 = 20^\circ$; Euler angles are given by: (a) $\alpha = 0^\circ, \beta = 45^\circ, \gamma = 0^\circ$; (b) $\alpha = 30^\circ, \beta = 60^\circ, \gamma = 90^\circ$.

Chapter 5

Electromagnetic Plane Wave Scattering by a System of Two Parallel Uniformly Lossy Dielectric Prolate Spheroids

5.1 Introduction

By means of modal series expansions of electromagnetic fields in terms of prolate spheroidal vector wave functions (following the procedures shown in chapter 4), an exact solution is obtained for the electromagnetic scattering by two uniformly lossy dielectric prolate spheroids in parallel orientation. Since the two spheroids are in parallel configuration, the Euler angles (α, β, γ) used in rotational-translational addition theorems [24]-[26] are, in the present case, given by $\alpha \rightarrow 0^\circ$, $\beta \rightarrow 0^\circ$ and $\gamma \rightarrow 0^\circ$. Thus translational addition theorems [19] can be considered as a special case of rotational-translational addition theorems when $\alpha \rightarrow 0^\circ$, $\beta \rightarrow 0^\circ$ and $\gamma \rightarrow 0^\circ$. Numerical results in the form of curves for normalized bistatic and monostatic radar cross sections are given in the resonance region for a variety of two-body system of uniformly lossy dielectric prolate spheroids in parallel orientation having different distances of separation.

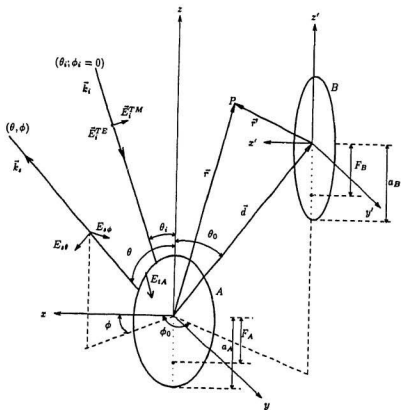


Figure 5.1: Scattering geometry for a system of two parallel uniformly lossy dielectric prolate spheroids with arbitrary incidence and polarization of a plane electromagnetic wave.

5.2 Formulation of the Problem

Consider a system of two parallel uniformly lossy dielectric prolate spheroids as shown in Fig. 5.1. Unprimed coordinates refer to spheroid A and primed coordinates refer to spheroid B . The center O' of spheroid B has spherical coordinates (d, θ_0, ϕ_0) with respect to $Oxyz$. A point P has spheroidal coordinates (ξ, η, ϕ) and (ξ', η', ϕ') with respect to (x, y, z) -system and (x', y', z') -system respectively.

Let us consider a monochromatic plane electromagnetic wave of wavelength λ and of unit amplitude propagating in free space. This wave is propagating in the $x - z$ plane ($\phi_i = 0$) at an angle $\theta_i (\leq \pi/2)$ made with the z -axis, and is incident on $A - B$ system. The media outside and inside the scatterers are assumed to be non-ferromagnetic.

Let the electric field \vec{E}_i of the incident plane wave be linearly polarized in an arbitrary direction. This can be decomposed into two orthogonally polarized \vec{E} vectors \vec{E}_{iTE} and \vec{E}_{iTM} . \vec{H}_i vector is decomposed into orthogonally polarized \vec{H} vectors \vec{H}_{iTE} and \vec{H}_{iTM} . Thus the polarization angle γ_p (the angle which the incident electric field makes with the normal to the plane of incidence ($x - z$ plane)) is such that for TE polarization $\gamma_p = 0$ and for TM polarization $\gamma_p = \pi/2$.

The incident electric field in unprimed coordinate system can be expressed in generalized matrix product [20]

$$\vec{E}_{iA} = \vec{M}_{iA}^{(1)T} \mathbf{I}_A \quad (5.1)$$

In (5.1) a boldface character means a column vector and T indicates the transpose of a matrix. The elements of $\vec{M}_{iA}^{(1)}$ are the normalized spheroidal vector wave functions corresponding to radial function of first kind evaluated with respect to $h_1 (= 2\pi F_A/\lambda)$ which is real. The elements of \mathbf{I}_A are the known incident field

expansion coefficients given in [20] (also refer to (4.2)). The limiting expressions for the elements of I_A when $\gamma_p = 0$ and $\theta_i \rightarrow \pi/2$ are given in [7] (also refer equation (3.39)).

In the presence of spheroid B there will be a non-plane wave type of field incident on spheroid A , which is the E -field scattered from spheroid B . This scattered field from spheroid B can be written in the generalized column vector product [20]

$$\vec{E}_{iB} = \vec{M}_{iB}^{(4)T} \beta \quad (5.2)$$

where, in terms of primed coordinate system of spheroid B , $\vec{M}_{iB}^{(4)T}$ is a column vector whose elements are the outgoing normalized spheroidal vector wave functions corresponding to radial function of fourth kind evaluated with respect to h_1 and β represents a column vector whose elements are the corresponding unknown expansion coefficients.

Now for boundary conditions to hold good, this field in primed coordinates has to be expressed in terms of vector wave functions of first kind in unprimed coordinates. At this point it is necessary to invoke the Translational Addition Theorems [19] which transform each outgoing normalized spheroidal vector wave functions in primed coordinates into a series of incoming normalized spheroidal vector wave functions in unprimed coordinates for $r \leq d$. Thus following the analysis shown in [20], we can write:

$$\vec{E}_{iBA} = \vec{M}_{BA}^{(1)T} [T_{BA}]^T \beta \quad (5.3)$$

The elements of matrix $[T_{BA}]$ are the translational addition field expansion coefficients given in [19] and [20] (also refer Appendix E). Also the elements of the column vector $\vec{M}_{BA}^{(1)}$ are defined in Appendix I of [20] (also refer Chapter 4).

In response to the incident plane wave and the field scattered from spheroid B , the total field scattered by spheroid A is given as [20]:

$$\vec{E}_{sA} = \vec{M}_{sA}^{(4)T} \alpha \quad (5.4)$$

where, in terms of unprimed coordinate system of spheroid A , $\vec{M}_{sA}^{(4)}$ is a column vector whose elements are the outgoing normalized spheroidal vector wave functions corresponding to radial function of fourth kind evaluated with respect to h_1 and α represents a column vector whose elements are the corresponding unknown expansion coefficients.

Since the spheroid is composed of dielectric material there will be a transmitted component of E -field inside the spheroid A , which can be expanded as [23]:

$$\vec{E}_{tA} = \vec{M}_{tA}^{(1)T} \gamma \quad (5.5)$$

where, in terms of unprimed coordinate system of spheroid A , $\vec{M}_{tA}^{(1)}$ is a column vector whose elements are the normalized spheroidal vector wave functions of first kind evaluated with respect to h_2 which is complex. $h_2 = (2\pi F_A/\lambda)\sqrt{\epsilon'_A/\epsilon_0}$; $\epsilon'_A = \epsilon_A - j\sigma_A/\omega$, where ϵ_0 is permittivity of free space, and conductivity (σ_A) of the medium inside the spheroid A is not equal to zero. $\epsilon_{rA} = \epsilon'_A/\epsilon_0$ is complex relative permittivity of the medium inside spheroid A . γ represents a column vector whose elements are the corresponding unknown expansion coefficients.

Using the Maxwell's equation

$$\vec{H} = j k^{-1} (\epsilon/\mu)^{1/2} \nabla \times \vec{E} \quad (5.6)$$

where k is the wavenumber (or propagation constant), ϵ and μ are the permittivity and permeability of the medium respectively, we can obtain expansions

of the different H -fields inside and outside the scatterer in terms of appropriate normalized spheroidal vector wave functions from those of the corresponding E -fields. We do this by replacing \vec{M} by \vec{N} and multiplying each expansion by the appropriate value of $j(\epsilon/\mu)^{1/2}$.

The total E -field and H -field outside the spheroid B can be expanded in a manner identical to that for spheroid A but with respect to normalized spheroidal vector wave functions associated with primed spheroidal coordinates.

5.3 Application of Boundary Conditions

Boundary conditions require that across the surface of each spheroid the tangential components (η and ϕ) of the E -field and as well as those of H -field (assuming no surface current) must be continuous.

Applying the boundary conditions on the surface ($\xi = \xi_A$) of spheroid A , we get:

$$(\vec{M}_{iA}^{(1)T} \mathbf{I}_A + \vec{M}_{BA}^{(1)T} [T_{BA}]^T \beta + \vec{M}_{iA}^{(4)T} \alpha) \times \hat{\xi}|_{\xi=\xi_A} = \vec{M}_{iA}^{(1)T} \gamma \times \hat{\xi}|_{\xi=\xi_A} \quad (5.7)$$

$$(\vec{N}_{iA}^{(1)T} \mathbf{I}_A + \vec{N}_{BA}^{(1)T} [T_{BA}]^T \beta + \vec{N}_{iA}^{(4)T} \alpha) \times \hat{\xi}|_{\xi=\xi_A} = (\epsilon_A/\epsilon_1)^{1/2} \vec{N}_{iA}^{(1)T} \gamma \times \hat{\xi}|_{\xi=\xi_A} \quad (5.8)$$

Both sides of (5.7), (5.8) are scalar multiplied by the vector functions

$$\left\{ \begin{array}{l} l_\eta \hat{\eta} \\ l_\phi \hat{\phi} \end{array} \right\} S_{|m|, |m|+N} e^{\pm j(m \pm 1)\phi}, \quad N = 0, 1, 2, \dots$$

and the products are integrated over the surface of the spheroid A with respect to both η ($-1 \leq \eta \leq 1$) and ϕ ($0 \leq \phi \leq 2\pi$), where

$$l_\eta = j2F_A(\xi_A^2 - \eta^2)^{1/2}$$

$$l_\phi = 2F_A(\xi_A^2 - \eta^2)$$

for equation (5.7) and

$$l_\eta = 2F_A^2(\xi_A^2 - \eta^2)^{3/2}/(\xi_A^2 - 1)^{1/2}$$

$$l_\phi = j2F_A^2(\xi_A^2 - \eta^2)/(\xi_A^2 - 1)$$

for equation (5.8) as given in [23]. Utilizing the orthogonality properties of complex exponentials and angle functions [1], we obtain the following set of coupled algebraic equations of the form:

$$[P_{MA}] \gamma + [0] \delta + [Q_{MA}] \alpha + [R_{MBA}][T_{BA}]^T \beta = [R_{MA}] \mathbf{I}_A \quad (5.9)$$

$$[P_{NA}] \gamma + [0] \delta + [Q_{NA}] \alpha + [R_{NBA}][T_{BA}]^T \beta = [R_{NA}] \mathbf{I}_A \quad (5.10)$$

where the elements of $[P_{MA}]$, $[Q_{MA}]$, $[R_{MBA}]$, $[P_{NA}]$, $[Q_{NA}]$, $[R_{NBA}]$, $[R_{MA}]$ and $[R_{NA}]$ are defined in [20] and [23] (also refer Appendix B).

By applying the boundary conditions on the surface ($\xi = \xi_B$) of spheroid B , and performing subsequent η - and ϕ -integrations we obtain the a set of coupled algebraic equations in a manner similar to that of spheroid A .

$$[0] \gamma + [P_{MB}] \delta + [R_{MAB}][T_{AB}]^T \alpha + [Q_{MB}] \beta = [R_{MB}] \mathbf{I}_B \quad (5.11)$$

$$[0] \gamma + [P_{NB}] \delta + [R_{NAB}][T_{AB}]^T \alpha + [Q_{NB}] \beta = [R_{NB}] \mathbf{I}_B \quad (5.12)$$

where the elements of $[P_{MB}]$, $[Q_{MB}]$, $[R_{MAB}]$, $[P_{NB}]$, $[Q_{NB}]$, $[R_{NAB}]$, $[R_{MB}]$ and $[R_{NB}]$ are defined in Appendix B. The elements of \mathbf{I}_B , the known expansion coefficients corresponding to series expansion of E -field and H -field incident on spheroid B , are given by equation (4.2), but evaluated with respect to primed coordinates. Thus according to [23], we finally get

$$\begin{bmatrix} [P_{MA}] & [0] & [Q_{MA}] & [R_{MBA}][T_{BA}]^T \\ [P_{NA}] & [0] & [Q_{NA}] & [R_{NBA}][T_{BA}]^T \\ [0] & [P_{MB}] & [R_{MAB}][T_{AB}]^T & [Q_{MB}] \\ [0] & [P_{NB}] & [R_{NAB}][T_{AB}]^T & [Q_{NB}] \end{bmatrix} \begin{bmatrix} \gamma \\ \delta \\ \alpha \\ \beta \end{bmatrix} = \begin{bmatrix} [R_{MA}] \mathbf{I}_A \\ [R_{NA}] \mathbf{I}_A \\ [R_{MB}] \mathbf{I}_B \\ [R_{NB}] \mathbf{I}_B \end{bmatrix} \quad (5.13)$$

Equation (5.13) can be written in the form

$$\mathbf{S} = [G]\mathbf{I} \quad (5.14)$$

where

$$\mathbf{S} = \begin{bmatrix} \gamma \\ \delta \\ \alpha \\ \beta \end{bmatrix} \quad (5.15)$$

$$\mathbf{I} = \begin{bmatrix} \mathbf{I}_A \\ \mathbf{I}_B \end{bmatrix} \quad (5.16)$$

$$[G] = \begin{bmatrix} [P_{MA}] & [0] & [Q_{MA}] & [R_{MBA}] [T_{BA}]^T \\ [P_{NA}] & [0] & [Q_{NA}] & [R_{NBA}] [T_{BA}]^T \\ [0] & [P_{MB}] & [R_{MAB}] [T_{AB}]^T & [Q_{MB}] \\ [0] & [P_{NB}] & [R_{NAB}] [T_{AB}]^T & [Q_{NB}] \end{bmatrix}^{-1} \begin{bmatrix} [R_{MA}] & [0] \\ [R_{NA}] & [0] \\ [0] & [R_{MB}] \\ [0] & [R_{NB}] \end{bmatrix} \quad (5.17)$$

All the elements of matrix $[G]$ are defined in Appendix B. $[G]$ is the generalized system matrix which is independent of the direction and polarization of the incident wave. Solution in the form $\mathbf{S} = [G]\mathbf{I}$ eliminates the process of repeatedly solving a new set of equations for new angle of incidence, which is a great advantage in numerical computation.

5.4 Far-Field Expansions and Scattering Cross sections

Of practical interest is the scattered field in the far zone of the system for $|r| \rightarrow \infty$. The asymptotic forms of spheroidal vector functions are obtained by neglecting ξ^{-2} and its higher inverse power terms. Thus in the far zone the scattered E -field with respect to the origin O of spheroid A , which is chosen to be the global origin,

is given by [20]:

$$\begin{aligned}\vec{E}_e &= \vec{E}_{eA} + \vec{E}_{eB} \\ &= \frac{e^{-jkr}}{kr} [F_\theta(\theta, \phi) \hat{\theta} + F_\phi(\theta, \phi) \hat{\phi}]\end{aligned}\quad (5.18)$$

where

$$\begin{aligned}F_\theta(\theta, \phi) &= F_{\theta A}(\theta, \phi) + F_{\theta B}(\theta, \phi) \\ F_\phi(\theta, \phi) &= F_{\phi A}(\theta, \phi) + F_{\phi B}(\theta, \phi)\end{aligned}\quad (5.19)$$

where $F_{\theta A}(\theta, \phi)$, $F_{\phi A}(\theta, \phi)$, $F_{\theta B}(\theta, \phi)$ and $F_{\phi B}(\theta, \phi)$ are defined in [20].

The expressions needed for calculation of bistatic and monostatic radar cross sections in the far field are given by equations (3.63) – (3.65).

5.5 Results of Numerical Computation

Numerical results are presented in the form of normalized bistatic and monostatic (backscattering) radar cross sections in the far field for a system of two parallel uniformly lossy dielectric prolate spheroids, each with axial ratio $a/b = 2$ and 10, and with different values of complex relative permittivity (ϵ_r), and displacement of their centers specified by (d, θ_0, ϕ_0) . Since the series expansions of the E and H -fields in terms of the spheroidal vector wave functions are infinite in extent, one has to truncate accordingly the matrices given in (5.13). The truncation scheme used here, is the one that was discussed in previous chapters. For each m , N in $S_{|m|, |m|+N}$ can be given as $N = 0, 1, 2, \dots, n_t - 1$. Also it is found that ϕ -harmonics $(0)\phi, (\pm 1)\phi, (\pm 2)\phi$ give at least two significant digit accuracy in the computed results of the radar cross sections. In order to study the scattering characteristics in the resonance region we choose $a_A = a_B = \lambda/4$.

Fig. 5.2 shows the computed normalized bistatic cross section corresponding to axial excitation ($\theta_i = 0$) of two identical uniformly lossy dielectric spheroids with $\epsilon_{rA} = \epsilon_{rB} = 2 - j0.5$, each of semimajor axis length of $\lambda/4$ placed in contact with each other end to end, the centers of two spheroids being separated along z -axis by: (a) $\lambda/2$, (b) λ . In Fig. 5.3 the normalized bistatic cross section is shown for $\epsilon_{rA} = \epsilon_{rB} = 4 - j0.5$. From Fig. 5.2 and Fig. 5.3 we observe that as the axial ratio changes from 2 to 10 there is a decrease in magnitude of bistatic cross section in both E -plane and H -plane. This is due to the reduction in the available scattering area for the thin spheroid ($a/b = 10$). Also due to more pronounced effect of multiple scattering, as d increases E -plane and H -plane bistatic cross sections show more oscillations.

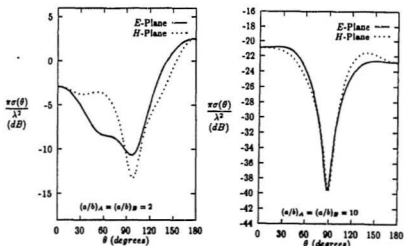
Fig. 5.4 represents the plots of normalized monostatic cross section in terms of TE and TM polarizations of incident field for two identical lossy spheroids with $\epsilon_{rA} = \epsilon_{rB} = 2 - j0.5$, in contact end to end with their centers separated along z -axis by: (a) $d = \lambda/2$, (b) $d = \lambda$. In Fig. 5.5 shows the plots of normalized monostatic cross section for $\epsilon_{rA} = \epsilon_{rB} = 4 - j0.5$. From Fig. 5.4 and Fig. 5.5 we observe that minima occur at almost at the same positions as in Fig. 5.2 and Fig. 5.3, and also as d increases we observe that monostatic cross section corresponding to both TE and TM polarizations of incident wave show more oscillations, which is due to more pronounced effect of multiple scattering. We also notice that at $\theta_i = 0^\circ$, the magnitude of monostatic radar cross section corresponding to TE polarization of incident excitation is equal to that corresponding to TM polarization of incident wave, unlike what we have observed in Fig. 4.4 and Fig. 4.5.

When the two spheroids are displaced along the z -axis specified by the coordi-

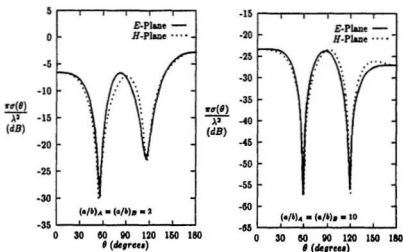
nates $d = \lambda/2$, $\theta_0 = 90^\circ$, $\phi_0 = 0^\circ$, as shown in Fig. 5.6(a) and Fig. 5.6(b), we find that for fat spheroid ($a/b = 2$) there is a difference in magnitudes of monostatic cross section for TE and TM polarizations of incident wave, but these magnitudes are almost same for the thin spheroid ($a/b = 10$) — this behavior is same as that explained in [20] and [23]. When the two spheroids were arbitrarily oriented (refer Fig. 4.6) there was a significant difference in the value of monostatic cross section at $\theta_i = 0^\circ$ for TE and TM polarization of incident wave.

In Fig. 5.7 the variation of monostatic cross section as function of aspect angle is presented for two spheroids of different values of axial ratio and complex relative permittivity. The center O' of spheroid B has spherical coordinates $d = \lambda/2$, $\theta_0 = 60^\circ$, $\phi_0 = 20^\circ$ with respect to $Oxyz$ -system: (a) $\epsilon_{rA} = 2 - j0.5$, $\epsilon_{rB} = 3 - j0.5$; (b) $\epsilon_{rA} = 2 - j0.1$, $\epsilon_{rB} = 3 - j0.1$; (c) $\epsilon_{rA} = 3 - j0.5$, $\epsilon_{rB} = 4 - j0.5$; (d) $\epsilon_{rA} = 3 - j0.1$, $\epsilon_{rB} = 4 - j0.1$.

It is to be noted, while obtaining results for monostatic cross section we consider the variation of θ_i from 0° to 90° because the spheroids are in parallel orientation with respect to each other.

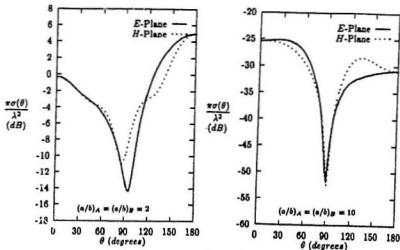


(a) $d = \lambda/2$.

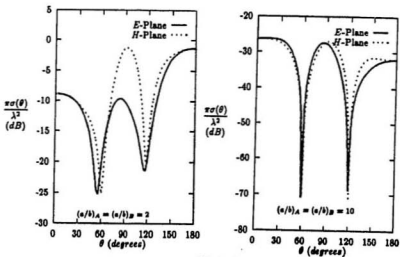


(b) $d = \lambda$.

Figure 5.2: Normalized bistatic cross section $\pi\sigma(\theta)/\lambda^2$ for TE polarization of incident wave, as a function of scattering angle (θ) for two identical lossy dielectric prolate spheroids with axial ratios 2 and 10, each with semi-major axis length $a_A = a_B = \lambda/4$, complex relative permittivity $\epsilon_{r,A} = \epsilon_{r,B} = 2 - j0.5$, and displaced along z -axis ($\theta_0 = 0^\circ, \phi_0 = 0^\circ$) by: (a) $d = \lambda/2$, (b) $d = \lambda$.



(a) $d = \lambda/2$.



(b) $d = \lambda$.

Figure 5.3: Normalized bistatic cross section $\pi\sigma(\theta)/\lambda^2$ for TE polarization of incident wave, as a function of scattering angle (θ) for two identical lossy dielectric prolate spheroids with axial ratios 2 and 10, each with semi-major axis length $a_A = a_B = \lambda/4$, complex relative permittivity $\epsilon_{rA} = \epsilon_{rB} = 4 - j0.5$, and displaced along z -axis ($\theta_0 = 0^\circ, \phi_0 = 0^\circ$) by: (a) $d = \lambda/2$, (b) $d = \lambda$.

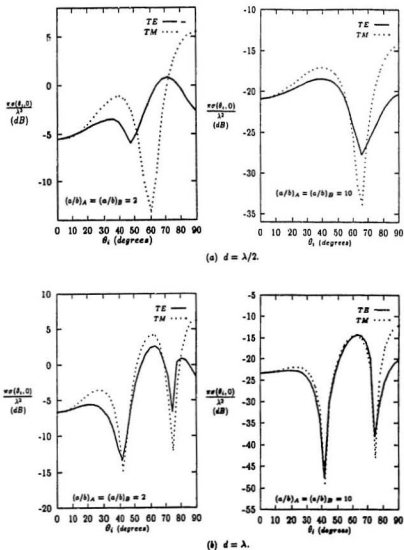


Figure 5.4: Normalized monostatic cross section $\pi\sigma(\theta_i, 0)/\lambda^2$ as a function of aspect angle (θ_i) for two identical lossy dielectric prolate spheroids with axial ratios 2 and 10, each with semi-major axis length $a_A = a_B = \lambda/4$, complex relative permittivity $\epsilon_{r,A} = \epsilon_{r,B} = 2 - j0.5$, and displaced along x -axis ($\theta_0 = 0^\circ, \phi_0 = 0^\circ$) by: (a) $d = \lambda/2$, (b) $d = \lambda$.

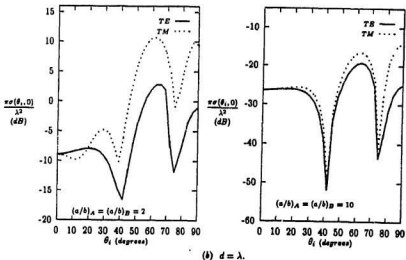
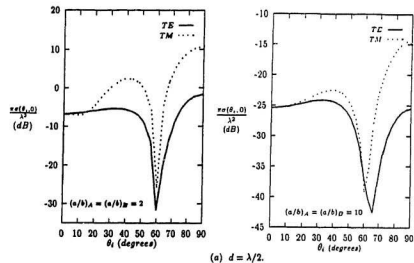


Figure 5.5: Normalized monostatic cross section $\pi\sigma(\theta_l, 0)/\lambda^2$ as a function of aspect angle (θ_l) for two identical lossy dielectric prolate spheroids with axial ratios 2 and 10, each with semi-major axis length $a_A = a_B = \lambda/4$, complex relative permittivity $\epsilon_{r,A} = \epsilon_{r,B} = 4 - j0.5$, and displaced along x -axis ($\theta_0 = 0^\circ$, $\phi_0 = 0^\circ$) by: (a) $d = \lambda/2$, (b) $d = \lambda$.

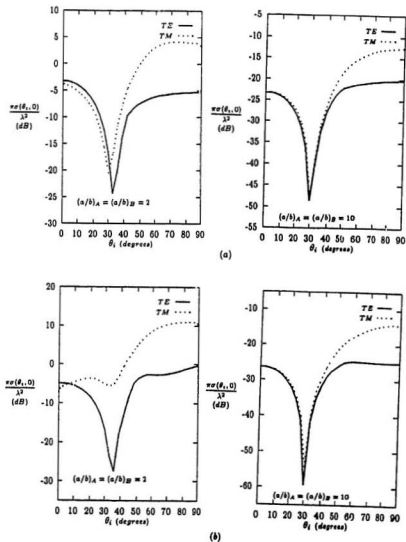


Figure 5.6: Normalized monostatic cross section as a function of aspect angle (θ_i) for two identical lossy dielectric prolate spheroids with axial ratios 2 and 10, each with semi-major axis length $a_A = a_B = \lambda/4$, and displaced along x-axis ($\theta_0 = 90^\circ, \phi_0 = 0^\circ$) by $d = \lambda/2$: (a) $\epsilon_{rA} = \epsilon_{rB} = 2 - j0.5$; (b) $\epsilon_{rA} = \epsilon_{rB} = 4 - j0.5$.

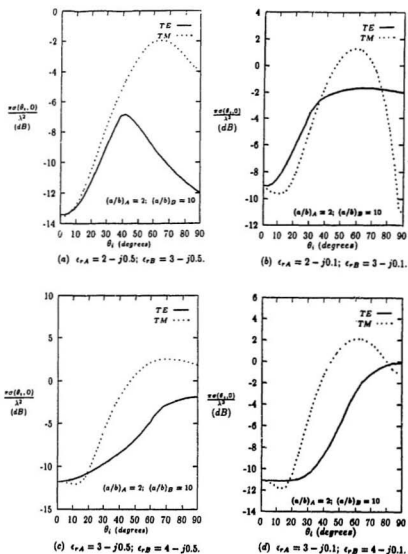


Figure 5.7: Normalized monostatic cross section as a function of aspect angle (θ_1) for two lossy dielectric prolate spheroids with axial ratios 2 and 10 respectively, each with semi-major axis length $a_A = a_B = \lambda/4$, and displaced along the direction $d = \lambda/2$, $\theta_0 = 60^\circ$, $\phi_0 = 20^\circ$: (a) $\epsilon_{rA} = 2 - j0.5$, $\epsilon_{rB} = 3 - j0.5$ (b) $\epsilon_{rA} = 2 - j0.1$, $\epsilon_{rB} = 3 - j0.1$ (c) $\epsilon_{rA} = 3 - j0.5$, $\epsilon_{rB} = 4 - j0.5$ (d) $\epsilon_{rA} = 3 - j0.1$, $\epsilon_{rB} = 4 - j0.1$.

Chapter 6

Conclusion

Exact analytical solutions for the problem of electromagnetic scattering by a single uniformly lossy dielectric prolate spheroid, a system of two uniformly lossy dielectric prolate spheroids in arbitrary configuration, and as a special case a system of two parallel uniformly lossy dielectric prolate spheroids have been obtained. Numerical results in the form of curves for normalized bistatic and monostatic radar cross sections are given for a variety of uniformly lossy dielectric prolate spheroids in the resonance region. Also for two-body scattering, different arbitrary configurations and parallel configurations of the spheroids having different distances of separation have been considered by using rotational-translational addition theorems and translational addition theorems respectively. Since no frequency approximation is involved in our present analysis, the solution obtained is valid for all frequencies.

By choosing Euler angles $\alpha = 0^\circ, \beta = 0^\circ, \gamma = 0^\circ$ for scattering by a system of two lossy dielectric spheroids in general orientation Chapter 4, [41], [42], results obtained were found to be identical with that obtained for a system of two lossy spheroids in parallel configuration (Chapter 5 of the present thesis) which employed only translational addition theorems [19]. Some of the results of Chapter

5 were presented in [43]. Also results were cross checked and were found to be in agreement with that of [20], [27], [23] and [29] by choosing appropriate values of relative permittivity of the medium inside the spheroid, ϵ_r and Euler angles (α, β, γ) .

It was shown that the system matrix $[G]$, in the equation $S = [G]I$, is independent of the direction and polarization of the incident wave. Solution in the form $S = [G]I$ eliminates the process of repeatedly solving a new set of equations for new angle of incidence, which is a great advantage in numerical computation.

Also since rotational-translational addition theorems and translational addition theorems assume the simplest forms for normalized vector wave functions because they translate like scalar wave functions, formulation of the two body scattering problem is simplified. However, because of the limitation in the size of the region within which the rotational-translational addition theorems and translational addition theorems available in literature are valid, the center to center distance between the spheroids for some non-axially displaced cases is restricted to $d \geq a$, where a is length of semi-major axis of the spheroid. If this restriction can be eliminated, then it will be possible to solve the problem of scattering by a system of two closely spaced spheroids for all non-axially displaced cases with distance of separation $d < a$.

Although specifically prolate spheroids have been considered, it is possible to obtain the solution for scattering by oblate spheroids by making suitable transformations in prolate spheroidal vector wave functions [1].

The present study finds applications in electromagnetic scattering from aircrafts and missiles [40], rain drops, ice crystals, biological particles e.g. bacterial cells [13] and in biomedical engineering such as tumors in human bodies [30].

Bibliography

- [1] C. Flammer, *Spheroidal Wave Functions*, Stanford University Press, Stanford, CA 1957.
- [2] J. A. Stratton, P. M. Morse, L. J. Chu, J. D. C. Little and F. J. Corbató, *Spheroidal Wave Functions*, The Technology Press of M. I. T., Cambridge, Mass., and John Wiley and Sons, New York, 1956.
- [3] F. V. Schultz, "Scattering by a prolate spheroid", *Report UMM-42*, Willow Run Research Center, University of Michigan, Ann Arbor, Michigan, 1950.
- [4] K. M. Siegel, F. V. Schultz, B. H. Gere and F. B. Sleator, "The theoretical and numerical determination of the radar cross section of a prolate spheroid", *IRE Trans., Antennas and Propag.*, Vol. Ap-4, No. 3, pp. 266-275, July 1956.
- [5] N. Reitlinger, "Scattering of a plane wave incident on a prolate spheroid at an arbitrary angle", *Memo No. 2868-506-M*, The University of Michigan Laboratory, Ann Arbor, Michigan, 1957.
- [6] B. P. Sinha, "Electromagnetic scattering from conducting prolate spheroids in the resonance region", *Ph. D. Dissertation*, University of Waterloo, Canada, March 1974.

- [7] B. P. Sinha and R. H. MacPhie, "Electromagnetic scattering by prolate spheroids for plane waves with arbitrary polarization and angle of incidence," *Radio Sci.*, vol. 12, pp. 171-184, Mar.- Apr., 1977.
- [8] J. Dalmas and R. Deleuil, "Scattering of electromagnetic wave by a prolate and a half prolate spheroid lying on a Plane with axial incidence", *Optica Acta*, Vol. 27, No. 5, pp. 637-649, May 1980.
- [9] J. Dalmas, "Scattering of electromagnetic wave by an ellipsoid with an elongated revolution of infinite conduction at non-axial incidence", *Optica Acta*, Vol. 28, No. 7, pp. 933-948, July 1981.
- [10] J. Dalmas, "Scattering indicators of an ellipsoid with elongated revolution of infinite conduction at oblique incidence", *Optica Acta*, Vol. 28, No. 9, pp. 1277-1287, Sept. 1981.
- [11] S. Asano and G. Yamamoto, "Light scattering by a spheroidal particle", *Applied Optics*, Vol. 14, No. 1, pp. 29-49, Jan 1975.
- [12] P. Barber and C. Yeh, "Scattering of electromagnetic waves by arbitrarily shaped dielectric bodies", *Applied Optics*, Vol. 14, No. 12, pp. 2864-2872, Dec. 1975.
- [13] S. Asano and M. Sato, "Light scattering by randomly oriented spheroidal particles", *Applied Optics*, Vol. 19, No. 6, pp.962-974, May 1980.
- [14] S. Asano, "Light scattering by horizontally oriented spheroidal particles", *Applied Optics*, Vol. 22, No. 9, pp. 1390-1396, May 1983.

- [15] M. F. Cooray, "Electromagnetic scattering by dielectric prolate spheroids," *M. Eng. thesis*, Memorial University of Newfoundland, St. John's, NF A1B 3X5, Canada, 1986.
- [16] J. H. Bruning and Y. T. Lo, "Multiple scattering of EM waves by spheres, Part I and II," *IEEE Trans. Antennas Propagat.*, vol. AP-19, pp. 378-400, May 1971.
- [17] O. R. Cruzan, "Translational addition theorems for spherical vector wave functions," *Quart. Appl. Math.*, vol. 20, pp. 33-40, Apr. 1962.
- [18] S. Stein, "Addition theorems for spherical wave functions," *Quart. Appl. Math.*, vol. 19, pp. 15-24, Apr. 1961.
- [19] B. P. Sinha and R. H. MacPhie, "Translational addition theorems for spheroidal scalar and vector wave functions," *Quart. Appl. Math.*, vol. 38, pp. 143-158, July 1980.
- [20] B. P. Sinha and R. H. MacPhie, "Electromagnetic plane wave scattering by a system of two parallel conducting prolate spheroids," *IEEE Transactions on Antennas and Propagation*, vol. AP-31, No. 2, March 1983.
- [21] J. Dalmas and R. Deleuil, "Multiple scattering of electromagnetic waves from two infinitely conducting prolate spheroids which are centered in a plane perpendicular to their axes of revolution", *Radio Sci.*, Vol. 20, pp. 575-581, 1985.
- [22] J. Dalmas and R. Deleuil, "Translational addition theorems for spheroidal scalar and vector wave functions M^r and N^r ", *Quart. Appl. Math.*, vol. 38, pp. 143-158, 1980.

- [23] M. F. Cooray, I. R. Ciric and B. P. Sinha, "Electromagnetic scattering by a system of two parallel dielectric prolate spheroids," *Canadian Journal of Physics*, Vol. 68, Nos. 4 & 5, pp. 376-384, 1990.
- [24] R. H. MacPhie, J. Dalmas and R. Deleuil, "Rotational-translational addition theorems for scalar spheroidal wave functions", *Quart. Appl. Math.*, vol. 44, No. 4, pp. 737-749, Jan. 1987.
- [25] J. Dalmas, R. Deleuil and R. H. MacPhie, "Rotational-translational addition theorems for vector spheroidal wave functions", *Quart. Appl. Math.*, vol. 47, No. 2, pp. 351-364, Jan. 1989.
- [26] M. F. Cooray and I. R. Ciric, "Rotational-translational addition theorems for vector spheroidal wave functions", *COMPEL*, vol. 8, No. 3, pp. 151-166, Jan. 1989.
- [27] M. F. Cooray and I. R. Ciric, "Electromagnetic wave scattering by a system of two spheroids of arbitrary orientation", *IEEE Trans. Antennas Propagat.*, vol. 37, No. 5, May 1989.
- [28] M. F. Cooray and I. R. Ciric, "Analytic solution for electromagnetic scattering by spheroids with non-parallel axes", *Proc. Symp. Antenna Tech. Appl. Electromagn. (ANTEM)*, Winnipeg, MB, Canada, Aug. 10-12, 1988.
- [29] M. F. Cooray and I. R. Ciric, "Scattering of electromagnetic waves by a system of two dielectric spheroids of arbitrary orientation", *IEEE Trans. Antennas Propagat.*, vol. 39, No. 5, May 1991.
- [30] R. Zimmer, "Contribution a l'etude de l'evolution de la Temperature induite par un champ electromagnetique hyperfrequence dans un ellipsoide de rev-

- olution — Application a la Thermotherapie des tumeurs mammaires", *Ph. D. Dissertation*, Universite de Provence (Aix-Marseille I), September 1984.
- [31] T. Oguchi, "Eigenvalues of spheroidal wave functions and their branch points for complex values of propagation constants", *Radio Science*, Vol. 5, Nos. 8, 9, pp. 1207-1214, Aug.-Sept. 1970.
- [32] A. R. Sebak and B. P. Sinha, "Scattering by a conducting spheroidal object with dielectric coating at axial incidence", *IEEE Trans. on Antennas and Propag.*, Vol. 40, No. 3, pp. 268-274, March 1992.
- [33] B. P. Sinha, R. H. MacPhie and T. Prasad, "Accurate computation of eigenvalues for prolate spheroidal wave functions", *IEEE Trans., Antennas and Propag.*, Vol. AP-21, No. 3, pp. 406-407, May 1973.
- [34] B. P. Sinha and R. H. MacPhie, "On the computation of the prolate spheroidal radial functions of the second kind", *Journ. of Mathematical Physics*, Vol. 16, No. 12, pp. 2378-2381, Dec. 1975.
- [35] S. M. Selby, *Handbook of Tables for Mathematics*, Cleveland: CRC Press, 1975.
- [36] E. Kreyszig *Advanced Engineering Mathematics*, Wiley Eastern Limited, 5th edition, 1983.
- [37] J. A. Stratton, *Electromagnetic Theory*, Mc-Graw Hill Book Co., New York, 1941.
- [38] A. R. Edmonds, *Angular Momentum in Quantum Mechanics*, Princeton, NJ: Princeton Univ. Press, 1957.

- [39] A. S. Davydov, *Quantum Mechanics*, Pergamon Press Limited, Addison-Wesley Publishing Company, Inc., 1965.
- [40] J. W. Crispin Jr., R. F. Goodrich and K. M. Seigel, "A theoretical method for the calculation of the radar cross sections of aircrafts and missiles", *The University of Michigan Laboratory Report No. 2591-1-H*, Ann Arbor, Michigan, 1959.
- [41] S. Nag and B. P. Sinha, "Electromagnetic scattering by a system of two uniformly lossy dielectric prolate spheroids in arbitrary orientation", *IEEE AP-S International Symposium and URSI Radio Science Meeting*, University of Washington, Seattle, Washington, June 19 - 24, 1994.
- [42] S. Nag and B. P. Sinha "Electromagnetic plane wave scattering by a system of two uniformly lossy dielectric prolate spheroids in arbitrary orientation", *IEEE Trans. Antennas Propagat.*, to appear.
- [43] S. Nag and B. P. Sinha, "Electromagnetic scattering by a system of two parallel uniformly lossy dielectric prolate spheroids", *6th Biennial IEEE Conference on Electromagnetic Field Computation*, Grenoble Aix-les-Bains, France, July 5-7, 1994.

Appendix A

Computation of Complex Eigen Values

Since the dielectric medium of the scatterer is of complex relative permittivity, complex eigen values $\lambda_{mn}(h)$, where $n = |m|, |m|+1, |m|+2, \dots$, and m is any positive integer including zero, are evaluated for the spheroidal scalar wave functions corresponding to transmitted components of E -field and H -field expansions.

Oguchi has calculated the eigen values of spheroidal wave functions for complex values of propagation constants in [31]. Zimmer also has computed complex eigen values for spheroidal wave functions assuming $e^{-j\omega t}$ time variation of time-harmonic electromagnetic field [30]. Thus in [30] the complex value of propagation constant is given by

$$k = (\omega\sqrt{\epsilon_0\mu_0})\sqrt{\epsilon/\epsilon_0 + j\sigma/(\omega\epsilon_0)}$$

Sebak and Sinha have calculated complex eigen values corresponding to prolate spheroidal functions in order to study the scattering by a conducting spheroidal object with lossy dielectric coating at axial incidence [32].

In this thesis we consider $e^{j\omega t}$ time variation of time-harmonic electromagnetic

field. So the complex value of propagation constant is given by

$$k = (\omega\sqrt{\epsilon_0\mu_0})\sqrt{\epsilon/\epsilon_0 - j\sigma/(\omega\epsilon_0)}$$

In the present work, the algorithm developed in [33], [6] for real eigen value computation has been used to calculate complex eigen values. In this appendix we present the code for calculation of complex eigen values required for angle functions and radial functions computation. We also present tables of eigenvalues $\lambda_{mn}(h)$, $m = 0, 1, 2, 3$, $n = |m|, |m| + 1, |m| + 2, \dots, |m| + 5$ corresponding to prolate radial and angle functions for axial ratio of length $a/b = 2$ and $a/b = 10$, and different values of complex relative permittivity of the medium inside the spheroid. The computed eigen values are in excellent agreement with those given in [30].

Now from [1] we know that

$$a = F\xi \tag{A.1}$$

$$b = F\sqrt{\xi^2 - 1} \tag{A.2}$$

from which we find that

$$\xi = \frac{(a/b)}{\sqrt{(a/b)^2 - 1}} \tag{A.3}$$

Utilizing the relation $h = \sqrt{\epsilon_r} \cdot (k_1 a / \xi)$, where $\epsilon_r = \epsilon/\epsilon_0 - j\sigma/(\omega\epsilon_0)$ and $k_1 a = 2\pi a/\lambda$ being the relative size of the spheroid, we can find the complex value of h .

```

:
/* In the following code the computation of complex eigen values for
prolate spheroidal wave functions corresponding to complex values of
propagation constant is presented. The functions used for algebra of
complex quantities (declared below) are not defined in the present
code. */

typedef struct {
    double re1;
    double re2;
}
complex;

complex K = {
    0., 0.};
complex J = {
    0., 1.};

int m, n;
complex hc;
complex E2c, E3c, Ec, Alphac[50], Betac[50], Gammac[50],
Wc[50], CrC[50], eigenc[50][50];

complex cpow(complex,int); /* returns (complex)**(integer) */
complex cmult(complex,complex); /* returns (complex)*(integer) */
complex rmult(double,complex); /* returns (double)*(integer) */
complex csum(complex,complex); /* returns (complex)+(integer) */
complex cdiv(complex,complex); /* returns (complex)/(integer) */
complex csub(complex,complex); /* returns (complex)-(integer) */
complex calc_cpowpos(complex,complex); /* returns (complex)**(positive integer) */
complex calc_cpowneg(complex,complex); /* returns (complex)**(negative integer) */

main() {
    int in, cnt1, cnt2;

    m=0;
    for (cnt1=1; cnt1<=15; cnt1++){
        E2c=K;
        E3c=K;
        n=m;

```

```

    for (cnt2=1;cnt2≤15;cnt2++){
        in = 0;
        if ((n-m)%2 ≠0) in = 1;
        if (hc.re2≠0.) call.comeigen();
        n++;
    }
    m++;
}

void call.comeigen()
{
    int r,i,l,cnt3,flag;
    complex E1c,Xc,Yc,Zc,deltac;

    if ((n-m)%2==0) l=0;
    else if ((n-m)%2≠0) l=1;
    if (hc.re1≠0.) call.comfactor(l);
    Ec=K;
    if (cabs(hc)>4.0) Ec=csum(E2c,E3c);
    if (n==m) Ec=K;
    deltac.re1=0.001;
    deltac.re2=0.001;
    if (hc.re2 == 0.) deltac.re2 = 0.;
    if (hc.re1≠0.) Xc=call.comiteration(l);
    flag=0;
    for(cnt3=1;cnt3≤100;cnt3++)
    {
        if (flag≠0) continue;
        E1c=Ec;
        Yc=Xc;
        Ec=csum(Ec,deltac);
        if (hc.re1≠0.) Xc=call.comiteration(l);
        Zc=Xc;

        if ( fabs( cabs(Yc)-cabs(Zc) ) ≤ 0.0000001 )
        {
            /* (sw==0) => computation of eigen values corresponding to radial func. */
            /* (sw==1) => computation of eigen values corresponding to angle func. */

            if (hc==K && (sw==1))

```

```

printf("ANGLE FUNCTION EIGEN VALUE,lambda_{%d %d} for hc=K is :
%f\n",
m,n,(float)(n+n+n));

if ((n==m)&& (cabs(hc)>4.0)) {
E3c.re1=2.*(Ec.re1-m);
E3c.re2=2.*(Ec.re2-m);
}
if ((n>m) && (cabs(hc)>4.0)) E3c=csub(Ec,E2c);

if (cabs(hc)>4.0) E2c=Ec;

eigenc[m][n] = Ec;

if ((hc.re1!=0.)&&(sw==1)) /* Angle function eigen values */
printf("lambda_{%d %d}.re = %g, lambda_{%d %d}.im = %g\n",
m, n, Ec.re1, m, n, Ec.re2);
if ((hc.re1!=0.)&&(sw==0)) /* Radial function eigen values */
printf("lambda_{%d %d}.re = %g, lambda_{%d %d}.im = %g\n",
m, n, Ec.re1, m, n, Ec.re2);

Xc=call.comiteration(1);
flag=1;
}

else {
Ec=csum(cdiv(cmult(deltac,Yc),csub(Yc,Zc)),E1c);
Xc=call.comiteration(1);
deltac=cdiv(cmult(Xc,deltac),csub(Yc,Zc));
}
}
return;
}

void call.comfactor(int l)
{
int r,mf;

mf=0;
for (r=1;r<=40;r+=2) {
if (r>1) mf=1;
}
}

```

```

        calc.comAlphaBeta.Gamma(mf,r);
    }
    return;
}

complex call.comiteration(int l)
{
    int i,r;
    complex Xc;

    if ((n-m)%2==0) {
        Wc[0].re1=1.;
        Wc[0].re2=1.;
        if (hc.re2==0.) Wc[0].re2=0.;
        Wc[n-m+24]=K;
    }
    if ((n-m)%2!=0) {
        Wc[1].re1=1.;
        Wc[1].re2=1.;
        if (hc.re2==0.) Wc[1].re2=0.;
        Wc[n-m+25]=K;
    };
    for(r=1;r<=(n-m)+2;r+=2) calc.computerate(r);
    Wpc=Wc[n-m+2];
    i=n-m+22;
    if ((n-m)%2!=0) i++;

    for (r=1;r<=20+1;r+=2) calc.comdowniterate(i,r);
    Wnc=Wc[n-m+2];
    Xc=csub(Wpc,Wnc);
    return(Xc);
}

void calc.comAlphaBeta.Gamma(int mf,int r)
{
    if (sw == 1){ /* ... for Angle function .... */
        Alphac[r]=rmult(((2.*n+2.*r+3.)*(2.*m+2.*r+5.)/
            (double)((2.*m+r+2)*(2.*m+r+1))),cpow(hc,-2));
        Betac[r] = csun(rmult(-(m+r)*(m+r+1),cmult(J,J)),
            rmult((2*(m+r)*(m+r+1)-2*m*m-1)/

```

```

        (double)(((2*m+2*r-1)*(2*m+2*r+3))),cpow(hc,2));
Gammac[r]=rmult(-((r*(r-1)*(2*m+2*r+3)*(2*m+2*r+5)
/(double)((2*m+2*r-3)*(2*m+2*r-1)*(2*m+r+2)*(2*m+r+1)))
*(double)(mf)),cmult(J,J));
}
if (sw == 0) { /* ... for Radial function .... */
    Alphac[r]=rmult(-(((2*m+2*r+3)*(2*m+2*r+5))/((r+2.)*(r+1.))),cpow(hc,-2));
    Betac[r]=caum(rmult(-(m+r)*(m+r+1),cmult(J,J)),
        rmult(((2*r+r+2*r*(2*m+1)+2*m-1))
/(double)((2.*m+2.*r-1.)*(2.*m+2.*r+3.))))),cpow(hc,2));
    Gammac[r]=rmult(-(((r+2*m-1)*(r+2*m)*(2*m+2*r+3)*(2*m+2*r+5)
/(double)((2.*m+2.*r-3.)*(2.*m+2.*r-1.)*(r+2.)*(r+1.))))
*(double)(mf)),cmult(J,J));
}
return;
}
void calc.computerate(int r)
{
    Nc[r+2]=csub(cmult(Alphac[r],csub(Ec,Betac[r])),cdiv(Gammac[r],Nc[r]));
    return;
}
void calc.comdowniterate (int i,int r)
{
    Nc[i-r]=cdiv(Gammac[i-r],csub(cmult(Alphac[i-r],csub(Ec,Betac[i-r])),Nc[i-r+2]));
    return;
}
:

```

$$\left. \begin{aligned} a/b &= 10 \\ k_1 a &= \pi/2 \\ \epsilon_r &= 2 - j0.5 \end{aligned} \right\} h = 2.22725 - j0.274187$$

$\lambda_{\{0\ 0\}}$.re = 1.34384, $\lambda_{\{0\ 0\}}$.im = -0.27189
 $\lambda_{\{0\ 1\}}$.re = 4.77309, $\lambda_{\{0\ 1\}}$.im = -0.64738
 $\lambda_{\{0\ 2\}}$.re = 8.73859, $\lambda_{\{0\ 2\}}$.im = -0.718595
 $\lambda_{\{0\ 3\}}$.re = 14.5753, $\lambda_{\{0\ 3\}}$.im = -0.667017
 $\lambda_{\{0\ 4\}}$.re = 22.5148, $\lambda_{\{0\ 4\}}$.im = -0.640477
 $\lambda_{\{0\ 5\}}$.re = 32.489, $\lambda_{\{0\ 5\}}$.im = -0.62952

$\lambda_{\{1\ 1\}}$.re = 2.88558, $\lambda_{\{1\ 1\}}$.im = -0.199015
 $\lambda_{\{1\ 2\}}$.re = 8.00835, $\lambda_{\{1\ 2\}}$.im = -0.478564
 $\lambda_{\{1\ 3\}}$.re = 14.3, $\lambda_{\{1\ 3\}}$.im = -0.577297
 $\lambda_{\{1\ 4\}}$.re = 22.3727, $\lambda_{\{1\ 4\}}$.im = -0.599691
 $\lambda_{\{1\ 5\}}$.re = 32.3997, $\lambda_{\{1\ 5\}}$.im = -0.605346
 $\lambda_{\{1\ 6\}}$.re = 44.4132, $\lambda_{\{1\ 6\}}$.im = -0.607484

$\lambda_{\{2\ 2\}}$.re = 6.65765, $\lambda_{\{2\ 2\}}$.im = -0.154081
 $\lambda_{\{2\ 3\}}$.re = 13.5795, $\lambda_{\{2\ 3\}}$.im = -0.381455
 $\lambda_{\{2\ 4\}}$.re = 21.9594, $\lambda_{\{2\ 4\}}$.im = -0.486818
 $\lambda_{\{2\ 5\}}$.re = 32.1343, $\lambda_{\{2\ 5\}}$.im = -0.534555
 $\lambda_{\{2\ 6\}}$.re = 44.2281, $\lambda_{\{2\ 6\}}$.im = -0.558966
 $\lambda_{\{2\ 7\}}$.re = 58.2843, $\lambda_{\{2\ 7\}}$.im = -0.5731

$\lambda_{\{3\ 3\}}$.re = 12.5217, $\lambda_{\{3\ 3\}}$.im = -0.124852
 $\lambda_{\{3\ 4\}}$.re = 21.3021, $\lambda_{\{3\ 4\}}$.im = -0.317195
 $\lambda_{\{3\ 5\}}$.re = 31.7002, $\lambda_{\{3\ 5\}}$.im = -0.421425
 $\lambda_{\{3\ 6\}}$.re = 43.9221, $\lambda_{\{3\ 6\}}$.im = -0.479637
 $\lambda_{\{3\ 7\}}$.re = 58.0573, $\lambda_{\{3\ 7\}}$.im = -0.51463
 $\lambda_{\{3\ 8\}}$.re = 74.1457, $\lambda_{\{3\ 8\}}$.im = -0.537195

$$\left. \begin{array}{l} a/b = 10 \\ k_1 a = \pi/2 \\ \epsilon_r = 4 - j0.5 \end{array} \right\} h = 3.13192 - j0.194986$$

lambda_{0 0}.re = 2.27345, lambda_{0 0}.im = -0.202386
 lambda_{0 1}.re = 7.19015, lambda_{0 1}.im = -0.562536
 lambda_{0 2}.re = 11.6549, lambda_{0 2}.im = -0.729614
 lambda_{0 3}.re = 17.3297, lambda_{0 3}.im = -0.708674
 lambda_{0 4}.re = 25.1235, lambda_{0 4}.im = -0.664279
 lambda_{0 5}.re = 35.035, lambda_{0 5}.im = -0.643592

lambda_{1 1}.re = 3.61559, lambda_{1 1}.im = -0.168357
 lambda_{1 2}.re = 9.83907, lambda_{1 2}.im = -0.437745
 lambda_{1 3}.re = 16.6007, lambda_{1 3}.im = -0.570878
 lambda_{1 4}.re = 24.7913, lambda_{1 4}.im = -0.608676
 lambda_{1 5}.re = 34.8406, lambda_{1 5}.im = -0.614908
 lambda_{1 6}.re = 46.8586, lambda_{1 6}.im = -0.615189

lambda_{2 2}.re = 7.24088, lambda_{2 2}.im = -0.138349
 lambda_{2 3}.re = 15.0577, lambda_{2 3}.im = -0.358157
 lambda_{2 4}.re = 23.8907, lambda_{2 4}.im = -0.478232
 lambda_{2 5}.re = 34.2738, lambda_{2 5}.im = -0.534787
 lambda_{2 6}.re = 46.4703, lambda_{2 6}.im = -0.561997
 lambda_{2 7}.re = 60.5839, lambda_{2 7}.im = -0.576646

lambda_{3 3}.re = 13.0024, lambda_{3 3}.im = -0.115839
 lambda_{3 4}.re = 22.5411, lambda_{3 4}.im = -0.302595
 lambda_{3 5}.re = 33.3709, lambda_{3 5}.im = -0.413737
 lambda_{3 6}.re = 45.8362, lambda_{3 6}.im = -0.477229
 lambda_{3 7}.re = 60.1163, lambda_{3 7}.im = -0.514793
 lambda_{3 8}.re = 76.297, lambda_{3 8}.im = -0.538439

$$\left. \begin{aligned} a/b &= 2 \\ k_1 a &= \pi/2 \\ \epsilon_r &= 2 - j0.5 \end{aligned} \right\} h = 1.93857 - j0.238649$$

lambda_{0 0}.re = 1.06377, lambda_{0 0}.im = -0.22527
 lambda_{0 1}.re = 4.13042, lambda_{0 1}.im = -0.506446
 lambda_{0 2}.re = 8.0484, lambda_{0 2}.im = -0.535578
 lambda_{0 3}.re = 13.9361, lambda_{0 3}.im = -0.497172
 lambda_{0 4}.re = 21.8977, lambda_{0 4}.im = -0.481079
 lambda_{0 5}.re = 31.8809, lambda_{0 5}.im = -0.474385

lambda_{1 1}.re = 2.68628, lambda_{1 1}.im = -0.157907
 lambda_{1 2}.re = 7.53693, lambda_{1 2}.im = -0.370553
 lambda_{1 3}.re = 13.7401, lambda_{1 3}.im = -0.437124
 lambda_{1 4}.re = 21.7931, lambda_{1 4}.im = -0.452182
 lambda_{1 5}.re = 31.8144, lambda_{1 5}.im = -0.456744
 lambda_{1 6}.re = 43.8255, lambda_{1 6}.im = -0.458776

lambda_{2 2}.re = 6.50519, lambda_{2 2}.im = -0.120115
 lambda_{2 3}.re = 13.2054, lambda_{2 3}.im = -0.293536
 lambda_{2 4}.re = 21.4861, lambda_{2 4}.im = -0.369997
 lambda_{2 5}.re = 31.6162, lambda_{2 5}.im = -0.404698
 lambda_{2 6}.re = 43.6866, lambda_{2 6}.im = -0.422811
 lambda_{2 7}.re = 57.7292, lambda_{2 7}.im = -0.433477

lambda_{3 3}.re = 12.3989, lambda_{3 3}.im = -0.0964408
 lambda_{3 4}.re = 20.9919, lambda_{3 4}.im = -0.243131
 lambda_{3 5}.re = 31.2903, lambda_{3 5}.im = -0.320558
 lambda_{3 6}.re = 43.4567, lambda_{3 6}.im = -0.363701
 lambda_{3 7}.re = 57.5583, lambda_{3 7}.im = -0.389783
 lambda_{3 8}.re = 73.625, lambda_{3 8}.im = -0.406706

$$\left. \begin{aligned} a/b &= 2 \\ k_1 a &= \pi/2 \\ \epsilon_r &= 4 - j0.5 \end{aligned} \right\} h = 2.72599 - j0.169714$$

λ_{00} .re = 1.85301, λ_{00} .im = -0.174734
 λ_{01} .re = 6.05629, λ_{01} .im = -0.456712
 λ_{02} .re = 10.2368, λ_{02} .im = -0.553012
 λ_{03} .re = 15.9755, λ_{03} .im = -0.522249
 λ_{04} .re = 23.8481, λ_{04} .im = -0.494313
 λ_{05} .re = 33.7943, λ_{05} .im = -0.482347

λ_{11} .re = 3.27521, λ_{11} .im = -0.137771
 λ_{12} .re = 8.96967, λ_{12} .im = -0.346202
 λ_{13} .re = 15.4882, λ_{13} .im = -0.435784
 λ_{14} .re = 23.6146, λ_{14} .im = -0.458211
 λ_{15} .re = 33.6528, λ_{15} .im = -0.462409
 λ_{16} .re = 45.6695, λ_{16} .im = -0.463242

λ_{22} .re = 6.96509, λ_{22} .im = -0.110234
 λ_{23} .re = 14.3514, λ_{23} .im = -0.279673
 λ_{24} .re = 22.9581, λ_{24} .im = -0.365712
 λ_{25} .re = 33.2364, λ_{25} .im = -0.405231
 λ_{26} .re = 45.3818, λ_{26} .im = -0.424715
 λ_{27} .re = 59.4674, λ_{27} .im = -0.435581

λ_{33} .re = 12.7734, λ_{33} .im = -0.0909213
 λ_{34} .re = 21.9469, λ_{34} .im = -0.234486
 λ_{35} .re = 32.5643, λ_{35} .im = -0.316341
 λ_{36} .re = 44.9092, λ_{36} .im = -0.3625
 λ_{37} .re = 59.1179, λ_{37} .im = -0.38998
 λ_{38} .re = 75.2534, λ_{38} .im = -0.407476

$$h = 3.95 - j0.626$$

lambda_{0 0}.re = 3.12359, lambda_{0 0}.im = -0.6452
lambda_{0 1}.re = 9.63126, lambda_{0 1}.im = -1.93797
lambda_{0 2}.re = 14.924, lambda_{0 2}.im = -2.85644
lambda_{0 3}.re = 20.5275, lambda_{0 3}.im = -3.01137
lambda_{0 4}.re = 28.0948, lambda_{0 4}.im = -2.80456
lambda_{0 5}.re = 37.9083, lambda_{0 5}.im = -2.67226

lambda_{1 1}.re = 4.34254, lambda_{1 1}.im = -0.582803
lambda_{1 2}.re = 11.7608, lambda_{1 2}.im = -1.60812
lambda_{1 3}.re = 19.144, lambda_{1 3}.im = -2.24785
lambda_{1 4}.re = 27.5121, lambda_{1 4}.im = -2.48653
lambda_{1 5}.re = 37.586, lambda_{1 5}.im = -2.5287
lambda_{1 6}.re = 49.6032, lambda_{1 6}.im = -2.52473

lambda_{2 2}.re = 7.84581, lambda_{2 2}.im = -0.50345
lambda_{2 3}.re = 16.6376, lambda_{2 3}.im = -1.35478
lambda_{2 4}.re = 26.0172, lambda_{2 4}.im = -1.88779
lambda_{2 5}.re = 36.6576, lambda_{2 5}.im = -2.15872
lambda_{2 6}.re = 48.9759, lambda_{2 6}.im = -2.28586
lambda_{2 7}.re = 63.1546, lambda_{2 7}.im = -2.34946

lambda_{3 3}.re = 13.5122, lambda_{3 3}.im = -0.434438
lambda_{3 4}.re = 23.8795, lambda_{3 4}.im = -1.16447
lambda_{3 5}.re = 35.2097, lambda_{3 5}.im = -1.63756
lambda_{3 6}.re = 47.9611, lambda_{3 6}.im = -1.91809
lambda_{3 7}.re = 62.4097, lambda_{3 7}.im = -2.08313
lambda_{3 8}.re = 78.6961, lambda_{3 8}.im = -2.18469

The above eigen values are in good agreement with those obtained in [30].

$$h = 7.61 - j2.47$$

lambda_{0 0}.re = 6.83423, lambda_{0 0}.im = -2.4805
lambda_{0 1}.re = 20.9442, lambda_{0 1}.im = -7.47411
lambda_{0 2}.re = 33.8823, lambda_{0 2}.im = -12.6123
lambda_{0 3}.re = 45.4058, lambda_{0 3}.im = -18.4051
lambda_{0 4}.re = 52.7882, lambda_{0 4}.im = -24.4264
lambda_{0 5}.re = 58.4144, lambda_{0 5}.im = -25.2691

lambda_{1 1}.re = 7.90493, lambda_{1 1}.im = -2.45073
lambda_{1 2}.re = 22.1805, lambda_{1 2}.im = -7.3456
lambda_{1 3}.re = 35.295, lambda_{1 3}.im = -12.205
lambda_{1 4}.re = 46.9838, lambda_{1 4}.im = -16.726
lambda_{1 5}.re = 57.5356, lambda_{1 5}.im = -19.7899
lambda_{1 6}.re = 68.7774, lambda_{1 6}.im = -20.7089

lambda_{2 2}.re = 11.1155, lambda_{2 2}.im = -2.36803
lambda_{2 3}.re = 25.9056, lambda_{2 3}.im = -7.00486
lambda_{2 4}.re = 39.8299, lambda_{2 4}.im = -11.3073
lambda_{2 5}.re = 53.0915, lambda_{2 5}.im = -14.8562
lambda_{2 6}.re = 66.4108, lambda_{2 6}.im = -17.1825
lambda_{2 7}.re = 80.8356, lambda_{2 7}.im = -18.3154

lambda_{3 3}.re = 16.458, lambda_{3 3}.im = -2.24938
lambda_{3 4}.re = 32.0822, lambda_{3 4}.im = -6.56074
lambda_{3 5}.re = 47.2498, lambda_{3 5}.im = -10.3554
lambda_{3 6}.re = 62.3653, lambda_{3 6}.im = -13.3476
lambda_{3 7}.re = 78.079, lambda_{3 7}.im = -15.3914
lambda_{3 8}.re = 95.0398, lambda_{3 8}.im = -16.6281

The above eigen values are in good agreement with those obtained in [30].

Appendix B

Definition of Elements of $[G]$

By applying the appropriate boundary conditions and performing the η and ϕ integrations on the surfaces of the spheroids A and B we obtain the system equation $S = [G]I$, in which elements of $[G]$ given by equations (3.56), (4.90) and (5.17) are quasi-diagonal matrices.

It is to be noted that in Chapter 4 the size of the matrix $[R_{MB}]$ or $[R_{NB}]$ is different from that of $[R_{MA}]$ or $[R_{NA}]$; whereas in Chapter 5 the size of the matrix $[R_{MB}]$ or $[R_{NB}]$ is same as that of $[R_{MA}]$ or $[R_{NA}]$. Also in Chapter 3, the matrices $[P_M]$, $[Q_M]$, $[R_M]$, $[P_N]$, $[Q_N]$ and $[R_N]$ are respectively identical to $[P_{MA}]$, $[Q_{MA}]$, $[R_{MA}]$, $[P_{NA}]$, $[Q_{NA}]$ and $[R_{NA}]$.

The diagonal submatrices of $[P_{MA}]$ or $[P_{NA}]$ are given by $[P_{MA}]_m$ or $[P_{MA}]_m$ respectively ($m = 0, 1, 2, \dots$), and the off-diagonal submatrices are null matrices. Thus from Appendix III of [20]:

$$[P_{LA}]_0 = \begin{bmatrix} [\eta Y_{-1}^{+(1)}] & [\eta Y_0^{s(1)}] \\ [\phi Y_{-1}^{+(1)}] & [\phi Y_0^{s(1)}] \end{bmatrix} \quad (B.1)$$

$$[P_{\mathcal{L}\mathcal{A}}] = \begin{bmatrix} [\eta Y_{m-1}^{+(1)}] & [\eta Y_m^{s(1)}] & [0] & [0] \\ [\phi Y_{m-1}^{+(1)}] & [\phi Y_m^{s(1)}] & [0] & [0] \\ [0] & [0] & [\eta Y_{-(m-1)}^{-(1)}] & [\eta Y_{-m}^{s(1)}] \\ [0] & [0] & [\phi Y_{-(m-1)}^{-(1)}] & [\phi Y_{-m}^{s(1)}] \end{bmatrix}, \quad m \geq 1 \quad (\text{B.2})$$

\mathcal{L} is M or N according as Y is normalized spheroidal vector wave function \vec{M} or \vec{N} respectively, evaluated with respect to h_2 .

The diagonal submatrices of $[Q_{MA}]$ is given by

$$[Q_{\mathcal{K}\mathcal{A}}]_0 = - \begin{bmatrix} [\eta X_{-1}^{+(4)}] & [\eta X_0^{s(4)}] \\ [\phi X_{-1}^{+(4)}] & [\phi X_0^{s(4)}] \end{bmatrix} \quad (\text{B.3})$$

$$[Q_{\mathcal{K}\mathcal{A}}] = - \begin{bmatrix} [\eta X_{m-1}^{+(4)}] & [\eta X_m^{s(4)}] & [0] & [0] \\ [\phi X_{m-1}^{+(4)}] & [\phi X_m^{s(4)}] & [0] & [0] \\ [0] & [0] & [\eta X_{-(m-1)}^{-(4)}] & [\eta X_{-m}^{s(4)}] \\ [0] & [0] & [\phi X_{-(m-1)}^{-(4)}] & [\phi X_{-m}^{s(4)}] \end{bmatrix}, \quad m \geq 1 \quad (\text{B.4})$$

\mathcal{K} is M or N according as X is normalized spheroidal vector wave function \vec{M} or \vec{N} respectively, evaluated with respect to h_1 .

For $[R_{MA}]$ or $[R_{NA}]$ we can similarly write its submatrices as:

$$[R_{\mathcal{K}\mathcal{A}}]_0 = \begin{bmatrix} [\eta X_{-1}^{+(1)}] & [\eta X_1^{-(1)}] \\ [\phi X_{-1}^{+(1)}] & [\phi X_1^{-(1)}] \end{bmatrix} \quad (\text{B.5})$$

$$[R_{\mathcal{K}A}] = \begin{bmatrix} [\eta X_{m-1}^{+(1)}] & [\eta X_{m+1}^{-(1)}] & [0] & [0] \\ [\phi X_{m-1}^{+(1)}] & [\phi X_{m+1}^{-(1)}] & [0] & [0] \\ [0] & [0] & [\eta X_{-(m+1)}^{+(1)}] & [\eta X_{-(m-1)}^{-(1)}] \\ [0] & [0] & [\phi X_{-(m+1)}^{+(1)}] & [\phi X_{-(m-1)}^{-(1)}] \end{bmatrix}, \quad m \geq 1 \quad (\text{B.6})$$

\mathcal{K} is M or N according as X is \bar{M} or \bar{N} respectively, evaluated with respect to h_1 .

For $[R_{MBA}]$ or $[R_{NBA}]$ used in Chapter 4 the submatrices are

$$[R_{\mathcal{K}BA}]_0 = - \begin{bmatrix} [\eta X_{-1}^{+(1)}] & [\eta X_1^{-(1)}] & [\eta X_0^{s(1)}] \\ [\phi X_{-1}^{+(1)}] & [\phi X_1^{-(1)}] & [\phi X_0^{s(1)}] \end{bmatrix} \quad (\text{B.7})$$

$$[R_{\mathcal{K}BA}] = - \begin{bmatrix} [\eta X_{m-1}^{+(1)}] & [\eta X_{m+1}^{-(1)}] & [\eta X_m^{s(1)}] & [0] & [0] & [0] \\ [\phi X_{m-1}^{+(1)}] & [\phi X_{m+1}^{-(1)}] & [\phi X_m^{s(1)}] & [0] & [0] & [0] \\ [0] & [0] & [0] & [\eta X_{-(m+1)}^{+(1)}] & [\eta X_{-(m-1)}^{-(1)}] & [\eta X_{-m}^{s(1)}] \\ [0] & [0] & [0] & [\phi X_{-(m+1)}^{+(1)}] & [\phi X_{-(m-1)}^{-(1)}] & [\phi X_{-m}^{s(1)}] \end{bmatrix}, \quad m \geq 1 \quad (\text{B.8})$$

\mathcal{K} is M or N according as X is \bar{M} or \bar{N} respectively, evaluated with respect to h_1 .

For $[R_{MBA}]$ or $[R_{NBA}]$ used in Chapter 5 the submatrices are

$$[R_{\mathcal{K}BA}]_0 = - \begin{bmatrix} [\eta X_{-1}^{+(1)}] & [\eta X_0^{s(1)}] & [\eta X_1^{-(1)}] \\ [\phi X_{-1}^{+(1)}] & [\phi X_0^{s(1)}] & [\phi X_1^{-(1)}] \end{bmatrix} \quad (\text{B.9})$$

$$[R_{KBA}] = - \begin{bmatrix} [\eta X_{m-1}^{+(1)}] & [0] & [\eta X_m^{+(1)}] & [0] & [\eta X_{m+1}^{-(1)}] & [0] \\ [\phi X_{m-1}^{+(1)}] & [0] & [\phi X_m^{+(1)}] & [0] & [\phi X_{m+1}^{-(1)}] & [0] \\ [0] & [\eta X_{-(m+1)}^{+(1)}] & [0] & [\eta X_{-m}^{+(1)}] & [0] & [\eta X_{-(m-1)}^{-(1)}] \\ [0] & [\phi X_{-(m+1)}^{+(1)}] & [0] & [\phi X_{-m}^{+(1)}] & [0] & [\phi X_{-(m-1)}^{-(1)}] \end{bmatrix}, \quad m \geq 1 \quad (\text{B.10})$$

\mathcal{K} is M or N according as X is \bar{M} or \bar{N} respectively, evaluated with respect to h_1 .

The submatrices $[X_m]$ are of the general form:

$$[X_m] = \begin{bmatrix} X_{m,0,|m|} & X_{m,0,|m|+1} & X_{m,0,|m|+2} \cdots \\ X_{m,1,|m|} & X_{m,1,|m|+1} & X_{m,1,|m|+2} \cdots \\ X_{m,2,|m|} & X_{m,2,|m|+1} & X_{m,2,|m|+2} \cdots \\ \vdots & \vdots & \vdots \end{bmatrix} \quad (\text{B.11})$$

where the elements of matrix in (B.11) are evaluated with respect to h_1 . The submatrices $[Y_m]$, with elements evaluated with respect to h_2 , have the same form as those of $[X_m]$. The elements of the submatrices $[X_m]$ and $[Y_m]$ are defined in Appendix C.

In Chapter 5, the submatrices $[P_{MB}]$, $[Q_{MB}]$, $[R_{MB}]$, $[R_{MAB}]$, $[P_{NB}]$, $[Q_{NB}]$, $[R_{NB}]$, $[R_{NAB}]$ have the same forms as those of $[P_{LA}]$, $[Q_{KA}]$, $[R_{KA}]$, $[R_{KBA}]$, but with corresponding elements being evaluated with respect to primed coordinate system attached to spheroid B . In Chapter 4, the submatrices $[P_{MB}]$, $[Q_{MB}]$, $[R_{MAB}]$, $[P_{NB}]$, $[Q_{NB}]$, $[R_{NAB}]$ have the same forms as those of $[P_{LA}]$, $[Q_{KA}]$, $[R_{KA}]$, $[R_{KBA}]$, but with corresponding elements being evaluated with respect to primed coordinate system attached to spheroid B . However the matrices $[R_{MB}]$ and $[R_{NB}]$ are different from $[R_{MA}]$ and $[R_{NA}]$. Thus in Chapter 4, for $[R_{MB}]$ or

$[R_{NB}]$ we can write:

$$[R_{KB}]_0 = \begin{bmatrix} [\eta X_{-1}^{+(1)'}] & [\eta X_{-1}^{-(1)'}] & [\eta X_0^{s'(1)}] \\ [\phi X_{-1}^{+(1)'}] & [\phi X_{-1}^{-(1)'}] & [\phi X_0^{s'(1)}] \end{bmatrix} \quad (\text{B.12})$$

$$[R_{KB}] = \begin{bmatrix} [\eta X_{m-1}^{+(1)'}] & [\eta X_{m+1}^{-(1)'}] & [\eta X_m^{s'(1)}] & [0] & [0] & [0] \\ [\phi X_{m-1}^{+(1)'}] & [\phi X_{m+1}^{-(1)'}] & [\phi X_m^{s'(1)}] & [0] & [0] & [0] \\ [0] & [0] & [0] & [\eta X_{-(m+1)}^{+(1)'}] & [\eta X_{-(m-1)}^{-(1)'}] & [\eta X_{-(m-1)}^{s'(1)}] \\ [0] & [0] & [0] & [\phi X_{-(m+1)}^{+(1)'}] & [\phi X_{-(m-1)}^{-(1)'}] & [\phi X_{-(m-1)}^{s'(1)}] \end{bmatrix}, \quad m \geq 1 \quad (\text{B.13})$$

\mathcal{K} is M or N according as X is \vec{M} or \vec{N} respectively, evaluated with respect to h'_i . $[X_m]$ has the same form as that given by equation (B.11).

Appendix C

Definition of $[\eta Q_m^{\pm(i)}]$, $[\eta Q_{m+2}^{\pm(i)}]$,
 $[\eta Q_{m+1}^{z(i)}]$, $[\phi Q_m^{\pm(i)}]$, $[\phi Q_{m+2}^{\pm(i)}]$, $[\phi Q_{m+1}^{z(i)}]$

In this appendix we define the elements of $[Q_m]$, where Q is equal to X when the field under consideration is E -field and is equal to Y when the field is H -field.

The submatrices of $[Q_m]$ are of the general form:

$$[Q_m] = \begin{bmatrix} Q_{m,0,|m|(c)} & Q_{m,0,|m|+1(c)} & Q_{m,0,|m|+2(c)} \cdots \\ Q_{m,1,|m|(c)} & Q_{m,1,|m|+1(c)} & Q_{m,1,|m|+2(c)} \cdots \\ Q_{m,2,|m|(c)} & Q_{m,2,|m|+1(c)} & Q_{m,2,|m|+2(c)} \cdots \\ \vdots & \vdots & \vdots \end{bmatrix} \quad (C.1)$$

c is equal to $(2\pi F/\lambda)$ or $(2\pi F\sqrt{\epsilon_r}/\lambda)$, where F and ϵ_r are semi-interfocal distance and complex relative permittivity of the spheroid respectively, according as the medium under consideration is outside or inside the spheroid.

The elements of the matrix in (C.1) for Q equal to X are given by the integrals in [20] and [15]:

$$\begin{aligned} \left(\eta\right)_{\phi} X_{m,t,n}^{\pm(i)}(c) &= \frac{1}{2\pi} \int_0^{2\pi} \int_{-1}^{+1} \begin{pmatrix} l_{\eta} \\ l_{\phi} \end{pmatrix} \cdot \left(\eta\right)_{m,n}^{\pm(i)}(c; \mathbf{r}) \\ &\cdot S_{m,|m|+t}(c, \eta) e^{-j(m\pm 1)\phi} d\eta d\phi \end{aligned} \quad (C.2)$$

$$\begin{aligned} \left(\eta\right)_{\phi} X_{m+1,t,n}^{\pm(i)}(c) &= \frac{1}{2\pi} \int_0^{2\pi} \int_{-1}^{+1} \begin{pmatrix} l_{\eta} \\ l_{\phi} \end{pmatrix} \cdot \left(\eta\right)_{m+1,n}^{\pm(i)}(c; \mathbf{r}) \\ &\cdot S_{m,|m|+t}(c, \eta) e^{-j(m+1)\phi} d\eta d\phi \end{aligned} \quad (C.3)$$

where

$$l_\eta = j2F(\xi^2 - \eta^2)^{1/2} \quad (\text{C.4})$$

$$l_\phi = 2F(\xi^2 - \eta^2) \quad (\text{C.5})$$

with J is the respective component of \bar{M} ; $t = 0, 1, 2, \dots$; \mathbf{r} being the spheroidal coordinate triad (ξ, η, ϕ) .

The submatrices $[Y_m]$ have the same form as those of $[X_m]$ with elements given as :

$$\begin{aligned} \begin{pmatrix} \eta \\ \phi \end{pmatrix} Y_{m,t,n}^{\pm(i)}(c) &= \frac{1}{2\pi} \int_0^{2\pi} \int_{-1}^{+1} \begin{pmatrix} l_\eta \\ l_\phi \end{pmatrix} \cdot \begin{pmatrix} \eta \\ \phi \end{pmatrix} J_{m,t}^{\pm(i)}(c; \mathbf{r}) \\ &\cdot S_{m,|m|+t}(c, \eta) e^{-j(m\pm 1)\phi} d\eta d\phi \end{aligned} \quad (\text{C.6})$$

$$\begin{aligned} \begin{pmatrix} \eta \\ \phi \end{pmatrix} Y_{m+1,t,n}^{\pm(i)}(c) &= \frac{1}{2\pi} \int_0^{2\pi} \int_{-1}^{+1} \begin{pmatrix} l_\eta \\ l_\phi \end{pmatrix} \cdot \begin{pmatrix} \eta \\ \phi \end{pmatrix} J_{m+1,t}^{\pm(i)}(c; \mathbf{r}) \\ &\cdot S_{m,|m|+t}(c, \eta) e^{-j(m+1)\phi} d\eta d\phi \end{aligned} \quad (\text{C.7})$$

where J is the respective component of \bar{N} ; $t = 0, 1, 2, \dots$, and

$$l_\eta = 2F^2(\xi^2 - \eta^2)^{3/2}/(\xi^2 - 1)^{1/2} \quad (\text{C.8})$$

$$l_\phi = j2F^2(\xi^2 - \eta^2)/(\xi^2 - 1) \quad (\text{C.9})$$

Explicit expressions of $X_{m,t,n}(c)$ are given in [7] and [15]. Explicit expressions of $Y_{m,t,n}(c)$ are given below.

For $n = |m|, |m| + 1, |m| + 2, \dots$ and $N = 0, 1, 2, \dots$ we have the following expressions for $Y_{m,N,n}(c)$:

$$\begin{aligned} \eta Y_{m,N,n}^{\pm(i)}(c) &= \left[(\xi_0^2 - 1) \frac{d^2}{d\xi^2} R_{m,m+n}^{(i)}(c, \xi) \Big|_{\xi=\xi_0} + \xi_0 \frac{d}{d\xi} R_{m,m+n}^{(i)}(c, \xi) \Big|_{\xi=\xi_0} \right] \\ &\cdot [(\xi_0^2 - 1)I_{3mNn} + I_{14mNn}] \\ &+ \xi_0 \frac{d}{d\xi} R_{m,m+n}^{(i)}(c, \xi) \Big|_{\xi=\xi_0} [(\xi_0 - 1)I_{4mNn} + I_{15mNn} + 2I_{14mNn}] \end{aligned}$$

$$\begin{aligned}
& - R_{m,m+n}^{(i)}(c, \xi) \Big|_{\xi=\xi_0} \left[I_{16mNn} - \frac{\xi_0^2}{\xi_0^2 - 1} I_{15mNn} \right] \\
& \mp (m \pm 1) R_{m,m+n}^{(i)}(c, \xi) \Big|_{\xi=\xi_0} \left[(\xi_0^2 - 1) I_{18mNn} + 2I_{4mNn} + \frac{1}{\xi_0^2 - 1} I_{15mNn} \right] \\
& - m(m \pm 1) R_{m,m+n}^{(i)}(c, \xi) \Big|_{\xi=\xi_0} \left[(\xi_0^2 - 1) I_{17mNn} + 2I_{3mNn} + \frac{1}{\xi_0^2 - 1} I_{14mNn} \right]
\end{aligned} \tag{C.10}$$

$$\begin{aligned}
\eta Y_{m+2,N,n}^{\pm(i)}(c) &= \left[(\xi_0^2 - 1) \frac{d^2}{d\xi^2} R_{m+2,m+n+2}^{(i)}(c, \xi) \Big|_{\xi=\xi_0} + \xi_0 \frac{d}{d\xi} R_{m+2,m+n+2}^{(i)}(c, \xi) \Big|_{\xi=\xi_0} \right] \\
&\cdot \left[(\xi_0^2 - 1) I_{8mNn} + I_{19mNn} \right] \\
&+ \xi_0 \frac{d}{d\xi} R_{m+2,m+n+2}^{(i)}(c, \xi) \Big|_{\xi=\xi_0} \left[(\xi_0 - 1) I_{9mNn} + I_{20mNn} + 2I_{19mNn} \right] \\
&- R_{m+2,m+n+2}^{(i)}(c, \xi) \Big|_{\xi=\xi_0} \left[I_{21mNn} - \frac{\xi_0^2}{\xi_0^2 - 1} I_{20mNn} \right] \\
&\mp (m + 2 \pm 1) R_{m+2,m+n+2}^{(i)}(c, \xi) \Big|_{\xi=\xi_0} \left[(\xi_0^2 - 1) I_{23mNn} + 2I_{9mNn} \right. \\
&\left. + \frac{1}{\xi_0^2 - 1} I_{20mNn} \right] - (m + 2)(m + 2 \pm 1) R_{m+2,m+n+2}^{(i)}(c, \xi) \Big|_{\xi=\xi_0} \\
&\cdot \left[(\xi_0^2 - 1) I_{22mNn} + 2I_{8mNn} + \frac{1}{\xi_0^2 - 1} I_{19mNn} \right]
\end{aligned} \tag{C.11}$$

$$\begin{aligned}
\eta Y_{m+1,N,n}^{(i)}(c) &= 2 \left[(\xi_0^2 - 1)^{3/2} \frac{d}{d\xi} R_{m+1,m+n+1}^{(i)}(c, \xi) \Big|_{\xi=\xi_0} (I_{8mNn} - I_{5mNn}) \right. \\
&+ (\xi_0^2 - 1)^{1/2} \frac{d}{d\xi} R_{m+1,m+n+1}^{(i)}(c, \xi) \Big|_{\xi=\xi_0} (I_{24mNn} - I_{25mNn}) \\
&- \xi_0 (\xi_0^2 - 1)^{1/2} \frac{d^2}{d\xi^2} R_{m+1,m+n+1}^{(i)}(c, \xi) \Big|_{\xi=\xi_0} \left[(\xi_0^2 - 1) I_{5mNn} + I_{25mNn} \right] \\
&- \frac{d}{d\xi} R_{m+1,m+n+1}^{(i)}(c, \xi) \Big|_{\xi=\xi_0} \frac{2\xi_0^2}{(\xi_0^2 - 1)^{1/2}} I_{25mNn} \\
&+ \frac{(m+1)^2 \xi_0}{(\xi_0 - 1)^{3/2}} R_{m+1,m+n+1}^{(i)}(c, \xi) \Big|_{\xi=\xi_0} \left[(\xi_0^2 - 1) I_{26mNn} + 2(\xi_0^2 - 1) I_{5mNn} \right. \\
&\left. + I_{25mNn} \right] + \frac{2\xi_0}{(\xi_0^2 - 1)^{1/2}} R_{m+1,m+n+1}^{(i)}(c, \xi) \Big|_{\xi=\xi_0} I_{24mNn} \Big]
\end{aligned} \tag{C.12}$$

$$\begin{aligned}
\phi Y_{m,N,n}^{\pm(i)}(c) &= \frac{1}{(\xi_0^2 - 1)} R_{m,m+n}^{(i)}(c, \xi) \Big|_{\xi=\xi_0} [m J_{2^m N n} \pm J_{2^m N n}] \\
&\pm \left[\frac{d^2}{d\xi^2} R_{m,m+n}^{(i)}(c, \xi) \Big|_{\xi=\xi_0} + \frac{(1 \mp m)\xi_0}{(\xi_0^2 - 1)} \frac{d}{d\xi} R_{m,m+n}^{(i)}(c, \xi) \Big|_{\xi=\xi_0} \right. \\
&\left. \pm \frac{m}{(\xi_0^2 - 1)^2} R_{m,m+n}^{(i)}(c, \xi) \Big|_{\xi=\xi_0} \right] I_{1m N n} \quad (C.13)
\end{aligned}$$

$$\begin{aligned}
\phi Y_{m+2,N,n}^{\pm(i)}(c) &= \frac{1}{(\xi_0^2 - 1)} R_{m+2,m+n+2}^{(i)}(c, \xi) \Big|_{\xi=\xi_0} \\
&\cdot [(m+2)(J_{31m N n} + J_{32m N n}) \pm (J_{33m N n} - J_{31m N n})] \\
&\pm \left[\frac{d^2}{d\xi^2} R_{m+2,m+n+2}^{(i)}(c, \xi) \Big|_{\xi=\xi_0} + \frac{(1 \mp (m+2))\xi_0}{(\xi_0^2 - 1)} \frac{d}{d\xi} R_{m+2,m+n+2}^{(i)}(c, \xi) \Big|_{\xi=\xi_0} \right. \\
&\left. \pm \frac{(m+2)}{(\xi_0^2 - 1)^2} R_{m+2,m+n+2}^{(i)}(c, \xi) \Big|_{\xi=\xi_0} \right] I_{7m N n} \quad (C.14)
\end{aligned}$$

$$\begin{aligned}
\phi Y_{m+1,N,n}^{\pm(i)}(c) &= -\frac{2(m+1)}{(\xi_0^2 - 1)^{1/2}} \left[\frac{\xi_0}{(\xi_0^2 - 1)} R_{m+1,m+n+1}^{(i)}(c, \xi) \Big|_{\xi=\xi_0} I_{29m N n} \right. \\
&\left. + \frac{d}{d\xi} R_{m+1,m+n+1}^{(i)}(c, \xi) \Big|_{\xi=\xi_0} I_{2m N n} \right] \quad (C.15)
\end{aligned}$$

$$\begin{aligned}
\eta Y_{0,N,n}^{\pm(i)}(c) &= 2 \left[(\xi_0^2 - 1)^{1/2} \frac{d}{d\xi} R_{0,n}^{(i)}(c, \xi) \Big|_{\xi=\xi_0} \left\{ (\xi_0^2 - 1) J_{11m N n} + J_{12m N n} \right\} \right. \\
&- \xi_0 (\xi_0^2 - 1) \left\{ (\xi_0^2 - 1) J_{10m N n} + J_{13m N n} \right\} \frac{d^2}{d\xi^2} R_{0,n}^{(i)}(c, \xi) \Big|_{\xi=\xi_0} \\
&- (\xi_0^2 - 1)^{1/2} \frac{d}{d\xi} R_{0,n}^{(i)}(c, \xi) \Big|_{\xi=\xi_0} \left\{ (\xi_0^2 - 1) J_{10m N n} + J_{13m N n} \frac{(3\xi_0^2 - 1)}{(\xi_0^2 - 1)} \right\} \\
&\left. + \frac{2\xi}{(\xi_0^2 - 1)^{1/2}} R_{0,n}^{(i)}(c, \xi) \Big|_{\xi=\xi_0} I_{12m N n} \right] \quad (C.16)
\end{aligned}$$

$$\phi Y_{0,N,n}^{\pm(i)}(c) = 0 \quad (C.17)$$

The integrals I_{pmNn} , $p = 1, 2, \dots, 33$ have been defined in Appendix D.

In all the above expressions for $Y_{m,N,n}(c)$, $\frac{d^2}{d\xi^2} R_{m,m+n}^{(i)}(c, \xi)$ is evaluated utilizing the equation (2.28):

$$\begin{aligned} \frac{d^2}{d\xi^2} R_{m,m+n}^{(i)}(c, \xi) &= \left[\left\{ \lambda_{m,m+n} - c^2 \xi^2 + \frac{m^2}{\xi^2 - 1} \right\} R_{m,m+n}^{(i)}(c, \xi) \right. \\ &\quad \left. - 2\xi \frac{d}{d\xi} R_{m,m+n}^{(i)}(c, \xi) \right] / (\xi^2 - 1) \end{aligned} \quad (\text{C.18})$$

Using the computed values of $\lambda_{m,m+n}(c)$, $R_{m,m+n}^{(i)}(c, \xi)$ and $\frac{d}{d\xi} R_{m,m+n}^{(i)}(c, \xi)$ we can calculate $\frac{d^2}{d\xi^2} R_{m,m+n}^{(i)}(c, \xi)$ from (C.18).

Appendix D

Definition of Integrals

The integrals I_{pmNn} , $p = 1, 2, \dots, 33$ resulting out of η -matching are evaluated by using the recurrence relations of associated Legendre functions from p. 401 [37] and the integrals

$$\int_{-1}^1 P_{\mu}^m(\eta) P_{\nu}^m(\eta) d\eta = \frac{2}{(2\mu+1)} \frac{(\mu+m)!}{(\mu-m)!} \delta_{\mu\nu} \quad (D.1)$$

and [5]

$$\int_{-1}^1 P_{\mu}^{m+2}(\eta) P_{\nu}^m(\eta) d\eta = \begin{cases} 0, & \nu > \mu \\ -\frac{2}{(2\mu+1)} \frac{(\mu+m)!}{(\mu-m-2)!}, & \nu = \mu \\ -2(m+1) \frac{(\mu+m)!}{-(\mu-m)!} [1 + (-1)^{\mu+\nu}], & \nu < \mu \end{cases} \quad (D.2)$$

where $\delta_{\mu\nu}$ is Kronecker delta function. The evaluation of integrals I_{pmNn} , $p = 1, 2, \dots, 11$ is shown in [7]; here the results of integrals I_{pmNn} , $p = 12, 13, \dots, 33$ are included. It is to be noted that orthogonality property of complex exponentials is used for ϕ -matching. Also for simplicity, the expression d_{τ}^{mn} has been used in place of $d_{\tau}^{mn}(c)$. c is equal to $2\pi F/\lambda$ or $2\pi F\sqrt{\epsilon_r}/\lambda$, according as the propagation constant of the medium under consideration is real or complex.

For $m \geq 0$, we have

$$\begin{aligned}
I_{12mNn} &= \int_{-1}^1 \eta(1-\eta^2)^{3/2} \frac{d}{d\eta} S_{0n} S_{1,1+N} d\eta \\
&= 2 \sum_{q=0,1}^{\infty} \frac{q(q+1)}{(2q+1)} d_q^{2n} \left[\frac{(q-1)}{(2q-3)(2q-1)} \left\{ \frac{q^2 d_{q-2}^{1,1+N}}{2q+3} - \frac{(q-2)(q-3) d_{q-4}^{1,1+N}}{2q-5} \right\} \right. \\
&\quad \left. + \frac{q+2}{2q+5} \left\{ \frac{(q+1)^2 d_{q+1}^{1,1+N}}{(2q-1)(2q+1)} - \frac{(q+3)(q+4) d_{q+3}^{1,1+N}}{(2q+3)(2q+7)} \right\} \right], \quad (n+N) \text{ even} \\
&= 0, \quad (n+N) \text{ odd} \tag{D.3}
\end{aligned}$$

$$\begin{aligned}
I_{13mNn} &= \int_{-1}^1 (1-\eta^2)^{3/2} \frac{d}{d\eta} S_{0n} S_{1,1+N} d\eta \\
&= 2 \sum_{q=0,1}^{\infty} \frac{1}{(2q+1)} d_q^{2n} \left[\frac{(q+1)(q+2)(q+3)}{(2q+3)(2q+5)} \left\{ \frac{d_q^{1,1+N}}{2q+3} - \frac{d_{q+2}^{1,1+N}}{2q+7} \right\} \right. \\
&\quad \left. - \frac{2(q-1)q(q+1)(q+2)}{(2q-1)(2q+3)} \left\{ \frac{d_{q-2}^{1,1+N}}{2q-1} - \frac{d_{q+1}^{1,1+N}}{2q+3} \right\} \right. \\
&\quad \left. + \frac{q(q+1)(q+2)(q+3)}{(2q-3)(2q-1)} \left\{ \frac{d_{q-4}^{1,1+N}}{2q-5} - \frac{d_{q-2}^{1,1+N}}{2q-1} \right\} \right], \quad (n+N) \text{ even} \\
&= 0, \quad (n+N) \text{ odd} \tag{D.4}
\end{aligned}$$

$$\begin{aligned}
I_{14mNn} &= \int_{-1}^1 \eta(1-\eta^2) S_{m,m+n} S_{m,m+N} d\eta \\
&= 2 \sum_{q=0,1}^{\infty} \frac{(2m+q)!}{(2m+2q+1)q!} d_q^{2n} \\
&\quad \cdot \left[\frac{(2m+q+1)(2m+q+2)}{(2m+2q+3)(2m+2q+5)} \left\{ \frac{d_{q+1}^{m,m+N}}{2m+2q+3} - \frac{d_{q+3}^{m,m+N}}{2m+2q+7} \right\} \right. \\
&\quad \left. + \frac{(2m+1)q(2m+q+1)^2}{(2m+2q-1)(2m+2q+1)(2m+2q+3)} \left\{ \frac{d_{q-1}^{m,m+N}}{2m+2q-1} - \frac{d_{q+1}^{m,m+N}}{2m+2q+3} \right\} \right. \\
&\quad \left. - \frac{q(q-1)(q-2)}{(2m+2q-3)(2m+2q-1)} \left\{ \frac{d_{q-3}^{m,m+N}}{2m+2q-5} - \frac{d_{q-1}^{m,m+N}}{2m+2q-3} \right\} \right], \quad (n+N) \text{ odd} \\
&= 0, \quad (n+N) \text{ even} \tag{D.5}
\end{aligned}$$

$$\begin{aligned}
I_{15mNn} &= \int_{-1}^1 (1-\eta^2)^2 \frac{d}{d\eta} S_{m,m+n} S_{m,m+N} d\eta \\
&= 2 \sum_{q=1,0}^{\infty} \frac{(2m+q+1)!}{(2m+2q+1)(2m+2q+3)q!} d_q^{2n} \left[(2m+q+2) d_{q+1}^{m,m+n} \right. \\
&\quad \cdot \left. \left\{ \frac{(m+q+2)(2m+q+1)(2m+2q+5) + (m+q+1)(q+2)(2m+2q+1)}{(2m+2q+1)(2m+2q+3)(2m+2q+5)} \right\} \right]
\end{aligned}$$

$$\begin{aligned}
& + \left[\frac{(m+q+2)(q-1)q d_{q+1}^{m,m+n}}{(2m+2q-1)(2m+2q+1)} - \frac{(m+q+4)(2m+q+2)(2m+q+3)d_{q+3}^{m,m+n}}{(2m+2q+5)(2m+2q+7)} \right] \\
& - 2 \sum_{q=0,1}^{\infty} \left[\frac{(m+q)(2m+q+2)(2m+q+3)}{2m+q+5} \left\{ \frac{d_{q+1}^{m,m+N}}{2m+2q+3} - \frac{d_{q+3}^{m,m+N}}{2m+2q+7} \right\} \right] \\
& + \left\{ \frac{(m+q+1)(2m+q)(2m+2q+3) + (m+q)(q+1)(2m+2q-1)}{(2m+2q-1)(2m+2q+1)(2m+2q+3)} \right\} \\
& \cdot q d_{q+1}^{m,m+N} \frac{d_{q+1}^{m,m+n}(2m+2q+1)!}{(2m+2q+1)(2m+2q+3)}, \quad (n+N) \text{ odd} \\
& = 0, \quad (n+N) \text{ even} \tag{D.6}
\end{aligned}$$

$$\begin{aligned}
I_{16mNn} & = \int_{-1}^1 (1-\eta^2)^2 \eta^2 \frac{d}{d\eta} S_{m,m+n} S_{m,m+N} d\eta \\
& = I_{4mNn} - I_{16mNn} \tag{D.7}
\end{aligned}$$

$$\begin{aligned}
I_{17mNn} & = \int_{-1}^1 \frac{\eta}{(1-\eta^2)} S_{m,m+n} S_{m,m+N} d\eta \\
& = \sum_{q=0,1}^{\infty} \frac{(2m+q)!}{m \cdot q!} d_q^{m,m+n} \left[d_{q+1}^{m,m+N} + 2 \sum_{r=q+3}^{\infty} d_r^{m,m+N} \right] \\
& + 2 \sum_{r=1,0}^{\infty} \frac{(2m+r)!}{m \cdot r!} d_r^{m,m+N} \sum_{q=r+1}^{\infty} d_q^{m,m+n}, \quad (n+N) \text{ odd} \\
& = 0, \quad (n+N) \text{ even} \tag{D.8}
\end{aligned}$$

$$\begin{aligned}
I_{18mNn} & = \int_{-1}^1 \frac{d}{d\eta} S_{m,m+n} S_{m,m+N} d\eta \\
& = - \sum_{q=0,1}^{\infty} \frac{(2m+q)!}{q!} d_q^{m,m+n} \left[d_{q+1}^{m,m+N} + 2 \sum_{r=q+3}^{\infty} d_r^{m,m+N} \right] \\
& + 2 \sum_{r=1,0}^{\infty} d_r^{m,m+N} \sum_{q=r+1}^{\infty} d_q^{m,m+n} \frac{(2m+q)!}{q!}, \quad (n+N) \text{ odd} \\
& = 0, \quad (n+N) \text{ even} \tag{D.9}
\end{aligned}$$

$$\begin{aligned}
I_{19mNn} & = \int_{-1}^1 \eta(1-\eta^2) S_{m+2,m+n+2} S_{m,m+N} d\eta \\
& = 2 \sum_{q=0,1}^{\infty} \frac{(2m+q+4)!}{(2m+2q+5)q!} d_q^{m+2,m+n+2} \\
& \cdot \left[\frac{q}{(2m+2q+1)(2m+2q+3)} \left\{ \frac{d_{q-1}^{m,m+N}}{2m+2q-1} - 2 \frac{d_{q+1}^{m,m+N}}{2m+2q+5} \right\} \right] \\
& + \frac{(2m+q+5)}{(2m+2q+5)(2m+2q+7)} \left\{ \frac{d_{q+1}^{m,m+N}}{2m+2q+3} - 2 \frac{d_{q+3}^{m,m+N}}{2m+2q+9} \right\}
\end{aligned}$$

$$\begin{aligned}
& + \frac{1}{2m+2q+7} \left\{ \frac{(2m+q+5)a_{q+5}^{m,m+N}}{(2m+2q+9)(2m+2q+11)} \right. \\
& \left. + \frac{q a_{q+3}^{m,m+N}}{(2m+2q+3)(2m+2q+5)} \right\}, \quad (n+N) \text{ odd} \\
& = 0, \quad (n+N) \text{ even}
\end{aligned} \tag{D.10}$$

$$\begin{aligned}
I_{20mNn} & = \int_{-1}^1 (1-\eta^2)^2 \frac{d}{d\eta} S_{m+2,m+n+2} S_{m,m+N} d\eta \\
& = 2 \sum_{q=0,1}^{\infty} \frac{(2m+q+4)!}{(2m+2q+5)q!} a_q^{m,m+n} \\
& \cdot \left[\frac{q(m+q+3)}{(2m+2q+1)(2m+2q+3)} \left\{ \frac{a_{q-1}^{m,m+N}}{2m+2q-1} - \frac{2a_{q+1}^{m,m+N}}{2m+2q+5} \right\} \right. \\
& - \frac{(2m+q+5)(m+q+2)}{(2m+2q+5)(2m+2q+7)} \left\{ \frac{a_{q+1}^{m,m+N}}{2m+2q+3} - \frac{2a_{q+3}^{m,m+N}}{2m+2q+9} \right\} \\
& - \frac{1}{2m+2q+7} \left\{ \frac{(m+q+3)a_{q+5}^{m,m+N}}{(2m+2q+3)(2m+2q+5)} \right. \\
& \left. - \frac{(m+q+2)(2m+q+5)a_{q+3}^{m,m+N}}{(2m+2q+9)(2m+2q+11)} \right\}, \quad (n+N) \text{ odd} \\
& = 0, \quad (n+N) \text{ even}
\end{aligned} \tag{D.11}$$

$$\begin{aligned}
I_{21mNn} & = \int_{-1}^1 (1-\eta^2)^2 \eta^2 \frac{d}{d\eta} S_{m+2,m+n+2} S_{m,m+N} d\eta \\
& = I_{0mNn} - I_{20mNn}
\end{aligned} \tag{D.12}$$

$$\begin{aligned}
I_{22mNn} & = \int_{-1}^1 \frac{\eta}{(1-\eta^2)} S_{m+2,m+n+2} S_{m,m+N} d\eta \\
& = - \sum_{q=0,1}^{\infty} \frac{2(2m+q-2)!}{q!} \left\{ (2m+q-1)(2m+q) \left[(q+2)a_{q+1}^{m,m+N} \right. \right. \\
& + (2m+2q+3) \sum_{r=q+3}^{\infty} a_r^{m,m+N} \left. \right] \sum_{r=q}^{\infty} a_r^{m+2,m+n+2} \\
& - 2m \left[q a_{q-1}^{m,m+N} + (2m+2q-1) \sum_{r=q+1}^{\infty} a_r^{m,m+N} \right] \\
& \cdot \sum_{t=q}^{\infty} (2m+2t+3) \sum_{r=t}^{\infty} a_r^{m+2,m+n+2} \left. \right\}, \quad (n+N) \text{ odd} \\
& = 0, \quad (n+N) \text{ even}
\end{aligned} \tag{D.13}$$

$$I_{23mNn} = \int_{-1}^1 \frac{d}{d\eta} S_{m+2,m+n+2} S_{m,m+N} d\eta$$

$$\begin{aligned}
&= - \sum_{q=1,0}^{\infty} , \frac{2(2m+q-2)!}{q!} \{ (2m+q-1)(2m+q) [-q(m+q+1)d_q^{m+2,m+n+2} \\
&+ (m+2)(2m+2q+3) \sum_{r=q+1}^{\infty} , d_r^{m+2,m+n+2}] \sum_{r=q+2}^{\infty} , d_r^{m,m+N} \\
&+ 2m(2m+2q-1) \sum_{t=q}^{\infty} , [-t(m+t+1)d_{t-1}^{m+2,m+n+2} + (m+2)(2m+2t+3) \\
&\cdot \sum_{r=t+1}^{\infty} , d_r^{m+2,m+n+2}] \sum_{r=q}^{\infty} , d_r^{m,m+N} \} , (n+N) \text{ odd} \\
&= 0, (n+N) \text{ even} \tag{D.14}
\end{aligned}$$

$$\begin{aligned}
I_{24m,Nn} &= \int_{-1}^1 \eta(1-\eta^2)^{3/2} \frac{d}{d\eta} S_{m+1,m+n+1} S_{m,m+N} d\eta \\
&= 2 \sum_{q=0,1}^{\infty} , \frac{(2m+q+2)!}{(2m+2q+3)q!} d_q^{m+1,m+n+1} \\
&\cdot \left[\frac{(m+q+2)}{(2m+2q+1)} \left\{ \frac{q(q-1)d_{q-2}^{m,m+N}}{(2m+2q-3)(2m+2q-1)} \right. \right. \\
&+ \left. \left. \frac{(2m+1)d_q^{m,m+N}}{(2m+2q-1)(2m+2q+3)} - \frac{(2m+q+2)d_{q+2}^{m,m+N}}{(2m+2q+3)(2m+2q+5)} \right\} \right. \\
&\cdot \left. \frac{(2m+q+3)(m+q+1)}{(2m+2q+5)} \left\{ \frac{(q+1)d_q^{m,m+N}}{(2m+2q+1)(2m+2q+3)} \right. \right. \\
&+ \left. \left. \frac{(2m+1)d_{q+2}^{m,m+N}}{(2m+2q+3)(2m+2q+7)} - \frac{(2m+q+4)d_{q+4}^{m,m+N}}{(2m+2q+7)(2m+2q+9)} \right\} \right] , (n+N) \text{ even} \\
&= 0, (n+N) \text{ odd} \tag{D.15}
\end{aligned}$$

$$\begin{aligned}
I_{26m,Nn} &= \int_{-1}^1 (1-\eta^2)^{3/2} S_{m+1,m+n+1} S_{m,m+N} d\eta \\
&= 2 \sum_{q=0,1}^{\infty} , \frac{(2m+q+2)!}{(2m+2q+3)q!} d_q^{m+1,m+n+1} \\
&\cdot \left[\frac{(2m+q+3)(2m+q+4)}{(2m+2q+5)} \left\{ \frac{d_q^{m,m+N}}{(2m+2q+1)(2m+2q+3)} \right. \right. \\
&+ \left. \left. \frac{d_{q+4}^{m,m+N}}{(2m+2q+7)(2m+2q+9)} - \frac{2d_{q+2}^{m,m+N}}{(2m+2q+3)(2m+2q+7)} \right\} \right. \\
&- \left. \frac{q(q-1)}{(2m+2q+1)} \left\{ \frac{d_{q-2}^{m,m+N}}{(2m+2q-3)(2m+2q-1)} \right. \right. \\
&+ \left. \left. \frac{d_{q+2}^{m,m+N}}{(2m+2q+3)(2m+2q+5)} - \frac{2d_q^{m,m+N}}{(2m+2q-1)(2m+2q+3)} \right\} \right] , (n+N) \text{ even}
\end{aligned}$$

$$= 0, \quad (n + N) \text{ odd} \quad (D.16)$$

$$\begin{aligned} I_{2mNn} &= \int_{-1}^1 \frac{1}{(1 - q^2)^{1/2}} S_{n+1, m+1+1} S_{m, n+N} dq \\ &= 2 \sum_{r=0,1}^{\infty} \frac{1}{(2m + q)^r} d_{q^r, m+N} d_{q^{r+1, m+1+1}} \\ &+ 2 \sum_{r=0,1}^{\infty} \sum_{k=r+2}^{\infty} \frac{(2m + r)!}{r!} d_{q^r, m+N} d_{q^{r+1, m+N+1}} (n + N) \text{ even} \\ &= 0, \quad (n + N) \text{ odd} \end{aligned} \quad (D.17)$$

$$\begin{aligned} I_{2mNn} &= \int_{-1}^1 (1 - q^2)^{1/2} \frac{d}{dq} \left[(1 - q^2)^{1/2} \frac{d}{dq} S_{m, n+N} \right] S_{m, n+N} dq \\ &= \sum_{r=0,1}^{\infty} \frac{1}{q^r} \frac{1}{(2m + q)^r} \\ &\cdot \left[(m + 1) d_{q^r, m+N} \sum_{r=2q+2}^{\infty} d_{q^r, n+n} - (m - 1) d_{q^r, m+n} \sum_{r=2q+2}^{\infty} d_{q^r, m+N} \right. \\ &\left. - \frac{q(m + q) + (q + 1)(m + q + 1)}{2m + 2q + 1} d_{q^r, m+n} d_{q^r, m+N} \right], \quad (n + N) \text{ even} \\ &= 0, \quad (n + N) \text{ odd} \end{aligned} \quad (D.18)$$

$$\begin{aligned} I_{2mNn} &= \int_{-1}^1 (1 - q^2)^{1/2} \frac{d}{dq} \left[\frac{q}{(1 - q^2)^{1/2}} S_{m, m+1} \right] S_{m, m+N} dq \\ &= \sum_{r=0,1}^{\infty} \frac{(m + 2q + 1)(2m + q)^r}{m(2m + 2q + 1)q^r} d_{q^r, m+n} d_{q^r, m+N} + \sum_{r=0,1}^{\infty} \frac{(2m + r)!}{m r!} \\ &\cdot \left[(m + 1) d_{q^r, m+N} \sum_{k=r+2}^{\infty} d_{q^k, m+n} \right. \\ &\left. - (m - 1) d_{q^r, m+1} \sum_{k=r+2}^{\infty} d_{q^k, m+N} \right], \quad (n + N) \text{ even} \\ &= 0, \quad (n + N) \text{ odd} \end{aligned} \quad (D.19)$$

$$\begin{aligned} I_{2mNn} &= \int_{-1}^1 (1 - q^2)^{1/2} \frac{d}{dq} S_{m, m+n} S_{m, m+N} dq \\ &= -2 \sum_{q=0,1}^{\infty} \frac{(m + q + 1)(2m + q + 1)}{(2m + 2q + 3)(q + 1)} d_{q^{q+1, m+n+1}} d_{q^q, m+N} \\ &+ 2 \sum_{r=0,1}^{\infty} \frac{(m + 1)(2m + r)!}{r!} d_{q^r, m+N} \sum_{k=r+1}^{\infty} d_{q^k, m+n+1+1}, \quad (n + N) \text{ odd} \\ &= 0, \quad (n + N) \text{ even} \end{aligned} \quad (D.20)$$

$$\begin{aligned}
I_{30mNn} &= \int_{-1}^1 \eta^2 S_{m+2,m+n+2} S_{m,m+N} d\eta \\
&= -2 \sum_{q=0,1}^{\infty} \frac{(2m+q+1)!}{(2m+2q+5)q!} d_r^{m+2,m+n+2} \\
&\quad \cdot \left[\frac{(2m+q+2)(2m+q+3)}{(2m+q+7)} \left\{ \frac{(q+3)d_{q+2}^{m,m+N}}{(2m+2q+5)} + \frac{(2m+q+4)d_{q+4}^{m,m+N}}{(2m+2q+9)} \right\} \right. \\
&\quad \left. + \frac{(2m+q+4)q}{(2m+2q+3)} \left\{ \frac{(q+1)d_r^{m,m+N}}{(2m+2q+1)} + \frac{(2m+q+2)d_{q+2}^{m,m+N}}{(2m+2q+5)} \right\} \right] \\
&\quad + 2 \sum_{r=0,1}^{\infty} \frac{(m+1)(2m+r)!}{(2m+2r+1)r!} d_r^{m,m+N} \sum_{q=r}^{\infty} \left[\frac{(q+1)(2m+2q+1)}{(2m+2q+5)} \right. \\
&\quad \left. + \frac{(2m+q+4)q}{(2m+2q+5)} \right] d_r^{m+2,m+n+2} + 2 \sum_{q=0,1}^{\infty} \frac{(m+1)(2m+q)!}{(2m+2q+5)q!} d_q^{m+2,m+N+2} \\
&\quad \cdot \left[\frac{(2m+q+2)(2m+2q+1)}{(2m+2q+5)} d_{q+2}^{m,m+N} + \frac{(q+1)q}{(2m+2q+1)} d_q^{m,m+N} \right] \\
&\quad + 2 \sum_{r=0,1}^{\infty} \frac{(m+1)(2m+r)!}{(2m+2r+1)r!} d_r^{m,m+N} \sum_{q=r+2}^{\infty} \left[\frac{(2m+q+1)(2m+2q+4)}{(2m+2q+5)} \right. \\
&\quad \left. + \frac{(q+1)q}{(2m+2q+5)} \right] d_q^{m+2,m+n+2}, \quad (n+N) \text{ even} \\
&= 0, \quad (n+N) \text{ odd} \tag{D.21}
\end{aligned}$$

$$\begin{aligned}
I_{31mNn} &= \int_{-1}^1 \eta \frac{d}{d\eta} S_{m+2,m+n+2} S_{m,m+N} d\eta \\
&= - \sum_{q=1,0}^{\infty} \frac{2(2m+q-2)!}{q!} \left\{ \frac{(2m+q-1)(2m+q)}{(2m+2q+3)} \right\} \left[-q(m+q+1)d_q^{m+2,m+n+2} \right. \\
&\quad \left. + (m+2)(2m+2q+3) \sum_{r=q+1}^{\infty} d_r^{m+2,m+n+2} \right] \left[(q+2)d_{q+1}^{m,m+N} \right. \\
&\quad \left. + (2m+2q+3) \sum_{r=q+3}^{\infty} d_r^{m,m+N} \right] - m \left[q d_{q-1}^{m,m+N} + (2m+2q-1) \sum_{r=q+1}^{\infty} d_r^{m,m+N} \right] \\
&\quad \cdot \sum_{t=q}^{\infty} \left[-t(m+t+1)d_{t-1}^{m+2,m+n+2} \right. \\
&\quad \left. + (m+2)(2m+2t+3) \sum_{r=t+1}^{\infty} d_r^{m+2,m+n+2} \right] \Big\}, \quad (n+N) \text{ even} \\
&= 0, \quad (n+N) \text{ odd} \tag{D.22}
\end{aligned}$$

$$I_{32mNn} = \int_{-1}^1 \frac{1}{(1-\eta^2)} S_{m+2,m+n+2} S_{m,m+N} d\eta$$

$$\begin{aligned}
&= - \sum_{q=0,1}^{\infty} \frac{2(2m+q-2)!}{q!} \left\{ (2m+q-1)(2m+q)(2m+2q+3) \sum_{r=q}^{\infty} {}_r d_r^{m+2,m+n+2} \right. \\
&\quad \cdot \sum_{r=q+2}^{\infty} {}_r d_r^{m,m+N} - 2m(2m+2q-1) \sum_{r=q}^{\infty} {}_r d_r^{m,m+N} \\
&\quad \left. \cdot \left[\sum_{t=q}^{\infty} (2m+2t+3) \sum_{r=t}^{\infty} {}_r d_r^{m+2,m+n+2} \right] \right\}, \quad (n+N) \text{ even} \\
&= 0, \quad (n+N) \text{ odd} \tag{D.23}
\end{aligned}$$

$$\begin{aligned}
I_{32mNn} &= \int_{-1}^1 (1-\eta^2) \frac{d^2}{d\eta^2} S_{m+2,m+n+2} S_{m,m+N} d\eta \\
&= 2I_{31mNn} + (m+2)^2 I_{32mNn} - \lambda_{m+2,m+n+2} I_{7mNn} + h^2 I_{30mNn} \tag{D.24}
\end{aligned}$$

In all the expressions of I_{pmNn} , $p = 1, 2, \dots, 33$, prolate spheroidal expansion coefficients $d_r^{m,n}$ are real or complex accordingly the propagation constant of the medium is real or complex.

Appendix E

Rotational-Translational Coefficients

E.1 The Euler Angles

Let us first define the Euler angles before defining the rotational-translational coefficients. An arbitrary rotation of a system of coordinates (x', y', z') with respect to a system of coordinates (x, y, z) is uniquely determined by three parameters — the three Euler angles (α, β, γ) [39]. Since we are using cartesian coordinate system, which is a right-handed system of coordinates, a positive direction of rotation is one that corresponds to the motion of right-handed screw. Let initially the (x', y', z') -axes coincide with the (x, y, z) -axes: position K . The Euler angles (α, β, γ) are defined by three consecutive rotations through which the set of (x', y', z') -axes goes from the position K to the final position K' . These three rotations are performed as follows (refer to Fig. E.1):

- (a) a rotation over an angle α ($0 \leq \alpha \leq 2\pi$) around the z -axis changes the system of axes to the position $K_1(x_1, y_1, z_1)$.
- (b) a rotation over an angle β ($0 \leq \beta \leq 2\pi$) around the new y_1 -axis changes the system of axes from the position K_1 to the position

$K_2(x_2, y_2, z_2)$.

(c) a rotation over an angle γ ($0 \leq \gamma \leq 2\pi$) around the z_2 -axis which is same as the z' -axis changes the system of axes from the position K_2 to the final position K' .

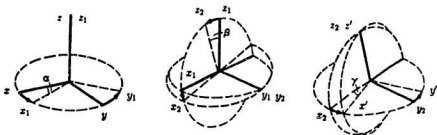


Figure E.1: The Euler Angles.

E.2 Rotational-Translational Coefficients

The elements of the matrices $[\Gamma]$ and $[\Gamma']$ defined in [28] are as follows.

$$[\Gamma] = \begin{bmatrix} [\Gamma]_{00} & [\Gamma]_{01} & [\Gamma]_{02} \cdots \\ [\Gamma]_{10} & [\Gamma]_{11} & [\Gamma]_{12} \cdots \\ [\Gamma]_{20} & [\Gamma]_{21} & [\Gamma]_{22} \cdots \\ \vdots & \vdots & \vdots \end{bmatrix} \quad (\text{E.1})$$

with

$$[\Gamma]_{00} = \begin{bmatrix} [\Gamma_1]_0^{-1} & [\Gamma_2]_1^{-1} & [\Gamma_3]_0^{-1} \\ [\Gamma_4]_{-1}^0 & [{}^*\Gamma_4]_1^0 & [\Gamma_5]_0^0 \end{bmatrix} \quad (\text{E.2})$$

$$[\Gamma]_{k\sigma} = \begin{bmatrix} [\Gamma_1]_{\sigma-1}^{-1} & [\Gamma_2]_{\sigma+1}^{-1} & [\Gamma_3]_{\sigma}^{-1} & [\Gamma_1]_{\sigma-(\sigma+1)}^{-1} & [\Gamma_2]_{\sigma-(\sigma-1)}^{-1} & [\Gamma_3]_{-\sigma}^{-1} \\ [\Gamma_4]_{\sigma-1}^0 & [{}^*\Gamma_4]_{\sigma+1}^0 & [\Gamma_5]_{\sigma}^0 & [\Gamma_4]_{\sigma-(\sigma+1)}^0 & [{}^*\Gamma_4]_{\sigma-(\sigma-1)}^0 & [{}^*\Gamma_5]_{-\sigma}^0 \end{bmatrix}, \sigma \geq 1 \quad (\text{E.3})$$

$$[\Gamma]_{r0} = \begin{bmatrix} [\Gamma_1]_0^{r-1} & [\Gamma_2]_1^{r-1} & [\Gamma_3]_0^{r-1} \\ [\Gamma_4]_{-1}^{r-1} & [* \Gamma_4]_1^r & [\Gamma_5]_0^r \\ [* \Gamma_2]_{-1}^{-(r-1)} & [* \Gamma_1]_1^{-(r-1)} & [* \Gamma_3]_0^{-(r-1)} \\ [\Gamma_4]_{-1}^{-r} & [* \Gamma_4]_1^{-r} & [\Gamma_5]_0^{-r} \end{bmatrix}, \quad \tau \geq 1 \quad (\text{E.4})$$

$$[\Gamma]_{\tau\sigma} = \begin{bmatrix} [\Gamma_1]_{\sigma-1}^{r-1} & [\Gamma_2]_{\sigma+1}^{r-1} & [\Gamma_3]_{\sigma}^{r-1} & [\Gamma_1]_{-(\sigma+1)}^{r-1} & [\Gamma_2]_{-(\sigma-1)}^{r-1} & [\Gamma_3]_{-\sigma}^{r-1} \\ [\Gamma_4]_{\sigma-1}^{r-1} & [* \Gamma_4]_{\sigma+1}^r & [\Gamma_5]_{\sigma}^r & [\Gamma_4]_{-(\sigma+1)}^r & [* \Gamma_4]_{-(\sigma-1)}^r & [\Gamma_5]_{-\sigma}^r \\ [* \Gamma_2]_{\sigma-1}^{-(r-1)} & [* \Gamma_1]_{\sigma+1}^{-(r-1)} & [* \Gamma_3]_{\sigma}^{-(r-1)} & [* \Gamma_2]_{-(\sigma+1)}^{-(r-1)} & [* \Gamma_1]_{-(\sigma-1)}^{-(r-1)} & [* \Gamma_3]_{-\sigma}^{-(r-1)} \\ [\Gamma_4]_{\sigma-1}^{-r} & [* \Gamma_4]_{\sigma+1}^{-r} & [\Gamma_5]_{\sigma}^{-r} & [\Gamma_4]_{-(\sigma+1)}^{-r} & [* \Gamma_4]_{-(\sigma-1)}^{-r} & [\Gamma_5]_{-\sigma}^{-r} \end{bmatrix} \quad \tau \geq 1, \quad \sigma \geq 1 \quad (\text{E.5})$$

The submatrices $[\Gamma_i]_{\sigma}^{\tau}$ and $[* \Gamma_i]_{\sigma}^{\tau}$, where $\tau, \sigma = \dots, -3, -2, -1, 0, 1, 2, 3, \dots$ and $i = 1, 2, 3, 4, 5$, are given by $C_i^{\tau} [\Gamma]_{\sigma}^{\tau}$ and $C_i^{*\tau} [\Gamma]_{\sigma}^{\tau}$ respectively, where C_i^{τ} are defined as follows:

$$\left. \begin{aligned} C_1^{\tau} &= \frac{1}{2}(1 + \cos \beta)[\cos(\alpha + \gamma) - j \sin(\alpha + \gamma)] \\ C_2^{\tau} &= -\frac{1}{2}(1 - \cos \beta)[\cos(\alpha - \gamma) + j \sin(\alpha - \gamma)] \\ C_3^{\tau} &= -\frac{1}{2} \sin \beta(\cos \gamma - j \sin \gamma) \\ C_4^{\tau} &= \sin \beta(\cos \alpha - j \sin \alpha) \\ C_5^{\tau} &= \cos \beta \end{aligned} \right\} \quad (\text{E.6})$$

$C_i^{*\tau}$ is the complex conjugate of C_i^{τ} , and

$$[\Gamma]_{\sigma}^{\tau} = \begin{bmatrix} (4)Q_{\sigma,|\sigma|}^{r,|\tau|} & (4)Q_{\sigma,|\sigma|+1}^{r,|\tau|} & (4)Q_{\sigma,|\sigma|+2}^{r,|\tau|} & \dots \\ (4)Q_{\sigma,|\sigma|}^{r,|\tau|+1} & (4)Q_{\sigma,|\sigma|+1}^{r,|\tau|+1} & (4)Q_{\sigma,|\sigma|+2}^{r,|\tau|+1} & \dots \\ (4)Q_{\sigma,|\sigma|}^{r,|\tau|+2} & (4)Q_{\sigma,|\sigma|+1}^{r,|\tau|+2} & (4)Q_{\sigma,|\sigma|+2}^{r,|\tau|+2} & \dots \end{bmatrix} \quad (\text{E.7})$$

where $(4)Q_{\mu\nu}^{mn}$ are rotational-translational expansion coefficients given below.

The elements of matrix $[\Gamma^{\tau}]$, given in equation (4.84), can be obtained from the corresponding elements of $[\Gamma]$ by replacing $(4)Q_{\mu\nu}^{mn}$ (given below) by $(4)Q_{\mu\nu}^{mn}$

and replacing C'_i by C_i , where C_i are given as:

$$\left. \begin{aligned} C_1 &= \frac{1}{2}(1 + \cos \beta)[\cos(\alpha + \gamma) + j \sin(\alpha + \gamma)] \\ C_2 &= -\frac{1}{2}(1 - \cos \beta)[\cos(\alpha - \gamma) + j \sin(\alpha - \gamma)] \\ C_3 &= \frac{1}{2} \sin \beta (\cos \alpha + j \sin \alpha) \\ C_4 &= -\sin \beta (\cos \gamma + j \sin \gamma) \\ C_5 &= \cos \beta \end{aligned} \right\} \quad (\text{E.8})$$

C_i^* is the complex conjugate of C_i .

Consider the translation from the coordinate system $O'x'y'z'$ to the system $Ox_{||}y_{||}z_{||}$ followed by the rotation of the system $Ox_{||}y_{||}z_{||}$ about the origin O through the Euler angles $(-\gamma, -\beta, -\alpha)$. The rotational-translational coefficients $({}^4)Q_{\mu,\nu}^{m,n}$ needed for the expansion of spheroidal wave functions in primed coordinates expressed in terms of functions in unprimed (global) coordinates are given as:

$$\begin{aligned} ({}^4)Q_{\mu,\nu}^{m,n}(\alpha, \beta, \gamma; d) &= \sum_{q=0,1}^{\infty} {}^4d_q^{m,n}(h) \sum_{r=0,1}^{\infty} {}^4j^{|m|+q-n+\nu-|\mu|-r} \frac{\Lambda_{\mu,|\mu|+r}}{N_{\mu\nu}(h)} d_r^{\mu\nu}(h) \\ &\cdot \sum_{c=-(|\mu|+r)}^{(|\mu|+r)} R_{\mu,|\mu|+r}^{c,|\mu|+r}(-\gamma, -\beta, -\alpha) ({}^4)b_{c,|\mu|+r}^{m,|\mu|+q}(d) \quad (\text{E.9}) \end{aligned}$$

where

$$({}^4)b_{c,l}^{m,s}(d) = (-1)^c \sum_{p=p_0, p_0+1}^{l+s} (-1)^p j^{l+p-s} (2l+1) a(m, s | -c, l, p) \Psi_{m-c,p}^{(4)}(d) \quad (\text{E.10})$$

in which $a(m, s | -c, l, p)$ are the linearization expansion coefficients [19], p_0 is the lower limit of $p = s + l, s + l - 2, \dots, |s - l|$ if $|s - l| \geq |m - c|$. If $|s - l| < |m - c|$, p_0 is replaced by $|m - c|$ or $|m - c| + 1$ according as $s + l + |m - c|$ is even or odd. The upper limit of p is given by $s + l$, and

$$\Psi_{m-c,p}^{(4)}(d) = z_p^{(4)}(kd) \cdot P_p^{m-c}(\cos \theta_d) \cdot e^{j(m-c)\phi_d} \quad (\text{E.11})$$

where $x_p^{(4)}(kd) = h_p^{(2)}(kd)$ is the spherical Hankel function of second kind and $P_p^{m-c}(\cos \theta_d)$ is the associated Legendre function of the first kind. $d_q^{mn}(h')$ and $d_q^{\mu\nu}(h)$ are the spheroidal expansion coefficients and $N_{\mu\nu}(h)$ is the normalization factor [1]. Also in (E.9) the following notations are used:

$$\Lambda_{ml} = \frac{2}{(2l+1)} \frac{(l+m)!}{(l-m)!} \quad (\text{E.12})$$

$$P_{m'l}^{ml}(\alpha, \beta, \gamma) = (-1)^{m'-m} \left[\frac{\Lambda_{m'l}}{\Lambda_{m'l}} \right]^{1/2} e^{im'\gamma} d_{m'm}^{(l)}(\beta) \cdot e^{im\alpha} \quad (\text{E.13})$$

$$d_{m'm}^{(l)}(\beta) = \left[\frac{(l+m')!(l-m')!}{(l+m)! (l-m)!} \right]^{1/2} \left(\cos \frac{\beta}{2} \right)^{m'+m} \cdot \left(\sin \frac{\beta}{2} \right)^{m'-m} \cdot P_{l-m'}^{(m'-m, m'+m)}(\cos \beta) \quad (\text{E.14})$$

where $P_{l-m'}^{(m'-m, m'+m)}(\cos \beta)$, the Jacobi polynomial of argument $\cos \beta$, is evaluated in the present work using the explicit expression [35]:

$$P_n^{(\lambda_1, \lambda_2)}(x) = \frac{1}{2^n} \sum_{t=0}^n \binom{n+\lambda_1}{t} \binom{n+\lambda_2}{n-t} (x-1)^{n-t} (x+1)^t \quad (\text{E.15})$$

Likewise, rotational-translational coefficients in the expansion of scalar spheroidal wave functions in unprimed coordinates expressed in terms of functions in primed coordinates for $r' \leq d$ is given by:

$$\begin{aligned} {}^{(4)}Q_{\mu, \nu}^{mn}(\alpha, \beta, \gamma; d) &= \sum_{q=0,1}^{\infty} d_q^{mn}(h) \sum_{k=-(|m|+q)}^{(|m|+q)} R_{k, |m|+q}^{m, |m|+q}(\alpha, \beta, \gamma) \\ &\cdot \sum_{r=0,1}^{\infty} j_{|m|+q-n+\nu-|\mu|-r} \frac{\Lambda_{\mu, |\mu|+r}}{N_{\mu\nu}(h')} d_r^{\mu\nu}(h') \cdot {}^{(4)}a_{\mu, |\mu|+r}^{k, |m|+q}(d) \end{aligned} \quad (\text{E.16})$$

where

$${}^{(4)}a_{\mu, |\mu|}^{k, |m|}(d) = (-1)^\mu \sum_{p=p_0, p_0+1}^{l+s} (-1)^p j^{l+p-s} (2l+1) \cdot a(k, s | -\mu, l | p) \Psi_{k-\mu, p}^{(4)}(d) \quad (\text{E.17})$$

E.3 Special Case: Translational Coefficients

Translational Addition Theorems can be obtained as a special case of Rotational-Translational Theorems when $\alpha \rightarrow 0$, $\beta \rightarrow 0$ and $\gamma \rightarrow 0$. Thus from (E.13) we find that

$$R_{m1}^{mi}(0, 0, 0) = \delta_{mm'} \quad (\text{E.18})$$

where $\delta_{mm'}$ is Kronecker delta function. Also when $\alpha \rightarrow 0$, $\beta \rightarrow 0$ and $\gamma \rightarrow 0$, the direction cosines $c_{ax'}$, $c_{ay'}$, $c_{az'}$, ($a = x, y, z$) are all equal to zero, except $c_{ax'}$, $c_{yy'}$ and $c_{zz'}$ which are equal to unity. Translational coefficients, deduced from rotational-translational coefficients in pp. 159-160, [26], are exactly same as the translational coefficients presented in [19].



